Central Actions of Cannabinoids: Insights on Endocannabinoid Signaling in the Lateral Habenula and Novel Actions of Cannabidiol on Amygdala Physiology

By

Nathan D. Winters

Dissertation

Submitted to the Faculty of the

Graduate School of Vanderbilt University

in partial fulfillment of the requirements

for the degree of

DOCTOR OF PHILOSOPHY

in

Pharmacology

May 12, 2023

Approved:

Danny Winder, Ph.D.

Sachin Patel, M.D., Ph.D.

Brad Grueter, Ph.D.

Erin Calipari, Ph.D.

Jennifer Blackford, Ph.D.

Dedicated to my parents, Dan and Kathy, whose unwavering love and support has allowed me to pursue all my passions and dreams in life.

ACKNOWLEDGEMENTS

As I near the conclusion of what has been undoubtedly the most trying, yet rewarding chapter of my life, I have many people to thank. First, I would like to thank my primary graduate school mentor, Sachin Patel. I am thankful for the risk Sachin took on me when he took me into the lab after leaving another lab, and his mentorship kept me pursuing impactful science while still allowing me to pursue the scientific topics that I was most passionate about. This freedom to explore has foundationally shaped me as a scientist and given me a level of independence that I would not have gotten in another lab. Sachin's high standards and willingness to always push new scientific boundaries are what initially drew me to his lab. Ultimately, this environment is what allowed me to push myself to my own high standards and pursue risky yet rewarding scientific endeavors. Sachin departed Vanderbilt during my final year of graduate school for a position as Chair of Psychiatry at Northwestern University. While this was certainly a challenging time for me personally as I remained at Vanderbilt, it is clearly a testament to the caliber of scientist that Sachin is. I am lucky to have trained with Sachin, and will always be grateful for his mentorship.

I would also like to thank my co-mentor, Brad Grueter. During my final year of graduate school, Brad took me into his lab as a "refugee" following Sachin's departure for Northwestern. Truth be told, this last year was one of the most mentally taxing of my life. That said, I was incredibly lucky to have a mentor like Brad to support me through this final leg of my graduate school journey. Brad has consistently been willing to talk about scientific ideas, non-science real life topics, and even just listen to me vent about my own struggles and frustrations that come with the final year of graduate school. Brad is a remarkably talented scientist with whom I share many scientific interests with, and our conversations have been tremendously helpful for both my science and my sanity. He has made me feel I was truly a part of the lab, and his mentorship and support has been instrumental in helping me keep things afloat and push through this past year.

I would also like to thank all my teachers and mentors throughout my earlier years, without whom I would not have made it to graduate school, much less completed a PhD. Firstly, my high school biology teacher, Jennifer Meritt, for her enthusiasm and encouragement during my senior year that ultimately fueled my motivation to pursue neuroscience in college. I had many great mentors during college, but 2 stand out in particular – Lora Becker and Andy Lampkins. Dr. Becker instilled in me my love and passion for neuroscience that has carried me all the way through graduate school. Dr. Lampkins was my first research mentor, and under his mentorship I truly discovered my love for the process of scientific research. I also have to mention Vanderbilt's own Dave Weaver. I spent a summer in Dave's lab doing undergraduate research. Dave gave me a lot of freedom to carry out my own project and was more patient than most when I had no idea what I was doing. This experience forced me to really *think* about the science I was doing and was ultimately what solidified my decision to pursue a PhD.

Lastly, but certainly not least, I want to thank all my friends and family (which of course includes my dog, Buddy). My parents, Dan and Kathy, for always supporting me in pursuing all of my passions, be that music or neuroscience. Thank you to my brothers Dakota and Casey, and sisters Dee, Dande, and Danielle for always cheering me on. To all of the rest of my family and friends, from Evansville to Nashville and beyond, there are too many of you to name everyone but know my love and gratitude to you are unending. Finally, my endless gratitude to my two biggest rocks that get me through each day, Natty and Buddy. My wonderful partner Natty has been unbelievably supportive and patient through the constant existential crisis that is a final year grad student, and I could never fully express my gratitude and love. Finally, Buddy – my dog and son I adopted my first year of grad school when I said I was going to get a fish. This little guy has been my single constant here in Nashville these last 6 years, and although he is mainly concerned with food at all times, he'll never know how much his unconditional love has meant to me and how his insanity has, ironically, kept me sane.

TABLE OF CONTENTS

DEDICATION ..... **ii**

ACKNOWLEDGEMENTS ..... **iii**

LIST OF FIGURES ..... **vii**

LIST OF TABLES ..... **ix**

Chapters .....

I. INTRODUCTION **1**

Preface 1

The Endocannabinoid System: Intersections with Stress and Lateral Habenula Physiology 1

Central Nervous System Physiology of the Endocannabinoid System 1

Endocannabinoid Modulation of Stress 7

Neuromodulation in the Lateral Habenula: The Case for Endocannabinoids 9

Monoamines 11

Corticotropin-Releasing Factor 14

Opioids 15

Endocannabinoids 17

Pharmacology of Phytocannabinoids 20

Δ9-Tetrahydrocannabinol (THC) 21

Cannabidiol (CBD) 23

Snake Oil or Misunderstood Medicine?: Barriers to Navigating the Therapeutic Utility of CBD 25

II. OPPOSING RETROGRADE AND ASTROCYTE-DEPENDENT ENDOCANNABINOID SIGNALING MECHANISMS REGULATE LATERAL HABENULA SYNAPTIC TRANSMISSION **30**

Abstract 31

Introduction 32

Results 33

Discussion 43

Materials and Methods 48

Supplemental Information 55

III. CANNABIDIOL DIFFERENTIALLY MODULATES SYNAPTIC RELEASE AND CELLULAR EXCITABILITY IN THE CENTRAL AND BASOLATERAL AMYGDALA 59

Abstract 60

Introduction 61

Results and Discussion 62

Materials and Methods 70

IV. CONCLUSIONS, LIMITATIONS, AND FUTURE DIRECTIONS 74

Physiology and Functions of the Multicellular Endocannabinoid System in the Lateral Habenula 74

Stress Plasticity in the Lateral Habenula Endocannabinoid System 80

Cannabidiol as a Therapeutic for Stress-Related Neuropsychiatric Disease 82

Summary 85

APPENDIX. TARGETING DIACYLGLYCEROL LIPASE REDUCES ALCOHOL CONSUMPTION IN PRECLINICAL MODELS 87

Abstract 88

Introduction 89

Results 90

Discussion 104

Materials and Methods 109

Supplemental Information 118

REFERENCES 129

LIST OF FIGURES

Figure 1-1: Schematic of Synaptic 2-AG Signaling 3

Figure 2-1: Endocannabinoids Differentially Regulate Glutamatergic and GABAergic Synapses in the Lateral Habenula 36

Figure 2-2: Distinct Inputs to the LHb are Differentially Regulated by Endocannabinoids 39

Figure 2-3: Astrocytic CB1 Receptors Positively Modulate Lateral Habenula Glutamate Release 41

Figure 2-S1, Related to Figure 2-1 55

Figure 2-S2, Related to Figure 2-2 56

Figure 2-S3, Related to Figure 2-3 57

Figure 3-1: Cannabidiol reduces GABAergic synaptic transmission in the CeA 63

Figure 3-2: Cannabidiol has no effect on synaptic transmission in the BLA 65

Figure 3-3: Cannabidiol exhibits cell type-specific modulation of CeA synaptic transmission ... 66

Figure 3-4: Cannabidiol decreases the cellular excitability of BLA and CeA neurons 68

Figure 3-5: Cannabidiol requires action potentials to modulate CeA GABAergic transmission . 69

Figure 4-1: Current model for synaptic functions of the eCB system in the LHb 74

Figure 4-2: Astrocytic CB1 Receptor Deletion Reduces Presynaptic GABA release 78

Figure 4-3: Neuronal DAGLα deletion does not occlude the effect of DAGL inhibition on sEPSC frequency 79

Figure A-1: Genetic deletion of DAGLα reduces voluntary alcohol intake 92

Figure A-2: Pharmacological inhibition of DAGL by DO34 reduces voluntary alcohol intake and produces similar brain lipid profiles in naïve and chronically drinking mice 94

Figure A-3: DO34 decreases EtOH intake across aversion-resistant and chronic intermittent models of EtOH drinking and does not precipitate negative affective phenotypes after chronic

EtOH drinking 98

Figure A-4: DO34 reduces reinstatement of EtOH drinking and does not precipitate negative affective phenotypes during protracted abstinence 102

Figure A-5: DO34 prevents EtOH suppression of posterior VTA GABA transmission 104

Figure A-S1: Chemical synthesis and spectroscopic characterization of (4-{[(2-Methyl-2-propanyl)oxy]carbonyl}-2-phenylpyperazinyl){4-[(4-trifluoromethoxy)phenyl]-1H-1,2,3-triazol-1-yl}metanone (DO53) 118

Figure A-S2: Vehicle treatment does not affect EtOH preference or consumption and DO34 reduces body weight only in male mice 119

Figure A-S3: DO53 treatment has no effect on body weight in female mice 120

Figure A-S4: DO34 does not alter blood ethanol concentrations 120

Figure A-S5: DO34 does not alter sucrose preference and 2-AG augmentation has no effect on EtOH drinking or body weight 121

Figure A-S6: Mice reliably drink quinine-adulterated EtOH and DO34 has variable but minimal effects on total fluid consumption across EtOH drinking models 122

Figure A-S7: DO34 treatment does not precipitate negative affective phenotypes after chronic drinking at 10% EtOH 123

Figure A-S8: DO34 treatment does not precipitate negative affective phenotypes after chronic drinking at 10% EtOH 124

Figure A-S9: EtOH reduces sIPSC amplitude onto putative dopamine neurons in the posterior VTA of DO34-treated slices 124

Figure A-S10: EtOH does not increase 2-AG levels measured by mass spectrometry in midbrain punches containing VTA 125

Figure A-S11: GTEx data on tissue-specific expression of DAGLA and DAGLB expression .. 126

Figure A-S12: GTEx data on the effect of DAGLA genetic variant rs11604261 on relative gene expression 127

LIST OF TABLES

Table A-S1: Detection methods for LC-MS/MS analysis of analytes and deuterated internal standards 128

CHAPTER I

INTRODUCTION

Preface

This chapter contains modified text from 1) a book chapter published in the *International Review of Neurobiology*[1] and 2) a book chapter under review for publication in *Marijuana and Madness, 3rd edition*[2]. The text sections from these chapters included here were authored by me.

The Endocannabinoid System: Intersections with Stress and Lateral Habenula Physiology

Central Nervous System Physiology of the Endocannabinoid System

The endocannabinoid (eCB) system is a broadly expressed, lipid-derived neuromodulatory system that is comprised of the cannabinoid receptors (CB1 and CB2), the eCB ligands (2-arachidonoylglycerol, 2-AG; anandamide, AEA; other minor eCB ligands), and the enzymes responsible for the synthesis and breakdown of the eCB ligands - 2-AG is synthesized postsynaptically via diacylglycerol lipase (DAGL) and primarily degraded presynaptically via monoacylglycerol lipase (MAGL), and to a more minor degree by other catabolic pathways, whereas AEA is synthesized postsynaptically via N-acyl phosphatidylethanolamine-specific phospholipase D and primarily degraded postsynaptically via fatty acid amide hydrolase[3]. The study of *Cannabis*-derived phytocannabinoid compounds, predates the discovery of the eCB system – the structures and stereochemistry of THC and CBD were first described in 1960s[4,5], whereas the first cannabinoid receptor (CB1) was functionally described in 1988[6] and cloned in 1990[7]. Indeed, the eCB system was largely discovered via efforts to elucidate the biological mechanisms subserving the psychotropic effects of the phytocannabinoid Δ^9-THC, discussed in the previous section of this chapter. Early hypotheses regarding the mechanism of THC posited that the highly hydrophobic nature of phytocannabinoid compounds led them to act by non-

specifically disrupting cellular membrane properties[8]. Later studies observed that the actions of THC and cannabimimetic compounds were stereoselective[9], drove cellular responses characteristic of a G protein-coupled receptor (GPCR)[10], and required active Gi proteins[11], suggesting cannabinoids exerted their effects through a selective GPCR and this was later confirmed via the cloning of CB1[7]. These seminal studies laid the foundation for the existence of the eCB system and catalyzed the continuously expanding field of study aimed at understanding eCB system physiology.

The eCB system is heavily expressed in the central nervous system (CNS) and has a variety of functions in other tissues as well, including in the gastrointestinal tract, cardiovascular system, reproductive organs, and various immune cells, among others. For the purposes of this chapter, we will focus on eCB functions within the CNS. Generally, eCBs act as retrograde signaling molecules that diffuse from the postsynaptic compartments of neurons to activate presynaptic cannabinoid receptors that act to decrease neurotransmitter release probability. In brief, eCBs are synthesized from lipid precursors within the postsynaptic compartment of neurons and travel retrogradely to activate presynaptic CB1 receptors that, in turn, reduce neurotransmitter release through a number of defined biochemical mechanisms. The CB1 receptor is a Class A GPCR and the most abundant GPCR in the brain (CB2 expression in the brain is low)[12,13]. CB1 couples to canonical Gi/o signaling mechanisms and reduces neurotransmitter release by activating presynaptic potassium channels, inhibiting presynaptic voltage-gated calcium channels, and reducing adenylate-cyclase and protein kinase A activity[3,14,15]. Collectively, the eCB system serves as a negative feedback loop at the synapse, and can be recruited in either a tonic or phasic (i.e., constitutive or on-demand) manner to regulate the efficacy of synaptic transmission (For reviews, see Refs. [3] and [16]). A schematic of synaptic 2-AG signaling (AEA omitted for clarity and relevance to the research in Chapter II) is provided below in **Figure 1-1**.

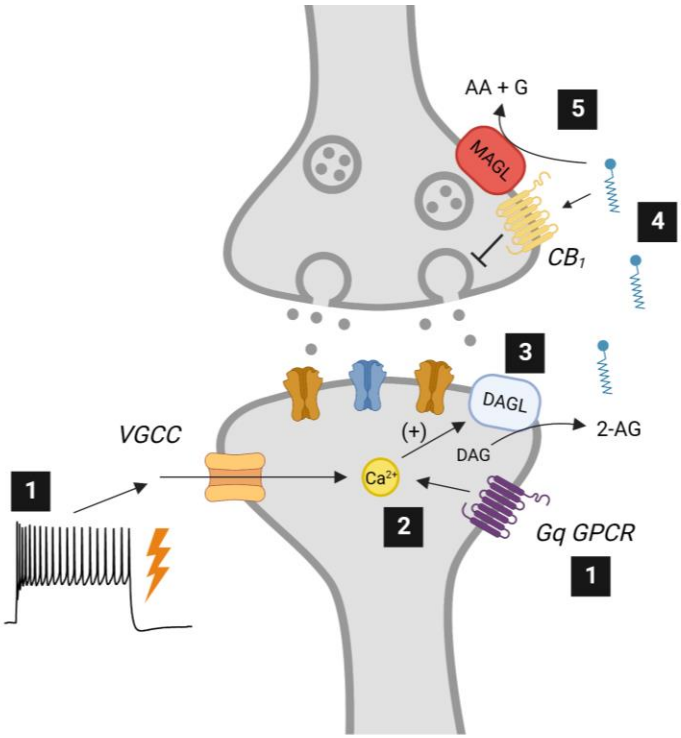

Figure 1-1: Schematic of Synaptic 2-AG signaling. 1) Increased postsynaptic activity and opening of voltage-gated Ca2+ channels (VGCCs) or activation of Gq GPCRs lead to **2)** increases in postsynaptic Ca2+ levels (Ca2+-independent forms of GPCR-driven 2-AG mobilization exist as well[3]. **3)** Increased Ca2+ levels stimulate the activity of DAGL, leading to the synthesis of 2-AG from diacylglycerol (DAG). **4)** 2-AG moves retrogradely across the synapse to activate presynaptic CB1 receptors and decrease neurotransmitter release. **5)** The 2-AG signal is terminated via hydrolysis of 2-AG molecules by MAGL to yield arachidonic acid (AA) and glycerol (G). Schematic created with Biorender.com.

The depth and complexity of the signaling mechanisms engaged by the eCB system is vast and the field is continuously expanding. For example, we will discuss CB1 receptor signaling mechanisms that extend beyond canonical Gi/o signaling at the presynaptic terminal. At the level of G proteins, CB1 has been shown to couple to couple to both Gs[17,18] and Gq[19] proteins under some conditions, although it is unclear what the direct physiological effects of these transduction mechanisms may be. The signaling of CB1 can also be modulated by a number of interacting proteins, including other GPCRs which may heterodimerize with CB1 influence its pharmacology and signal transduction. Reported heterodimerization partners for the CB1 include the μ opioid[20], dopamine D2[21], and adenosine 2A receptors[22,23], among others. Other non-GPCR proteins that

interact with and modulate CB1 have been described as well, such as cannabinoid receptor interacting protein 1a (CRIP1a), which binds to the C-terminus of CB1 to modulate receptor properties such as G protein coupling, constitutive activity, and cell surface expression[24,25]. Beyond the level of modulating molecular signals from the receptor, CB1 has been shown to be active in a number of cellular compartments outside of the presynaptic terminal of the neuron. For example, some cortical neurons exhibit a slow self-inhibition mediated by autocrine 2-AG signaling onto postsynaptic CB1 receptors to trigger G protein-activated inward-rectifier potassium (GIRK) channel conductance and hyperpolarization[26-28], thereby inhibiting cellular excitability via a unique postsynaptic CB1 mechanism. CB1 has also been described to exhibit intracellular (i.e., non-plasma membrane) signaling mechanisms, most notably being the description of CB1 on mitochondrial membranes, where it modulates bioenergetic metabolism in neurons[29]. CB1 activation on mitochondria negatively regulates cellular respiration, and this effect has been linked to the amnesic effects of cannabinoids[30]. Surprisingly, mitochondrial CB1 has been demonstrated to decrease synaptic release in some brain areas[31], a function conventionally ascribed to plasma membrane cannabinoid receptors. Of note, CB2 receptors also exhibit intracellular localization in brain tissue[32] (note - this study does not specify mitochondria) and mitochondrial cannabinoid receptors have been reported in other tissues as well[33]. CB1 receptors are also localized on non-neuronal cells in the CNS, most notably on astrocytes, discussed below.

Astrocytic eCB signaling is a rapidly emerging area of interest in the field[34,35]. CB1 receptors have been identified on astrocytes, and astrocytes respond to eCBs by mobilizing calcium to drive gliotransmitter release which can act on receptors present at the synapse[36,37]. For example, activation of CB1 receptors on astrocytes in the CA1 region of the hippocampus can potentiate glutamate release onto neurons via a mechanism involving presynaptic metabotropic glutamate receptor 1[37]. Other studies have and continue to identify similar signaling mechanisms, with the specific gliotransmission systems and synaptic effects varying by brain region. The behavioral

functions of glial eCB signaling remain poorly understood. One recent study identified that CB1 activation in the medial central amygdala (CeM) enhances synaptic GABA release and suppresses synaptic glutamate release, and activation of these astrocytes inhibits CeM neuron activity and suppresses the expression of learned fear[38]. Future studies will be needed to refine our understanding of glial eCB mechanisms in complex behaviors. At the cellular level, the signal transduction mechanisms mediating the effects of CB1 in astrocytes are not well defined – the presumed mechanism is a differential coupling of CB1 to Gq in astrocytes. This notion is supported by the evidence that eCB-elicited astrocytic Ca^{2+} signals and subsequent synaptic signaling require phospholipase C[36] and inositol 1,4,5-triphosphate (IP3) receptors[38] and are insensitive to pertussis toxin, an inhibitor of Gi/o proteins[37]. However, this assumption has not been experimentally validated via biochemical inhibition of Gq signaling or direct demonstration of Gq recruitment by CB1 in astrocytes. There is a pertussis toxin-insensitive member of the Gi/o subfamily, Gz[39], which is enriched in brain tissue[40,41]. Furthermore, Gi/o signaling in astrocytes can also mobilize Ca^{2+} signals[42], further complicating this assumption. Furthermore, one report has demonstrated that mitochondrial CB1 in astrocytes is required for eCB lateral potentiation in the hippocampus, for which the G protein signal transduction are not defined[43]. Further studies are needed to definitively elucidate the details of these mechanisms.

The complex physiology of the eCB system ultimately manifests in the dynamic regulation of myriad behaviors and physiological processes. While eCB regulation of stress and anxiety is a major function of eCB signaling, it is discussed in greater detail in the next section of this chapter and is therefore omitted from this section. A select number of other behavioral functions of eCBs are highlighted below:

- *Regulation of pain.* It is well documented that administration of exogenous cannabinoids leads to analgesia[44], suggesting a role for eCB signaling in modulating pain. Indeed, eCBs modulate pain processing at several levels. Peripheral nociceptive neurons express cannabinoid

receptors and both CB_1 and CB_2 receptors have been implicated in modulating peripheral pain processing[45-47]. The eCB system is also present in the spinal cord[48] and can modulate spinal pain transmission – intrathecal injection of cannabinoids produces analgesia[49] and spinal cord eCB levels increase in neuropathic pain states[50]. Finally, eCBs exhibit supraspinal mechanisms of pain modulation as well. eCB signaling within several brain areas, including the periaqueductal gray and rostral ventromedial medulla can promote analgesia via regulation of descending pain pathways[51]. See Refs. [52] and [53] for further reviews of eCB regulation of pain.

- *Regulation of sleep*. THC has sleep-promoting effects[54] and improved sleep quality is often reported as a motive for cannabis use[55], suggesting a role for the eCB system in natural sleep regulation. Indeed, brain eCB levels exhibit diurnal fluctuations in rodents. AEA and 2-AG show an inverse relationship in this context, with AEA levels highest during the dark (wakeful) phase, and 2-AG levels highest during the light (sleeping) phase[56]. Consistent with this, augmenting 2-AG levels by pharmacological inhibition of MAGL promotes some subtypes of sleep[57]. Similar observations have been made in humans as well – serum AEA levels were highest at waking and lowest before the onset of sleep in a small set of human subjects[58]. Further studies in rodents have begun to identify eCB-mediated mechanisms modulating the activity of brain areas involved regulating sleep and circadian rhythmicity, such as the suprachiasmatic nucleus[59,60], although how these mechanisms directly regulate sleep remains incompletely understood. See Ref. [61] for further review of eCB regulation of sleep.

In addition to these highlighted functions, the eCB system is involved in a variety of other behavioral functions as well, including (but not limited to) feeding behavior[62], learning and memory[63], and addiction[64]. Collectively, the eCB system is a complex neuromodulatory signaling system that plays pivotal roles in brain physiology and behavioral output. Further characterization

of the complex biology of this system and ongoing therapeutic development efforts will likely be synergistic in better leveraging the eCB system for the treatment of a wide range of disorders.

Endocannabinoid Modulation of Stress

Regulation of the physiological and behavioral response to stress is one of the most heavily studied functions of the eCB system. Central to the biological response to stress is the activation of the hypothalamic-pituitary-adrenal (HPA) axis. In brief, environmental stress leads to the activation of neurons in the paraventricular nucleus (PVN) of the hypothalamus, which release vasopressin and corticotropin-releasing factor (CRF) into portal vasculature. Vasopressin and CRF then stimulate cells in the pituitary to release adrenocorticotropin-releasing hormone (ACTH), which reaches the adrenal gland via the blood and stimulates adrenal cells to release glucocorticoids into systemic circulation (cortisol in humans and corticosterone in laboratory rodents) to mediate myriad physiological responses related to alterations in metabolic activity and immune function[65]. The eCB system has been intimately linked to the function of the HPA axis on several distinct levels. eCB involvement in HPA axis activity is made readily apparent by the observation that systemic antagonism of CB1 receptors is sufficient to elevate serum corticosterone levels[66,67]. A large body of work has identified that the eCB AEA likely mediates these observations – stress broadly decreases AEA levels in several brain areas[68,69], and blockade of AEA hydrolysis diminishes HPA axis activation[66,70]. These observations have collectively set forth a model by which tonic AEA signaling in corticolimbic brain circuitry acts as a “gatekeeper” to actively constrain HPA axis activity in the absence of environmental stress, and that stress-mediated reductions in AEA signaling are an important molecular event in the initiation of the stress response[71]. The other major brain eCB molecule, 2-AG, has also been linked to HPA axis function and is considered a critical mediator of HPA axis termination. In contrast to the effects of stress on AEA, stress drives increases in 2-AG levels across several brain areas[72,73]. In some brain areas, such as the medial prefrontal cortex, these changes occur on a more delayed

timescale than observed for reductions in AEA[72]. This is due to the requirement for glucocorticoid signaling to drive these elevations in 2-AG, as glucocorticoid receptor antagonism can inhibit 2-AG recruitment by stress[72] and corticosterone administration can elevate 2-AG levels in the absence of overt stress[74]. Furthermore, 2-AG levels have been shown to correlate with corticosterone after stress[75], and CB1 receptor antagonism can impair feedback inhibition of HPA axis activity[73] and potentiate and prolong the stress response[66,76], further supporting a role for 2-AG in terminating the stress response. Collectively, both AEA and 2-AG signaling play pivotal roles in modulating the central physiological effects of stress.

The role of eCB signaling in regulating the stress response has been established and further extended to be critical in buffering against the adverse effects of stress exposure. Excessive stress, or a lack a resiliency to stress, can manifest in the form of stress-related neuropsychiatric disorders, such as anxiety, posttraumatic stress disorder, and depression[71]. Given that eCB signaling, particularly 2-AG signaling, is critical for modulating the magnitude of and terminating the stress response, it follows that impairments in 2-AG signaling lead to enhanced susceptibility to the negative consequences of stress. Indeed, genetic depletion of 2-AG synthesis results in basal anxiety phenotypes[77] and dramatically increases susceptibility to stress in laboratory rodents[78]. Similar stress susceptibility effects are observed with pharmacological inhibition of 2-AG synthesis as well[78]. Individual basal differences in the efficiency of 2-AG signaling in limbic circuitry have been found to correlate with stress resiliency[78], and stress-induced disruptions of 2-AG control over corticolimbic connectivity have been implicated in the manifestation of anxiety[79]. Accordingly, there is robust preclinical evidence for the pharmacological augmentation of eCB levels as an effective means to promote stress resiliency and mitigate anxiety-like phenotypes[75,78,80], and thus there is much interest in targeting the eCB system for novel anxiolytic drugs[81]. Taken together, the eCB system presents a critical substrate for stress regulation and a compelling potential biological correlate for stress susceptibility and related affective pathology.

Future studies will likely answer the lingering hypotheses surrounding the druggability of the eCB system for the treatment of stress-related neuropsychiatric disorders.

Neuromodulation in the Lateral Habenula: The Case for Endocannabinoids

The lateral habenula (LHb) is an evolutionarily-conserved epithalamic brain structure that presents a critical node in the brain's broader stress-response network. The habenular complex, which includes the LHb along with the medial habenula (MHb), is an ancient brain structure that maintains a remarkably high degree of similarity across vertebrate species with regards to anatomy, general functions, and neural circuitry[82]. The LHb is well-positioned to regulate a diverse array of physiological and behavioral functions, owing to its circuitry acting as an integrative hub between a variety of forebrain inputs and midbrain monoamingeric centers. More specifically, the LHb is a midpoint nucleus in the diencephalic conduction system - the LHb receives diverse afferent input from limbic forebrain and basal ganglia structures[83,84] and relays that information flow to control the activity of midbrain monoamingeric centers, broadly regulating the activity of dopamine and serotonin systems across the brain[84]. Enhanced LHb activity is generally correlated with reductions in the activity and in dopaminergic and serotonergic neurons. The LHb is largely comprised of glutamatergic projection neurons[85] and achieves its inhibitory influence over dopamine and serotonin neurons via disynaptic feedforward inhibition mechanisms, most notably via excitation of GABAergic neurons of the rostromedial tegmental nucleus (RMTg), which then project to and inhibit DA and 5-HT neurons in the ventral tegmental area/substantia nigra[86] and raphe nuclei[87], respectively. Direct projections to monoaminergic nuclei exist as well[87,88], and these projections synapse onto both principal monoamine neurons and local GABAergic interneurons[89-91]. One report has also identified direct LHb excitation of medial ventral tegmental DA neurons that project to the medial prefrontal cortex, and activation of this projection elicits aversion[88]. This global negative control of the brain's monoamingeric networks results in the myriad functions of the LHb.

Among the most extensively studied functions of the LHb is its role in processing aversive environmental stimuli and negative reward. Indeed, owing in part to its negative constraint on midbrain reward circuitry, the LHb has been aptly suggested to be the brain's "anti-reward center"[92]. The LHb is highly responsive to diverse types of noxious stimuli, including (but not limited to) electrical foot shock, forced oral delivery of bitter tastants (e.g., quinine), and attack from social aggressors[93,94]. The LHb is also activated following the omission of expected reward (negative reward prediction error)[95,96] and is inhibited by unexpected reward presentation[95] or reward anticipation[97]. In line with its role in processing aversive stimuli, activation of the LHb in the absence of overt external stimuli is sufficient to drive an aversive-like state. Optogenetic activation of numerous afferent inputs to the LHb is aversive, including terminals from the lateral preoptic area (LPO)[98], entopeduncular nucleus (EPN)[99], or lateral hypothalamic area (LHA)[100], among others. Moreover, electrical stimulation[101] or optogenetic induction of burst firing activity[102] also produce a similar stress- or aversion-like state, and depressive-like behaviors are reversed by chemogenetic inhibition of LHb neurons[103] or ketamine inhibition of burst firing[102], further demonstrating the function of the LHb in encoding aversion. Lastly, although a somewhat poorly-defined relationship, there are several lines of evidence that suggest the LHb exerts regulatory control over the HPA axis[104-106], further establishing the role of the LHb and as a crucial component of the brain's stress response system.

Given the prominent role of the LHb in coding an aversive state, it follows that dysregulation and aberrant activity of the LHb have been associated with numerous neuropsychiatric disorders, most notably depression[107]. Indeed, LHb dysregulation has been observed across numerous animal models of depression[102,108,109] and observed in neuroimaging studies of humans presenting with symptoms of clinical depression[110]. Exposure to environmental stressors results in numerous physiological adaptations within the LHb, which has been proposed as a component of the pathophysiology of depression. Learned helplessness models in rodents exhibit enhanced

excitatory transmission onto LHb neurons, enhanced LHb neuron firing rates[111], and an increased proportion of LHb neurons with a tonic burst firing phenotype[102]. Cannulation of ketamine into the LHb reverses the aforementioned burst firing phenotype and alleviates the expression of depressive-like behaviors in rodents[102], positing the LHb is a potential cellular substrate for the antidepressant effects of ketamine. Collectively, a growing body of evidence supports the role of dysregulated LHb activity in mediating neuropsychiatric disease states.

Despite the increasingly evident role of the LHb in neuropsychiatric disease and our advances in understanding these mechanisms over the past two decades, a molecular understanding of the neuromodulatory signaling systems that ultimately shape and orchestrate LHb activity remain poorly understood. Numerous descriptive anatomical studies over the years have reported the expression of the molecular machinery (e.g., modulatory GPCRs) for known neuromodulatory systems in the LHb. However, despite their likely involvement in disease pathophysiology and high potential for druggability, few studies have interrogated the functionality of these systems with regards to their influence of synaptic and cellular activity in the LHb. There is likely a high degree of crosstalk between these systems, highlighting the importance of a holistic understanding of the broader LHb neuromodulatory signaling network. In the sections below, I will summarize relevant components of the sparse information surrounding what is known about a select number of these systems in the LHb, with a final emphasis on the eCB system and the foundational information that was the basis of the hypotheses explored in the research presented in Chapter II of this thesis.

Monoamines

Monoamines are aminergic amino acid-derived neuromodulatory signaling molecules, most notably dopamine, serotonin, and norepinephrine. These systems consist of their loci in midbrain structures and send projections widely across the brain, including to the LHb, to modulate a plethora of physiological and behavioral functions. Although there has been much focus on

understanding the role of the LHb in negatively regulating the activity of the brain's monoamine centers, several lines of evidence have demonstrated that the LHb itself is subject to direct reciprocal regulation via monoamine signaling.

There is evidence for tyrosine hydroxylase(+) terminals[112] and both dopamine (DA) D1- (D5[113]) and D2-like (D2[85], D4[112]) receptor expression in the LHb. Systemic DA agonists enhance LHb neuron firing[114] and local elevation of dopamine levels in the cat LHb[115] were shown to decrease downstream serotonergic output (an expected consequence of LHb excitation), supporting a role for endogenous DA signaling in the LHb. Furthermore, there is both physiological and behavioral evidence for the functionality of specific DA receptor subtypes in the LHb as well. D4 receptor activation promotes the activity of LHb neurons via both pre- and postsynaptic mechanisms[112]. Behaviorally, local manipulations of both D1- and D2-like DA receptors in rodents were shown to produce distinct effects on anxiety- and depressive-like behaviors and on aversive processing[116,117]. The LHb receives direct synaptic input from the VTA[118], which was posited as the most likely source of local dopaminergic innervation. Interestingly, no dopamine release from this projection has been detected[118] despite some cells expressing tyrosine hydroxylase[118,119]. Instead, this projection has been shown to co-release glutamate and GABA[120] with a stronger relative GABAergic component, resulting in net LHb inhibition and positive reinforcement[121]. Notably, one study has identified that the aforementioned D4 receptors are able to be activated by endogenous norepinephrine[122], proposing the intriguing possibility that norepinephrine could be responsible for LHb DA receptor activity. Further studies are needed to disentangle whether there is endogenous DA release in the LHb or this system is under the control of norepinephrine, as well as define its functional relevance in LHb physiology.

While still incompletely understood, serotonergic signaling in the LHb is better characterized relative to DA. LHb receives input from the dorsal raphe nuclei, and there is functional evidence for the release of serotonin (5-HT; 5-hydroxytryptamine) from this input[123]. More specifically, one

study demonstrated that continuous optogenetic excitation of dorsal raphe terminals in the LHb inhibited excitatory transmission onto LHb neurons via a 5-HT_{1B} receptor-dependent mechanism, and activation of this input produces and antidepressant-like effect[123]. One potential circuit target mediating these effects is the entopeduncular nucleus (EPN), from which excitatory transmission to the LHb is directly inhibited by serotonin[99]. Logically in line with this, intra-LHb 5-HT_{1B} receptor activation has been shown mitigate the anxiogenic effects of cocaine[124]. In contrast, bath application of 5-HT has broad and heterogeneous effects on glutamatergic input to LHb neurons, with cells showing increased or decreased presynaptic glutamate release[125]. These mixed observations can likely be attributed to different subtypes of 5-HT receptors in the LHb, which will be simultaneously engaged upon 5-HT bath application. Indeed, this study reported the involvement of 5-$HT_{2/3}$ receptors in the potentiating effects of 5-HT on glutamate release observed onto some cells[125]. Across the LHb, numerous subtypes of 5-HT receptors are expressed[126], with the 5-HT_{2C} receptor being particularly enriched in LHb neurons[85]. Future studies should further elucidate the contributions of distinct 5-HT receptor subtypes to regulating LHb synapses and output and the endogenous function of 5-HT modulation in the LHb.

The least studied and most poorly understood monoamine neuromodulator the LHb is norepinephrine (also referred to as noradrenaline). There is some evidence to suggest a noradrenergic innervation of the LHb by the locus coeruleus[127,128]. This is further supported by observations that electrical lesions of fiber tracts containing noradrenergic fibers originating from the locus coeruleus result in significant reductions in LHb norepinephrine tissue content[129]. At this time, there are no available reports of functional adrenergic receptors in LHb neurons. Interestingly, as mentioned above, norepinephrine can activate DA D4 receptors in the LHb, positing these receptors as a potential postsynaptic target for endogenous noradrenergic tone in the LHb[122]. This same study showed that inhibition of the DA transporter results in D4 receptor activation, with a substantially smaller effect following inhibition of the norepinephrine transporter,

suggesting that norepinephrine clearance in the LHb may occur primarily via the DA transporter. Beyond these studies, information on the physiological and behavioral functions of norepinephrine in the LHb is remarkably sparse. One study has reported that reduction of norepinephrine tone in the LHb via cannulations of an α2 adrenergic autoreceptor agonist (presumably inhibiting presynaptic norepinephrine release) decreased anxiety-like and ambulatory behavior[130], potentially owing to the excitatory actions of D4 receptors on LHb neuron activity[112]. The dearth of data on the functionality of noradrenergic innervation of the LHb renders it difficult to draw any causal conclusions from these studies, and a great deal of additional research is needed to convincingly establish a function for this modulatory system in the LHb.

Corticotropin-Releasing Factor

Corticotropin-releasing factor (CRF) is a peptide hormone most heavily studied for its signaling role in HPA axis function[131]. However, there is also an abundance of extrahypothalamic CRF that is expressed in numerous brain areas where it actively regulates many other aspects of neural circuitry related to the brain's stress response network with numerous implications for affective disorders and addiction[132-135], conditions which may be heavily influenced by the LHb[84]. Anatomical evidence suggests the presence of the CRF system within the LHb, based on immunoreactivity or reporter systems for both CRF peptide[136] and the type 1 CRF receptor (CRF1)[137-139]. Intriguingly, despite this anatomical evidence and intersectional implications of both CRF signaling and the LHb in neuropsychiatric disease, only one study to-date has addressed the function of CRF in LHb physiology[140]. Using *ex vivo* brain slice electrophysiology in rats, this study found that exogenous application of CRF to LHb brain slices caused a significant increase in the intrinsic excitability of LHb neurons, and this effect was dependent on CRF1 (a Gs-coupled GPCR) and protein kinase A (PKA) activation to have downstream effects on potassium channel activity. Furthermore, they showed that CRF application caused a selective reduction in presynaptic GABA release (with no effect on glutamate) onto LHb neurons that was mediated via

eCB signaling. Although this study did not provide any *in vivo* data addressing LHb CRF effects on behavioral output, they did find that a maternal deprivation model significantly increased LHb cellular excitability and this was mediated by enhanced PKA signaling tone. Furthermore, they found that the maternal deprivation model blunted the effects of CRF application on further increasing excitability, suggesting the possibility that this system may already be engaged by this stressor and thereby occlude further potentiation by CRF. Future studies should address whether CRF mobilization could be a mechanism engaged by stress to drive increased LHb activity following aversive experience, and what role this system might play in long-term LHb plasticity and disease pathophysiology. These questions could provide substantial translational value, particularly given the broader interest in pharmacologically antagonizing CRF1 for the treatment of affective and addiction-related disorders[141-143].

Opioids

The opioid system is a neuropeptide system with myriad physiological and behavioral functions, largely comprised of the mu, kappa, and delta opioid receptors and their cognate peptide ligands. There is evidence for the expression of both the mu[144,145] and kappa[146] opioid receptors in the LHb. Moreover, it is well established that the mu and kappa opioid systems are major regulators of both normal and pathological brain functions that overlap with many ascribed functions of the LHb[84], yet these systems remain largely unexplored in LHb physiology. These include functions such as pain[147-149], addiction[150,151], and affective disorders[150,152]. Both receptors are Gi/o-coupled GPCRs with largely inhibitory functions, but can be expressed both pre- and postsynaptically, leading to their rather complex neuromodulatory functions across the brain[149]. Indeed, sparse reports have demonstrated both pre- and postsynaptic actions of these receptors the LHb, discussed below.

The mu opioid receptor is the canonical opioid receptor associated with opioid analgesia and is the primary molecular target of opioid drugs, such as morphine[147]. Direct cannulation of

morphine into the LHb is sufficient to produce analgesia in some contexts[153,154]. Interestingly, this morphine-induced analgesia is not accompanied by manifestation of overt reward as is seen in other areas of the brain[153], suggesting there may be distinct neurocircuitry involved in LHb analgesia. The reported actions of the mu receptor on LHb neurons are rather complex – mu receptor activation hyperpolarizes only a subset of LHb neurons (a postsynaptic effect)[155], which could potentially be explained by its sparse expression in the LHb, relative to the neighboring medial habenula[145]. Mu receptor activation was also shown to have mixed effects on inhibiting both presynaptic glutamate and GABA release onto some LHb neurons[155]. The cellular or molecular traits that differentiate this heterogeneous synaptic response to mu opioid receptor activation remain to be determined. A later study found that the mu receptor exhibits circuit specificity with regard to the inhibition of presynaptic glutamate release, with the strongest inhibitory control of glutamate release from the LPO across the six inputs examined in the study[153], positing the LPO-LHb circuit as a potential novel cellular substrate for morphine analgesia. Another intriguing observation regarding the mu opioid receptor in the LHb is its necessity for the antidepressant effects of ketamine in rodents[156]. Ketamine has been shown to reduce burst firing activity in LHb neurons, and this has been proposed as one potential cellular mechanism subserving the rapid antidepressant effects of the drug[102]. The report by Klein *et al*. demonstrated the inhibition of mu opioid receptors blocked both the antidepressant effects of ketamine as well as its ability to reduce LHb activity, as shown by *ex vivo* calcium imaging[156]. The mechanism of this interaction is not understood but suggests a potentially complex interaction between the mu opioid system and glutamatergic transmission in the LHb, given the NMDA receptor antagonist actions of ketamine. A deeper understanding of mu opioid receptor function in the LHb could facilitate the development of less addictive analgesics and provide a mechanism to titrate the efficacy of antidepressants such as ketamine.

With regards to the kappa opioid receptor, only a single study has addressed its function in the LHb[157]. This study identified a bidirectional effect of kappa opioid receptor activation on cellular excitability, with two populations of cells responding in opposite directions. The differentiating factor between these opposing-response cell populations was found to be the presence or absence of cation currents mediated by hyperpolarization-activated, cyclic nucleotide-gated cation (HCN) channels. HCN current(-) cells showed decreased excitability after kappa receptor activation whereas cells that were HCN current(+) showed strongly increased excitability. The excitability changes induced by kappa opioid receptor activation required intact synaptic transmission, suggesting that modulation of synaptic release mediates these effects rather than changes in intrinsic membrane excitability. Accordingly, kappa receptors depressed glutamate release onto LHb neurons and exhibited a bidirectional effect on GABA, decreasing GABA release onto most cells but potentiating it onto a small subset of cells. Finally, a maternal deprivation model was able to completely occlude all kappa receptor effects on LHb neuron excitability, suggesting that this system may be dysregulated *in vivo* as a result of stress exposure. The findings of this study lay a basic framework for kappa receptor functions in the LHb and warrants further investigations as a potentially critical mediator of the LHb stress response.

Endocannabinoids

The eCB system presents one of the most intriguing neuromodulatory regulators of LHb functions, based on a series of sparse but surprising observations. The eCB system has been extensively outlined in previous sections, and as such only specific applications to the LHb will be addressed here. Electron microscopy has revealed heterogeneous expression of the CB1 receptor within the LHb. CB1 receptors are present on both excitatory and inhibitory axon terminals, postsynaptic dendritic compartments, mitochondria, and astrocytic membranes[158]. This anatomical information proposes a complex, multicellular role for eCB signaling within the LHb. Behaviorally, local eCB manipulations present intriguing findings – intra-LHb blockade of CB1

receptors produces an anxiolytic- and antidepressant-like effect in rodents, whereas CB1 activation produces a mild anxiogenic effect[158]. This is surprising given the stark contrast with systemic or limbic modulations – as outlined in greater detail in an earlier section, pharmacological or genetic blockade of eCB signaling generally promotes an anxiogenic or stress-susceptible phenotype[77,78,159]. Adding to the puzzling nature of these findings, eCB molecules in the LHb display a dynamic pattern in response to stress that mirrors that of some brain areas wherein eCB disruption is anxiogenic, such as the medial prefrontal cortex[79] – acute restraint stress exposure results in a delayed increase in LHb 2-AG levels after restraint[158] (a temporal 2-AG response that aligns with several corticolimbic brain structures[71]), with no significant effect on AEA levels[158]. Given these paradoxical behavioral observations along with the diverse LHb CB1 expression pattern and 2-AG recruitment by stress, how does the eCB system work to orchestrate LHb activity in a manner that may promote a stress-like phenotype?

A small number of studies have addressed some aspects of the physiological effects of CB1 receptor signaling in the LHb. However, they are not systemically focused on eCB regulation of LHb activity and do not provide the information needed to propose a mechanistic explanation for the antidepressant effects of intra-LHb CB1 blockade[158]. The first report of eCB system functionality in the LHb was a study exploring group I metabotropic glutamate receptor(mGluR)-driven long-term depression (LTD) of excitatory and inhibitory transmission onto LHb neurons[160]. This study found that group I mGluR activation resulted in LTD of both systems, but that only LTD of glutamate was dependent on eCB signaling at CB1 receptors. More specifically, mGluR1 activation mobilized eCBs to produce LTD at glutamatergic synapses, and this required the activity of postsynaptic protein kinase C. Further supporting CB1 receptor regulation of LHb glutamate release, application of the cannabinoid agonist WIN-55,212-2 suppressed electrically-evoked glutamate release, but the study did not address whether CB1 activation suppressed GABA release[160]. A later study from another group found that low-frequency stimulation elicited a

similar eCB-dependent LTD of glutamate release, and this eCB-dependent LTD was disrupted 24 hours after a single acute stress exposure[161]. The mechanism subserving this LTD disruption was found to be expressed postsynaptically via an upregulation of both α and β calcium/calmodulin-dependent protein kinase II (CaMKII) and could be reversed by CaMKII inhibition[161]. CaMKIIα has been shown to inhibit DAGL[162], which suggests that impairment of 2-AG synthesis underlies the stress-mediated LTD disruption[161]. One other study has reported CB1 receptor functionality at LHb synapses. The study addressed in the above section on CRF found that CRF application to LHb slices selectively depressed GABA, but not glutamate release via mobilization of eCBs and activation of CB1 receptors[140]. This is a contrast with the previous report that found that LTD of glutamate, but not GABA, was eCB-dependent[160], but it is important to consider the non-systematic nature of these reports as they did not simultaneously examine eCB control of both systems.

Two additional studies have reported behavioral modulations mediated via the LHb eCB system as well. Pharmacological augmentation of 2-AG or direct CB1 receptor activation was found to decrease alcohol intake in rodents[163]. Similar to the effects on anxiety- and depressive-like behaviors, LHb eCB modulations in this context produce phenotypes opposite to those elicited systemically – genetic or pharmacological *depletion* of systemic 2-AG signaling was found to reduce alcohol intake[164], directly opposing the results from LHb manipulations[163]. This study also found that intra-LHb eCB-CB1 signaling produced an analgesic effect, and blockade of LHb CB1 receptors exacerbated hyperalgesia associated with alcohol withdrawal[163]. The analgesic effects of intra-LHb CB1 activation are similar to those seen with local mu opioid receptor activation[153,154], suggesting there may be overlap between these systems within the LHb in the context of pain regulation. The activity of LHb CB1 receptors has also been shown to promote impulsive-like behavior in the context of cocaine seeking[165]. This study found that intra-LHb CB1 receptor blockade prevented effects of both cocaine and THC on enhancing premature responding in serial

reaction time and Go/NoGo cocaine-seeking tasks[165]. It is important to consider that these studies assessing LHb eCB signaling contributions to alcohol and cocaine-related behaviors address different domains of drug-seeking behavior (i.e., free self-administration vs. impulsivity in operant responding), but collectively suggest that the LHb eCB system may have complex influences on drug intake that may be substance-dependent.

These observations collectively present a strong case for the need for systematic investigation into how the eCB system regulates synaptic transmission in the LHb. A functional framework for how the eCB system orchestrates LHb activity could have broad implications for neuropsychiatric disorders, the subjective effects of exogenous cannabinoids, and the broader range of physiological and behavioral functions under LHb control[84]. How do eCBs control excitation-inhibition balance onto LHb neurons? What is the function of the distinct multicellular pools of CB1 receptors in the LHb (e.g., postsynaptic or astrocytic CB1 receptors)[158]? These unanswered questions form the basis for the hypotheses addressed in the research presented in Chapter II of this thesis.

Pharmacology of Phytocannabinoids

"Phytocannabinoid" generally refers to a broad class of bioactive and chemically-diverse compounds derived from plants of the genus *Cannabis*. *Cannabis*, also known as marijuana, is among the most widely used substances globally with human use dating back to 500 BC[166]. *Cannabis* is used largely for its medicinal and psychotropic effects. Purported medicinal uses for *Cannabis* include treatment of pain[167], anxiety[168], nausea (particularly in association with chemotherapy)[169], gastrointestinal irritability[170], and sleep abnormalities[61], among others. Furthermore, recreational use is widespread globally, lending to the aforementioned psychotropic properties of *Cannabis* that produce a "high" for users as well as for self-use for medicinal applications. This litany of applications for *Cannabis* has stimulated a multi-billion dollar industry in the United States[171], where it remains a Schedule I controlled substance at the federal level.

The *Cannabis* plant contains a plethora of phytocannabinoids, of which >100 have been identified[172]. Most notably among these are Δ^9-tetrahydrocannabinol (THC) and cannabidiol (CBD). THC is the primary psychoactive constituent of *Cannabis* and is responsible for the "high" experienced by *Cannabis* users. THC exerts its effects primarily through partial agonism of type-1 cannabinoid (CB1) receptors[173-176], whereas CBD is non-psychoactive and exerts its effects through complex polypharmacology that engages a variety of different molecular targets[177,178]. A majority of the therapeutic indications for *Cannabis* have been attributed to the actions of THC at cannabinoid receptors. However, there has been growing interest in the potential therapeutic applications of CBD given its purported effectiveness at treating a number of conditions and its desirable lack pf psychotropic activity[179]. In the sections below, I will review the basic pharmacology of THC and CBD, leading into a discussion around the barriers to elucidating the still-elusive mechanisms of CBD as a potential therapeutic compound.

Δ^9-Tetrahydrocannabinol (THC)

Δ^9-THC is the primary psychoactive constituent of *Cannabis*. Relative to other naturally occurring cannabinol compounds, such as Δ^8-THC or cannabinol, Δ^9-THC is the most abundant of these compounds derived from the plant[180]. However, in raw *Cannabis* plant material, levels of all cannabinol compounds, including Δ^9-THC, are low – these compounds exist as non-psychoactive carboxylic acid precursors. The precursor for Δ^9-THC is Δ^9-tetrahydrocannabinolic acid, which undergoes thermal decarboxylation upon heating, converting the molecule to bioactive Δ^9-THC[181]. This phenomenon is responsible for the need for users to heat *Cannabis*-derived products during or prior to use (smoking, cooking, etc). This acid precursor and decarboxylation process holds true for the many other phytocannabinoids as well, including CBD[182]. Following heating, *Cannabis* products yield active THC and are used via multiple routes of administration, predominantly inhalation or oral routes[183], which exhibit substantial differences in pharmacokinetics, bioavailability, and first-pass metabolism[184]. Inhalation generally exhibits

faster pharmacokinetics and higher bioavailability, whereas oral administration exhibits slow absorption, diminished bioavailability, and high first-pass hepatic metabolism[184]. Of note, 11-OH-THC is a major phase I metabolite of THC that exhibits a similar psychoactive profile to that of THC[185], largely mitigating a loss of psychotropic activity due to first-pass metabolism effects.

The bioactivity of THC and related cannabinoids occurs primarily via the *trans* levorotatory (-) stereoisomer[9] and is largely mediated by its actions as a partial agonist of the CB1 receptor[174-176], although THC may interact with a number of other molecular targets as well[173]. THC is widely viewed as the prototypical cannabinoid molecule, both by *Cannabis* users and in the cannabinoid research field. Indeed, significant structure-activity relationship and medicinal chemistry efforts in the early 1980's that centered around the THC chemical scaffold have led to development of cannabinoid compounds used for research applications, such as the cannabinoid full agonist CP55,940[186]. These early studies identified the core pharmacophore of THC and identified specific chemical modifications that could modify the potency of cannabinoids[187-191]. For example, hydroxylation of C11 and added steric bulk at the C3 hydrocarbon chain (based on the dibenzopyran numbering scheme) enhance potency, both features of the chemical structure of CP55,940 (see Ref. [173] for a more detailed review of the medicinal chemistry of THC). These modified cannabinoids were found to mimic the behavioral effects of THC *in vivo*, based on classic cannabinoid-elicited behavioral responses – THC elicits a wide array of physiological and behavioral effects, and many early studies have highlighted the ability of cannabinoid compounds to elicit a classical "tetrad" of behaviors in rodents – hypolocomotion, analgesia, catalepsy, and hypothermia[175,176,192], which was often used as a behavioral screen to identify compounds with cannabinoid activity. In humans, THC produces some similar effects, such as impaired movement and analgesia[193]. THC also produces a multitude of subjective effects in humans, including altered perception and hallucinations at high doses[193]. Both humans and animal models show a biphasic response to THC, with anxiolytic properties at low doses and exacerbated anxiety and aversion

at high doses[194-196], possibly due to differential engagement of distinct neural circuitry at varying doses[194].

THC (along with THC analogues) has numerous purported therapeutic utilities. Dronabinol is a synthetically-produced THC product that has approved indications for the treatment of anorexia associated with HIV/AIDS and chemotherapy-induced nausea[197]. A THC analog, nabilone, also has indications for the treatment of chemotherapy-induced nausea[198] and has also shown some efficacy in small-scale clinical trials investigating nabilone as a therapy for PTSD[199-201]. In addition to these approved indications, large bodies of evidence support various additional therapeutic applications of THC as well. One of the most notable is the treatment of pain. There is substantial evidence from human patient studies that *Cannabis* and THC products exhibit efficacy in mitigating chronic pain conditions[202]. Another major purported application for THC is the mitigation of anxiety. Anxiety relief is commonly reported as a major reason for *Cannabis* use[203]. This idea is further supported by the aforementioned clinical studies that have found modest efficacy for nabilone in treating PTSD symptomology[199-201]. These observations are promising but are somewhat confounded by the above mentioned biphasic anxiety response to THC[194] and purported anxiolytic properties of CBD[204-208], another major constituent of *Cannabis*. Numerous other applications for THC have been described as well, including epilepsy, irritable bowel syndrome, and sleep disorders, among others[193]. Data are mixed on many of these potential therapeutic applications of THC, and further research is warranted, including more rigorously controlled and systematic clinical trials.

Cannabidiol (CBD)

CBD is the major non-psychoactive constituent of *Cannabis* and has recently gained a tremendous amount of public interest, manifesting in a substantial expansion in the commercial availability of CBD products. This interest stems from the myriad purported medicinal uses for CBD and broad perceptions around CBD being a natural botanical product that offers an

alternative to synthetic pharmaceuticals[209]. CBD (or its acid precursor, cannabidiolic acid, prior to heating) is naturally found in high abundance in *Cannabis* plants[173], although many modern strains have been selectively bred to contain low levels of CBD, relative to THC[210]. Hemp, however, is a class of *Cannabis* cultivars that are particularly rich in CBD content, with very low levels of THC[173]. In contrast to THC, CBD does not activate cannabinoid receptors[177]. CBD engages a variety of molecular targets in the CNS and thus the biological mechanisms that may subserve its putative therapeutic actions are unclear[177]. Although CBD does not exhibit appreciable orthosteric binding at CB1 receptors, it can act as a CB1 negative allosteric modulator (NAM)[177]. As such, CBD is still considered to be an important regulator of the intoxicating effects of *Cannabis* and THC – *Cannabis* strains with elevated CBD levels (lower THC:CBD ratios) can show attenuated liability for adverse effects in some cases[210]. This likely occurs through CBD acting as a CB1 NAM to counteract THC engagement with CB1 receptors, although additional or alternative pharmacological targets may be involved in this phenomenon[211].

Non-CB1 receptor targets of CBD include a variety of GPCRs, ion channels, transporters, and transcription factors widely expressed across the CNS[177]. Indeed, a recent review article on the molecular pharmacology of CBD reported >65 proposed targets from the literature[178]. This polypharmacology likely contributes to the enigmatic and poorly understood biological actions of CBD. The 5-HT_{1A} receptor, a Gi/o-coupled GPCR, is one such target that has been proposed to be involved in the therapeutic actions of CBD, most notably its anxiolytic and antidepressant-like properties[212,213]. The data regarding CBD's mode of pharmacology at the 5-HT_{1A} receptor are conflicting. Some studies proposed that CBD acts as an agonist at 5-HT_{1A}, as evidenced by data from radioligand binding, [^{35}S]-GTPγS recruitment, and cAMP assays[214]. However, these studies were carried out in Chinese hamster ovary (CHO) cells, and a later study was unable to produce similar results in membranes prepared from rodent brainstem tissue[215]. Instead, this studied found that CBD potentiated the response of 8-OH-DPAT[215], a known 5-HT_{1A} orthosteric agonist,

suggesting CBD may act as a positive allosteric modulator at the 5-HT_{1A} receptor. Further complicating this interaction, a recent study using membranes prepared from human brain tissue reported data that suggested inverse agonist actions of CBD at the 5-HT_{1A} receptor[216]. Further studies aimed at disambiguating the actions of CBD at 5-HT_{1A} receptor should be a high priority given the posited role of 5-HT_{1A} in mediating some aspects of the therapeutic effects of CBD, particularly for neuropsychiatric disorders. Another notable target of CBD that may influence its therapeutic effects is the $GABA_A$ receptor, a ligand-gated Cl^- channel and the primary mediator of fast inhibitory transmission in the brain. CBD has been proposed to act as a positive allosteric modulator of $GABA_A$ receptors[217], although this study was carried out in *Xenopus* oocytes and remains to be corroborated by additional studies in native tissue preparations. Potentiation of $GABA_A$ receptors is a major mode of action for both barbiturates and benzodiazepines[218], and thus could have implications for the anxiolytic and antiepileptic properties of CBD. There are myriad other targets of CBD that may be involved these and other phenotypes and have been reviewed in detail elsewhere (See Ref. [177]). In addition to acute engagement of these molecular targets, CBD has also been proposed to exhibit some effects mediated via epigenetic modifications[219]. For example, two weeks of repeated dosing with CBD was shown cause profound alterations in DNA methylation states in the hippocampus in mice[220]. Collectively, the vastly complex polypharmacology of CBD highlights the need for a disentanglement of which of these molecular targets and interactions are physiologically relevant for the observed behavioral and therapeutic effects of the drug.

Snake Oil or Misunderstood Medicine?: Barriers to Navigating the Therapeutic Utility of CBD

The complex polypharmacology of CBD highlighted above contributes to an overarching problem facing this field, which is a global lack of understanding of the neurophysiological mechanisms of CBD and its therapeutic value. Indeed, there is a striking lack of systemic approach in the clinical data available for CBD (e.g., highly variable dosing and outcome

measures). The dearth of information regarding how CBD directly influences the physiology of the CNS renders it challenging to design systematic studies aimed at directly understanding its efficacy, especially in treating neuropsychiatric disorders. Despite the widespread interest in CBD in treating myriad conditions, the only approved indication for CBD is a product known as Epidiolex, which is used to treat the severe seizure disorders Dravet syndrome and Lennox-Gastaut syndrome[221]. There are multiple proposed mechanisms underlying the purported anticonvulsant properties of CBD, including interactions with transient receptor potential vanilloid 1 (TRPV1) via desensitizing the channel[222]. One of the most compelling mechanisms for the anticonvulsant properties of CBD, however, is preclinical evidence that CBD attenuates seizures via antagonism of G protein-coupled receptor 55 (GPR55). A study investing a mouse model of Dravet Syndrome (a clinical condition treated by CBD) demonstrated that CBD decreased seizure severity and duration and mitigated social deficits in these mice[223]. Mechanistically, this study demonstrated that CBD could enhance GABAergic transmission onto hippocampal dentate granule cells and decrease their firing, and this was mediated by a GPR55 antagonism-driven increase in local interneuron excitability[223]. This is one of few cases of compelling, preclinical mechanistic data that has clearly demonstrated translational value to humans, highlighting the need for a deeper mechanistic understanding of CBD at the neurophysiological level.

Another significant barrier to navigating proper research channels for CBD therapy relates to the relatively low affinity CBD exhibits for many of its proposed molecular targets. Many of the reports of molecular targets for CBD derived from *in vitro* studies utilize concentrations that exceed feasibly attainable *in vivo* concentrations, calling into question their physiological relevance[177,178]. For example, consider the study cited above that reported CBD agonism at the 5-HT_{1A} receptor using CHO cell preparations[214]. In the radioligand binding data from this study, while the authors do not report a calculated IC_{50} value, they report that CBD displaces [^{3}H]-8-OH-DPAT by 73% at a concentration of 16 µM[214]. Furthermore, another study reported IC_{50} values for

CBD displacement of [^{3}H]-8-OH-DPAT in human brain membrane preparations in the 46-129 µM range[216]. This may be somewhat mitigated by the report that CBD exhibited 5-HT_{1A} PAM activity at 100 nM[215]. However, the same study reported PAM activity was not observed at lower (31.6 nM) or higher (1 µM) CBD concentrations[215], complicating the interpretation of this finding. Similar concentration ranges are observed for the activating and desensitizing effects of CBD on TRPV1. Using HEK293 cells to express TRPV1, two studies have shown CBD-elicited channel activity in the 3-10 µM range[222,224]. These values align with radioligand binding data from one of these studies, which reported a K_i of 3.6 µM for CBD at TRPV1[224]. Similarly, EC_{50} values for the PAM activity of CBD at $GABA_A$ receptors varied within the 0.9-16.1 µM range, depending on receptor subunit composition[217]. GPR55, however, may exhibit higher affinity for CBD, which aligns with the preclinical evidence for GPR55 in mediating some of the anticonvulsant effects of CBD, as discussed above[223]. CBD was shown to antagonize [^{35}S]-GTPγS recruitment after GPR55 activation with an IC_{50} of 445 nM in this assay[225]. CBD antagonism of GPR55 has been demonstrated across numerous studies[226], including in a native tissue preparation (brain slices) at 1 µM (producing full blockade of experimental effects; antagonist effect is likely saturated at this concentration)[227]. Collectively, these observations indicate that this interaction is a likely candidate for mediating biologically meaningful effects at physiologically attainable CBD concentrations. The challenges and disconnects in making meaningful conclusions regarding the lower affinity targets of CBD, however, become clear when considering *in vivo* pharmacokinetic data for CBD, discussed below.

As with other cannabinoids, the primary routes of administration for CBD are inhalation (smoking or vaping) or oral. While CBD inhalation occurs during the smoking of *Cannabis* and there are CBD vaporizer products available, many of the CBD products marketed for medicinal use are formulated for oral administration (typically in an oil-based solution), including Epidiolex[228]. Although there is a dearth of human bioavailability data for CBD, it is estimated to

have an oral bioavailability of ~6% in humans (compared to ~31% from smoking[229]) in the fasted state, largely due to poor aqueous solubility and extensive first-pass metabolism[230]. Of note, multiple human studies have demonstrated that oral bioavailability can be improved by administration after a high-fat meal, as evidenced by severalfold increases in area under the curve values in fed vs. fasted patients[231,232]. Ultimately, the poor bioavailability of CBD leads to low systemic exposure after oral dosing and leads to the requirement for large doses in order to achieve efficacy. In animal studies, where much higher doses are administered relative to humans, plasma CBD concentrations have been observed in ranges that are compatible with the CBD concentrations used in many *in vitro* studies. For example, one study reported plasma and brain CBD concentrations >20 µM following a 120 mg/kg intraperitoneal dose[233]. In humans, clinical pharmacokinetic studies have reported plasma CBD concentrations in the low micromolar range, lending a degree of translational feasibility to some of the therapeutic mechanisms predicted from *in vitro* studies. Indeed, one study reported an average C_{max} of 413.6 and 346.1 ng/mL in children and adolescents after repeated dosing[234], which equates to approximately 1.1-1.3 µM. However, the dosing where these concentrations were observed in this study was 40 mg/kg, twice that of the maximum recommended dose for Epidiolex[228], which is 20 mg/kg. For this dose, the same study reported CBD plasma C_{max} values of 100.4 and 162.7 ng/mL[234], which equates to approximately 319-517 nM. Although these pharmacokinetic parameters approach the concentration ranges that may align with *in vitro* pharmacology data, it is important to consider that dosing in this range is atypical outside of formal Epidiolex regimens and clinical experimental settings. More standard oral dosing in the 10-20 mg range in humans produces plasma C_{max} values in the low nM range (for review of pharmacokinetics of CBD in humans see Ref. [235]). This is below the expected concentration range for CBD engagement with many of its molecular targets, which may lead to a lack of efficacy in clinical measures. In agreement with this idea, a recent review of dosing in clinical trials found positive outcomes associated with higher doses, in the 1-50 mg/kg range[236]. Although there is a clear correlation between oral dose and plasma

Cmax values, the collective data suggest this relationship may be non-linear at high doses[235]. This implies that dose escalation may be insufficient to improve systemic CBD exposure past an upper limit. More detailed data on the pharmacokinetics of CBD in humans are needed along with investigation into strategies to improve CBD bioavailability, be that by novel formulation methods or implementation of alternate routes of administration. Consideration of these concepts should be a priority in the design of clinical studies of CBD efficacy.

A collective contribution by the poorly understood neurophysiological mechanisms of CBD together with its pharmacokinetic disposition likely contribute to the lack of systematic, high-quality clinical information on the efficacy of CBD in therapeutic applications. An area of growing interest that particularly suffers from this lack of systematic clinical data or mechanistic insight is the use of CBD in the treatment of stress-related neuropsychiatric disorders, such as anxiety and PTSD. This application is supported by preclinical behavioral studies in rodents[205,237] and a number of small scale clinical trials and case studies in humans have reported efficacy in mitigating anxiety and PSTD symptomology[1,205]. However, larger scale clinical studies are needed to better examine the efficacy of PSTD in this context in humans. This area of research has the potential to be facilitated by more foundational preclinical mechanistic data on CBD pharmacodynamics in this context. How does CBD engage with brain circuitry involved in these phenotypes? What are the cellular mechanisms by which CBD may alter stress-related neurocircuitry? Novel mechanistic evidence for CBD modulation of a major emotional hub in the brain, the amygdala, forms the basis for the research presented in Chapter III of this thesis.

CHAPTER II

OPPOSING RETROGRADE AND ASTROCYTE-DEPENDENT ENDOCANNABINOID SIGNALING MECHANISMS REGULATE LATERAL HABENULA SYNAPTIC TRANSMISSION

Nathan D. Winters[1,2], Veronika Kondev[2,3], Niharika Loomba[3], Eric Delpire[3,4,5], Brad A. Grueter[1,2,3,4,5], and Sachin Patel[6,7*]

[1]Department of Pharmacology, Vanderbilt University School of Medicine, Nashville, TN, USA.

[2]Vanderbilt Center for Addiction Research, Vanderbilt University School of Medicine, Nashville, TN, USA.

[3]Vanderbilt Brain Institute, Vanderbilt University School of Medicine, Nashville, TN, USA.

[4]Department of Anesthesiology, Vanderbilt University School of Medicine, Nashville, TN, USA.

[5]Department of Molecular Physiology and Biophysics, Vanderbilt University School of Medicine, Nashville, TN, USA.

[6]Northwestern Center for Psychiatric Neuroscience, Department of Psychiatry and Behavioral Sciences, Feinberg School of Medicine, Northwestern University, Chicago, IL, USA.

[7]Lead contact.

*Correspondence: sachin.patel@northwestern.edu

ABSTRACT

The lateral habenula (LHb) encodes aversive states and its dysregulation is implicated in neuropsychiatric disorders, including depression. The endocannabinoid (eCB) system is a neuromodulatory signaling system that broadly serves to counteract the adverse effects of stress; however, CB1 receptor signaling within the LHb can paradoxically promote anxiogenic- and depressive-like effects. Current reports of synaptic actions of eCBs in the LHb are conflicting and lack systematic investigation of eCB regulation of excitatory and inhibitory transmission. Here we report that eCBs differentially regulate glutamatergic and GABAergic transmission in the LHb, exhibiting canonical and circuit-specific inhibition of both systems and an opposing potentiation of synaptic glutamate release mediated via activation of CB1 receptors on astrocytes. Moreover, simultaneous depression of GABA and potentiation of glutamate release increases net excitation-inhibition ratio onto LHb neurons, suggesting a potential cellular mechanism by which cannabinoids may promote LHb activity and subsequent anxious- and depressive-like aversive states.

INTRODUCTION

The lateral habenula (LHb) is a conserved epithalamic brain structure critical in guiding behavioral responses to aversive stimuli. Serving as in integrative hub between the forebrain and midbrain monoaminergic nuclei, the LHb regulates diverse physiological and behavioral functions [84]. Activation of the LHb is generally aversive and plays an increasingly evident role in neuropsychiatric disease, particularly in depression [107]. Despite this, the molecular systems orchestrating synaptic activity within the LHb are poorly understood. One system of particular interest is the endocannabinoid (eCB) system, as it strongly controls synaptic signaling in other brain areas [3] and is heavily implicated in the etiology of affective disorders [238].

The eCB system is a lipid-derived retrograde signaling system that generally functions to suppress presynaptic neurotransmitter release. It is comprised of the type 1 and 2 cannabinoid receptors (CB_1 and CB_2), the two major eCB ligands (2-arachidonoylglycerol, 2-AG; and anandamide, AEA), and their biosynthetic and degradative enzymes. In the LHb, CB_1 receptors are present on excitatory and inhibitory terminals, postsynaptic neuronal membranes, mitochondria, and astrocytic membranes [158]. Intra-LHb CB_1 activation promotes depressive- and anxiety-like phenotypes in rats, whereas CB_1 blockade exerts anxiolytic- and antidepressant-like effects [158]. How these divergent phenotypes are produced remains a major open question in the field, as eCB manipulations in the LHb produce phenotypes opposite to those elicited by systemic or corticolimbic eCB signaling, which generally promotes anxiolysis and stress resiliency [77-79,159]. Reports of eCB actions at LHb synapses are conflicting and do not adequately account for these observations. For example, eCBs have been shown to inhibit both GABA and glutamate release under some conditions [140,160] which would be predicted to have anxiogenic and anxiolytic effects, respectively. These observations highlight the need for systematic interrogation of eCB function at glutamatergic and GABAergic synapses in the LHb to provide insight into potential cellular mechanisms subserving the paradoxical aversive nature of eCBs in the LHb.

Using electrophysiology and pharmacology in acute brain slices, here we report opposing synaptic and astrocytic mechanisms by which eCBs differentially regulate LHb synaptic transmission. While we find circuit-specific canonical cannabinoid-mediated inhibition of evoked glutamate and GABA onto LHb neurons, our data uncover a novel astrocyte-dependent CB_1 mechanism potentiating spontaneous glutamate release. Collectively, our data identify opposing mechanisms of direct synaptic depression and indirect synaptic potentiation via eCB signaling in astrocytes, which may promote net LHb activity and potentially explain the pro-depressive effects of LHb CB_1 signaling. Furthermore, given the role of the LHb in depressive disorders, these findings may have broad implications for the cellular mechanisms underlying cannabinoid-associated depression [239] and the aversive effects of high-dose cannabinoids [168,204].

RESULTS

Endocannabinoids Differentially Regulate Glutamatergic and GABAergic Synapses in the Lateral Habenula

To assess eCB functionality at excitatory and inhibitory synapses in the LHb, we utilized patch clamp electrophysiology in acute *ex vivo* brain slices. Holding neurons near the reversal potentials for glutamate and GABA allowed for electrical isolation of both spontaneous excitatory and inhibitory postsynaptic currents (sEPSCs, sIPSCs) from single LHb neurons (**Figure 2-1A**). Electrically-isolated currents were predominantly glutamatergic or GABAergic, respectively (**Figure 2-S1A-B**), without significant contribution by glycine receptors [240,241] (**Figure 2-S1C**). Incubation of brain slices in the cannabinoid receptor agonist CP55,940 unexpectedly increased sEPSC frequency and amplitude (**Figure 2-1B-C**). In line with this, both the CB_1 inverse agonist Rimonabant (Rim) and the diacylglycerol lipase inhibitor DO34 significantly reduced sEPSC frequency (**Figure 2-1B-C**), suggesting the presence of a tonic positive modulatory 2-AG-CB_1 tone on spontaneous glutamate release. The monoacylglycerol lipase inhibitor JZL184 had no effect on sEPSC frequency or amplitude (**Figure 2-1B-C**). CP55,940 significantly reduced sIPSC

frequency and amplitude (**Figure 2-1D-E**), in line with canonical eCB actions at GABAergic synapses and in agreement with Authement, et al. [140]. None of the other compounds tested had a significant effect on sIPSC frequency or amplitude (**Figure 2-1D-E**). Rim also had no effect on pharmacologically-isolated sIPSCs measured at -70mV (**Figure 2-S1D**). When examining the sEPSC/sIPSC frequency ratio within cell, we found that CP55,940 significantly increased the excitation-inhibition (E/I) ratio onto LHb neurons, with no other compound exhibiting a significant effect on this measure (**Figure 2-1F**). These data suggest a differential role for 2-AG-CB_1 signaling at excitatory vs. inhibitory synapses with a shunting towards enhanced E/I ratio.

Contrasting our sEPSC data, it has been shown that CB_1 receptors inhibit evoked glutamate release in the LHb [160,161]; however, cannabinoid effects on evoked GABAergic transmission are not known. We therefore next examined the effects of cannabinoid receptor activation on evoked GABA release onto LHb neurons. We found that bath application of CP55,940 significantly reduced evoked IPSC (eIPSC) amplitude and caused a non-significant increase in the coefficient of variation (CV), another index of presynaptic release probability (**Figure 2-S1E-G**), confirming evoked GABA release is also inhibited by cannabinoid receptors. We next assessed activity-dependent engagement of eCB signaling at LHb synapses by measuring depolarization-induced suppression of excitation or inhibition (DSE, DSI). DSE/I is an electrophysiological method for eliciting phasic eCB release and short-term plasticity wherein brief depolarization of the postsynaptic cell triggers Ca^{2+} entry that results in the synthesis and retrograde release of 2-AG to depress neurotransmitter release via presynaptic CB_1 receptors [3,242]. For evoked EPSCs (eEPSCs), we found that 10s depolarization to +30 mV resulted in minimal effect on eEPSC amplitude. In contrast, depolarization to +30 mV resulted in a significant transient depression of eIPSC amplitude (**Figure 2-1G-H)**, and this effect was blocked by Rim (**Figure 2-1H, S1H**). This presence of DSI, but not DSE, at LHb synapses further supports our spontaneous transmission

data that suggest that the LHb eCB system exerts stronger inhibition of GABAergic transmission, and thus may serve to promote net synaptic excitation of LHb neurons.

Given the diverse distribution of CB_1 immunoreactivity in the rodent LHb, including postsynaptic and mitochondrial compartments [158], we also probed for potential effects of CB_1 activation on LHb neuron excitability. CP55,940 incubation had no effect on the number of action potentials fired in response to square wave current injection (**Figure 2-S1I**) and had no effect on resting membrane potential, input resistance, or tonic firing frequency in cell-attached configuration (**Figure 2-S1J-L**). These data suggest that the effects of CB_1 activation in the LHb are likely restricted to modulation of synaptic neurotransmitter release.

Distinct Inputs to the LHb are Differentially Regulated by Endocannabinoids

While previous studies have demonstrated cannabinoid receptors can depress electrically-evoked glutamate release onto LHb neurons [160,161], our data showing potentiation of sEPSCs suggest that distinct afferents to the LHb may be under divergent control of eCB signaling. To address this possibility, we utilized optogenetic projection targeting to isolate two distinct LHb inputs, the lateral preoptic area (LPO) and the entopeduncular nucleus (EPN). These inputs send dual component excitatory-inhibitory projections to the LHb, are generally aversive when activated, and have been implicated in behavioral states relevant to disease pathology [98,153,243]. We first examined eCB regulation of the LPO input, a hypothalamic structure which sends glutamate and GABA projections to the LHb via separate populations of neurons [98]. To target LPO synapses, we injected mice in the LPO with AAV5-CaMKIIa-ChR2(H134R)-eYFP and pharmacologically isolated optically-evoked EPSCs and IPSCs (oEPSCs; oIPSCs) in the LHb (**Figure 2-2A**). Examining the glutamatergic LPO-LHb circuit, we found robust depression of oEPSC amplitude upon bath application of CP55,940 (**Figure2- 2B-C**). There was no effect on the paired-pulse ratio (PPR) or CV (**Figure 2-2D**). With regards to the GABAergic LPO-LHb circuit,

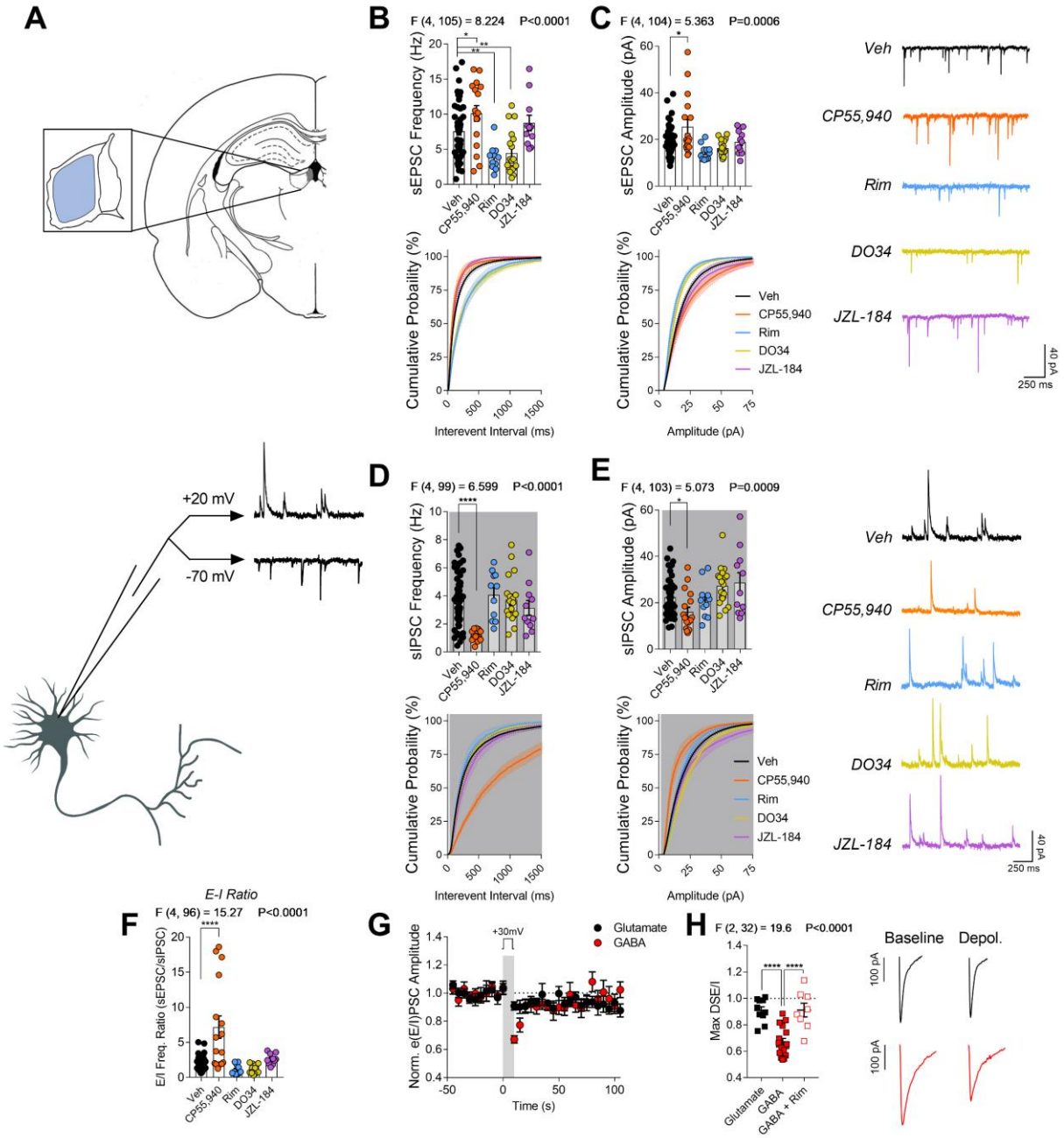

Figure 2-1: Endocannabinoids Differentially Regulate Glutamatergic and GABAergic Synapses in the Lateral Habenula

(A) Schematic of LHb recording territory and strategy for dual spontaneous excitatory/inhibitory recordings from single cells.

(B-C) Top: Effects of pharmacological manipulations of the 2-AG-CB_1 system on sEPSC (B) frequency and (C) amplitude (Vehicle n = 52, 18 mice; CP55,940 n = 17, 6 mice; Rim n = 11, 3 mice; DO34 n = 19/18, 5 mice; JZL-184, n = 11, 5 mice). Bottom: Associated cumulative probability plots for (B) interevent interval and (C) amplitude.

(D-E) Same as (B-C), for sIPSCs (Vehicle n = 50, 18 mice; CP55,940 n = 13/17, 6 mice; Rim n = 11, 3 mice; DO34 n = 19, 5 mice; JZL-184, n = 11, 5 mice).

(F) Same as (B-E) for excitation-inhibition ratio (Vehicle n = 46, 18 mice; CP55,940 n = 16, 6 mice; Rim n = 10, 3 mice; DO34 n = 19/18, 5 mice; JZL-184, n = 11, 5 mice).

(G-H) DSE (glutamate) and DSI (GABA) in LHb neurons. (G) Time course of normalized synaptic current amplitude. Depolarization step was 10s at +30mV. (H) Quantification of max DSE/DSI at the first sweep following depolarization. GABA + Rim time course in Figure S1G (Glutamate n = 10, 3 mice; GABA n = 17, 7 mice; GABA + Rim n = 8, 3 mice).

Data are mean ± SEM; n = number of cells. Data analyzed by one-way ANOVA with Holm-Sidak multiple comparisons relative to (B-F) vehicle or (H) between all groups. F and P values for ANOVA and significance for post-hoc multiple comparisons shown on relevant panels (*p<.05, **p<0.01, ****p<0.0001).

we found depression of oIPSC amplitude upon CP55,940 application (**Figure 2-2B, E**), as well as an increase in the PPR and non-significant increase in the CV (**Figure 2-2F**). These data suggest that the LPO-LHb circuit is regulated by cannabinoid receptors, with stronger relative control of the glutamate input (**Figure 2-S2A**). To probe tonic and phasic eCB regulation of this circuit, we examined the effects of Rim on release probability by delivering a 250ms pulse train at 20Hz and by analysis of DSE/I. At the glutamate LPO input, Rim accelerated synaptic depression of oEPSC amplitude, indicative of increased release probability (**Figure 2-2G**) and revealing tonic CB_1 inhibition of LPO-LHb glutamatergic transmission. This contrasts our sEPSC data but is in line with canonical retrograde synaptic eCB mechanisms. With regards to phasic 2-AG release, our DSE protocol did not detect DSE at the LPO-LHb circuit (**Figure 2-2H**). At the GABAergic LPO input, Rim had no effect on presynaptic release probability and we did not detect DSI (**Figure 2-2I-J**).

We next examined eCB regulation of the EPN input, a basal ganglia structure that sends a dual-component projection wherein glutamate and GABA are released from the same terminals [243]. To do this, we injected AAV5-Ef1a-DIO-ChR2-eYFP into the EPN of Somatostatin-Cre (SST-IRES-Cre) mice (**Figure 2-2K**). This approach selectively targets the SST+ glutamate/GABA co-releasing neurons of the EPN and avoids a distinct excitatory EPN-LHb circuit [244]. We found that

bath application of CP55,940 had no significant effect on oEPSC or oIPSC amplitude or any other release measure examined, except a small but significant increase in the glutamate PPR (**Figures 2-2L-P, 2-S2B**). Furthermore, Rim had no effect on release probability of glutamate or GABA and CB_1-sensitive DSE/DSI were absent at this input (**Figure 2-2Q-T**). These data provide evidence for circuit specificity in eCB modulation of LHb synapses and identify that the LPO input is inhibited by canonical synaptic eCB mechanisms. These data further support previous data showing cannabinoid inhibition of evoked glutamate release [160,161] and together with our sEPSC data suggest that there may be opposing eCB mechanisms that can inhibit or potentiate synaptic glutamate release in distinct contexts.

Astrocytic CB_1 Receptors Positively Modulate Lateral Habenula Glutamate Release

We next sought to further investigate the opposing effect of CB_1 receptor activation on spontaneous vs. evoked glutamatergic transmission and probed the mechanisms underlying the potentiating effects of eCB signaling on sEPSCs seen in **Figure 2-1B.** We first sought to exclude the possibility of indirect network effects due to the lack of synaptic blockers in these earlier experiments. We repeated the Rim and DO34 experiments in the presence of the $GABA_A$ receptor blocker picrotoxin, as well as the $GABA_B$ receptor antagonist CGP 54626. As shown before, blockade of the 2-AG-CB_1 axis by Rim or DO34 significantly reduced sEPSC frequency (**Figure 2-S3A**), confirming that these findings are not related to indirect effects of GABAergic transmission. To probe the reversibility of this mechanism, we next treated all slices with DO34 to deplete constitutive 2-AG signaling to determine if cannabinoid receptor activation by an exogenous agonist could restore the reduced glutamate release observed in this condition. Indeed, CP55,940 significantly enhanced sEPSC frequency in DO34-treated slices relative to slices treated with DO34 alone (**Figure 2-S3B),** confirming the bidirectionality of this potentiating 2-AG-CB_1 tone.

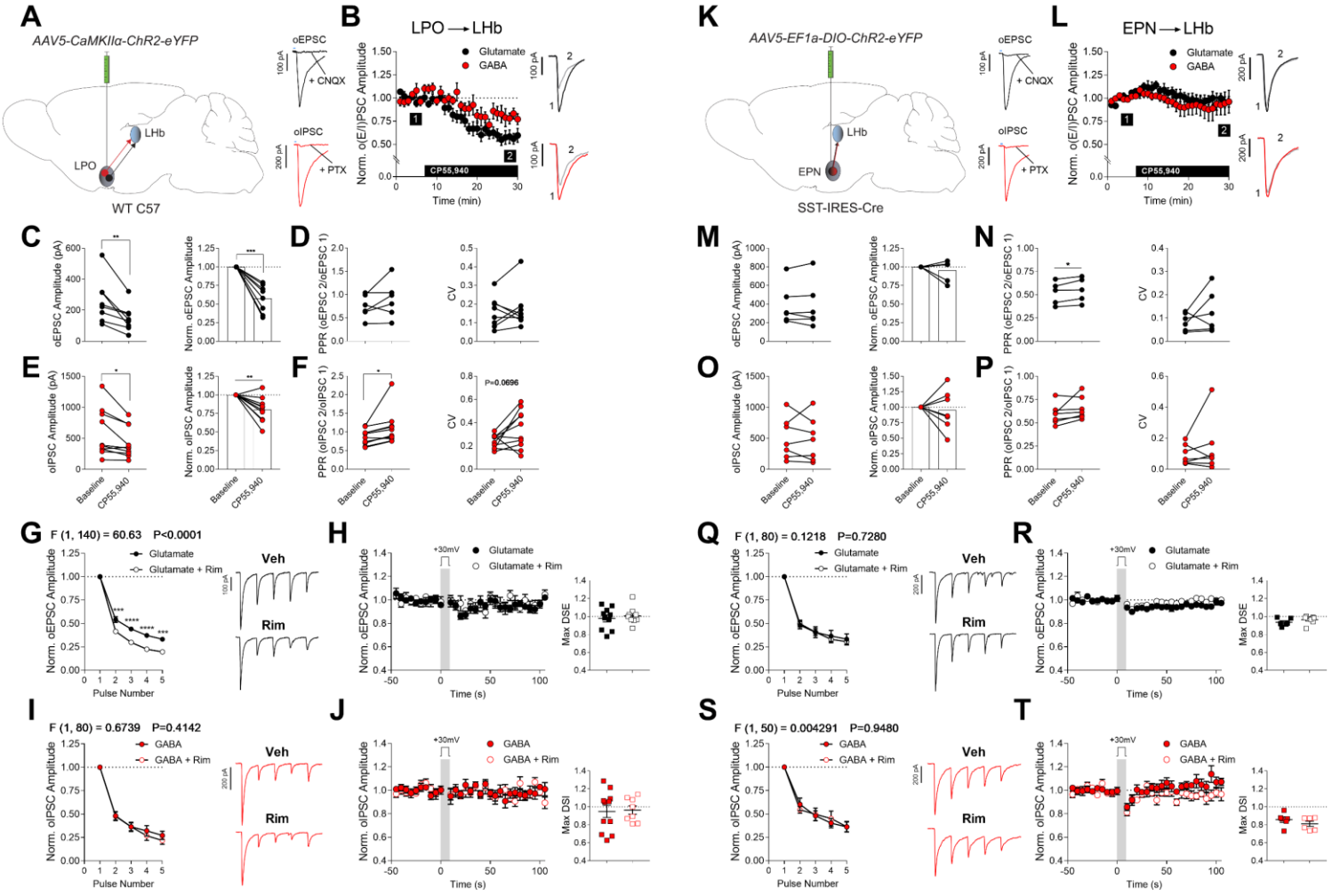

Figure 2-2: Distinct Inputs to the LHb are Differentially Regulated by Endocannabinoids

(A) Schematic of strategy for optogenetic study of the LPO- LHb circuit; pharmacological validation of oEPSCs and oIPSCs. CNQX, AMPA antagonist; PTX, $GABA_A$ antagonist.

(B) Time course of CP55,940 bath application effects on oEPSC and oIPSC amplitude at LPO-LHb synapses. Timepoints 1 and 2 represent baseline and last two minutes of drug application, respectively. (Glutamate n = 8, 6 mice; GABA = 13, 7 mice).

(C-F) CP55,940 effects on LPO-LHb (C) oEPSC amplitude, (D) oEPSC PPR and CV, (E) oIPSC amplitude, and (F) oIPSC PPR and CV at baseline and post-drug application (oEPSC amplitude, CV n = 8, 6 mice; oEPSC PPR n = 6, 4 mice; oIPSC amplitude, PPR, CV n = 10, 6 mice).

(G) Rim effects on LPO-LHb oEPSC amplitude during a 250ms 20 Hz pulse train, normalized to Pulse 1 (n = 17, 4 mice).

(H) DSE at LPO-LHb synapses. Left: Time course of normalized oEPSC amplitude. Depolarization step was 10s at +30mV. Right: Quantification of max DSE at the first sweep following depolarization. (Glutamate n = 10, 3 mice; Glutamate + Rim n = 9, 3 mice).

(I) Same as (G) for LPO-LHb oIPSCs (GABA n = 10, 4 mice; GABA + Rim n = 8, 3 mice).

(J) DSI at LPO-LHb synapses. Same as (H) for LPO-LHb oIPSCs (GABA n = 11, 4 mice; GABA + Rim n = 8, 3 mice).

(K) Same as (A) for the EPN-LHb circuit.

(L) Same as (B) for EPN-LHb oEPSC and oIPSC amplitude. (Glutamate n = 6, 5 mice; GABA = 7, 4 mice).

(M-P) Same as (C-F) for EPN-LHb oEPSCs and oIPSCs. (oEPSC amplitude, CV = 6, 5 mice; oEPSC PPR n = 5, 5 mice; oIPSC amplitude, PPR, CV n = 7, 4 mice).

(Q) Same as (G) for EPN-LHb oEPSCs (Glutamate n = 9, 3 mice; Glutamate + Rim n = 9, 3 mice).

(R) DSE at EPN-LHb synapses. Same as (H) for EPN-LHb oEPSCs (Glutamate n = 6, 3 mice; Glutamate + Rim n = 8, 3 mice).

(S) Same as (G) for EPN-LHb oIPSCs (GABA n = 6, 3 mice; GABA + Rim n = 6 mice).

(T) DSI at EPN-LHb synapses. Same as (H) for EPN-LHb oIPSCs (GABA n = 6, 3 mice; GABA + Rim n = 6, 3 mice).

Data are mean ± SEM except paired data; n = number of cells. Data analyzed by (C-F, M-P) two-tailed paired t-test, (G, I, Q, S) two-way ANOVA with Holm-Sidak multiple comparisons between control and Rim, or (H, J, R, T; right) two-tailed t-test. Significance for t-tests, ANOVA F and P values for main effect of drug, and significance for post-hoc multiple comparisons shown on relevant panels (*p<.05, **p<0.01, ***p<0.001, ****p<0.0001).

One mechanism by which eCBs have been reported to enhance synaptic transmission is via CB_1 signaling in astrocytes. A growing body of literature has demonstrated that astrocytes express CB_1 receptors that couple to intracellular Ca^{2+} mobilization and subsequent gliotransmission, which can modulate synaptic release [36-38,60,245]. Supporting this hypothesis, astrocyte membranes exhibit the highest relative density of CB_1 receptor immunoreactivity in the rodent LHb [158]. To determine whether LHb astrocytic CB_1 receptors were functional, we monitored astrocyte Ca^{2+} signals as a functional readout for these receptors from mice generated to genetically-encode the Ca^{2+} indicator GCaMP6f selectively in astrocytes (Aldh1l1-Cre/ERT2::Ai95D) (**Figure 2-3A**). In *ex vivo* brain slices from these mice, we delivered a local pressure pulse application of CP55,940 to examine local Ca^{2+} responses (**Figure 2-3B**). Application of CP55,940 resulted in a time-locked local elevation in bulk fluorescent Ca^{2+} signals near the site of drug application, and this effect

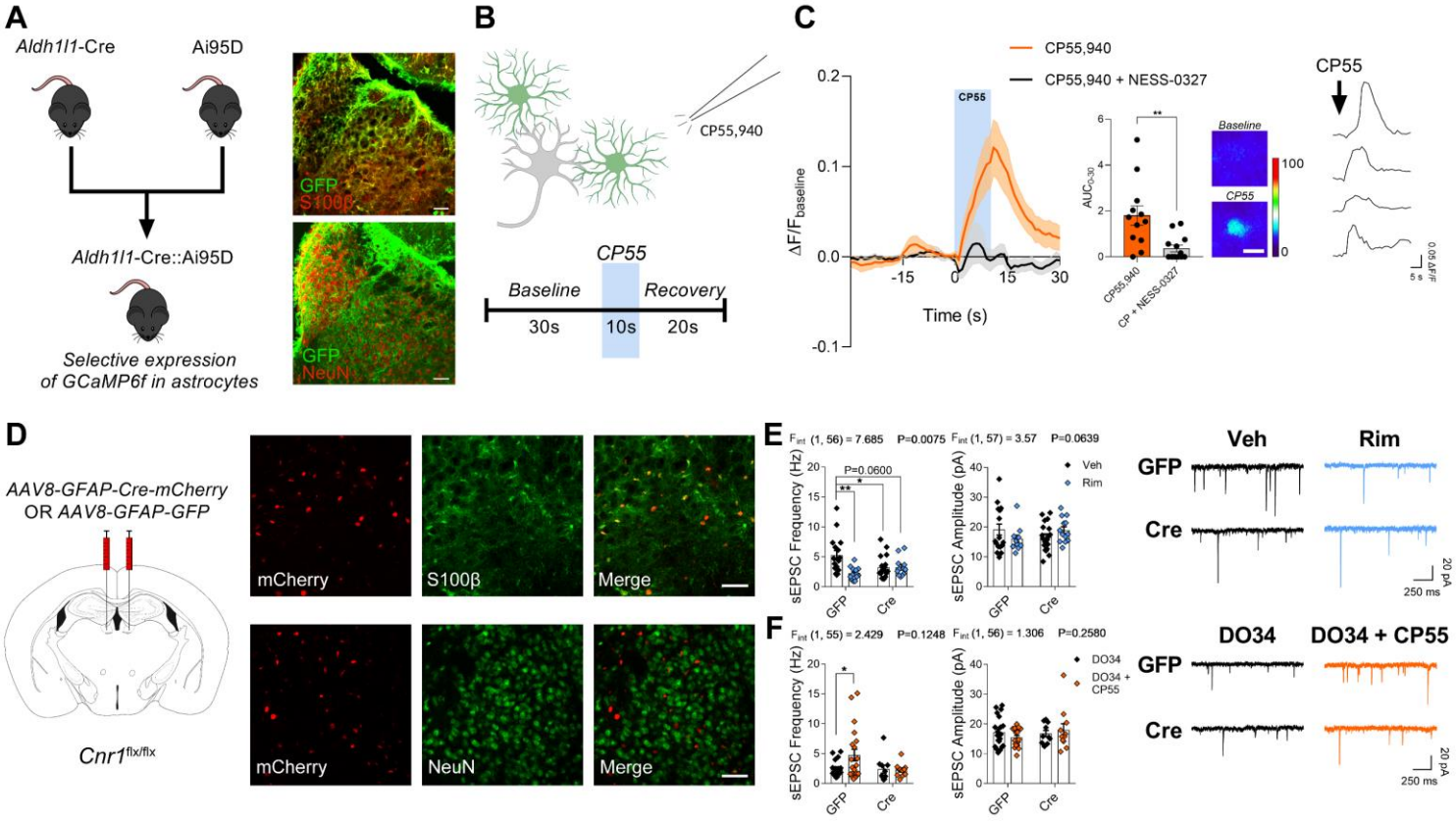

Figure 2-3: Astrocytic CB_1 Receptors Positively Modulate Lateral Habenula Glutamate Release

(A) Left: Breeding scheme for Aldh1l1-Cre::Ai95D mice. Right: Staining in LHb for canonical astrocyte and neuron markers against GFP staining for GCaMP6f. Scale bar = 50 µm.

(B) Schematic of experimental approach for *ex vivo* Ca^{2+} imaging in astrocytes (green).

(C) Effect of local CP55,940 application on astrocyte Ca^{2+} signals. Left: ΔF/F at drug application site and positive area under the curve (AUC) from 0-30s. (CP55,940 n = 12, 3 mice; CP + NESS-0327 n = 13, 3 mice). Right: Widefield pseudo-colored ΔF/F-adjusted images of a pre-identified cell pre vs post CP55,940 application; sample traces from individual cells. Scale bar = 10 µm.

(D) Left: Schematic for viral injections in the LHb. Right: Staining for canonical astrocyte and neuron markers against expression of GFAP-Cre-mCherry. Scale bar = 50 µm. See also Figure S3C.

(E) Effects of astrocytic CB_1 receptor deletion and Rim on sEPSC frequency and amplitude (GFP Veh n = 16/17, 5 mice; GFP Rim n = 13, 5 mice; Cre Veh n = 19, 6 mice; Cre Rim = 13/14, 6 mice).

(F) Same as (E) for DO34 ± CPP55,940 effects. (GFP DO34 n = 18/20, 6 mice; GFP DO34 + CP55 n = 20/19, 6 mice; Cre DO34 n = 10, 4 mice; Cre DO34 + CP55 = 11, 4 mice).

Data are mean ± SEM; n = number of cells. Data analyzed by (C) Mann-Whitney U test or (E-F) two-way ANOVA with Holm-Sidak multiple comparisons (E) between all groups or (F) between DO34 and DO34 + CP55 within each virus genotype. Significance for U-test, F and P values for drug x virus interaction for ANOVA, and significance for post-hoc multiple comparisons shown on relevant panels (*p<.05, **p<0.01).

was blocked by the CB_1 antagonist NESS-0327 (**Figure 2-3C**), confirming the selectivity of CB_1 receptors in mediating this effect. These data support previous reports of astrocytic CB_1 coupling to intracellular Ca^{2+} signaling in other brain regions and confirm the presence of functional CB_1 receptors coupling to this mechanism in the LHb.

To directly test the hypothesis that astrocytic CB_1 receptors are involved in the tonic potentiation of glutamate release, we selectively deleted CB_1 receptors from LHb astrocytes by viral expression of Cre recombinase under the astrocytic glial fibrillary acidic protein (GFAP) promoter (AAV8-GFAP-Cre-mCherry) in the LHb of *Cnr1*$^{flx/flx}$ mice (**Figures 2-3D, 2-S3C**). These mice express a floxed allele for the CB_1 receptor gene, which we have previously demonstrated exhibit functional CB_1 deletion in the presence of Cre [79]. Using this approach, we found again that Rim significantly reduced sEPSC frequency onto LHb neurons from animals injected with a control virus (AAV8-GFAP-GFP), but notably, this effect was absent in LHb neurons from slices expressing Cre (**Figure 2-3E**). Furthermore, neurons from the Cre-vehicle condition exhibited a significantly reduced sEPSC frequency relative to GFP-vehicle control slices (**Figure 2-3E**), suggesting that astrocytic CB_1 receptor deletion mimics and occludes the effect of Rim on sEPSC frequency. These data demonstrate that the tonic 2-AG-CB_1 tone that maintains physiological glutamatergic tone is mediated through astrocytic CB_1 receptors. We further demonstrated the involvement astrocytic CB_1 receptors in potentiating LHb glutamate release by examining CP55,940-induced potentiation of sEPSCs following 2-AG depletion by DO34. We found that CP55,940 significantly potentiated sEPSC frequency onto LHb neurons from GFP-injected control

mice as seen in **Figure 2-S3B**, and this effect was absent in neurons from Cre-injected mice (**Figure 2-3F**). Injection of AAV9-hSynapsin-GFP-Cre to delete CB_1 receptors from LHb neurons did not occlude the Rim-induced reduction in sEPSC frequency, controlling for off-target viral leak into neurons and further demonstrating the astrocytic specificity of these effects (**Figure 2-S3D**). Taken together, these data identify astrocytic CB_1 as the source for the tonic positive eCB regulation of LHb glutamate release and demonstrate that stimulation of these receptors can potentiate glutamate release under conditions of depleted 2-AG signaling. Moreover, astrocytic CB_1 deletion had no effect on group I metabotropic glutamate receptor (mGluR)-driven long-term depression of evoked glutamate release (**Figure 2-S3E**), which has been shown to be eCB-dependent [160]. Astrocytic CB_1 deletion also did not eliminate CP55,940-induced depression of eEPSCs (**Figure 2-S3F**) or sIPSCs (**Figure 2-S3G**), indicating that canonical cannabinoid-mediated synaptic depression does not require local astrocytic CB_1 and providing further support for distinct and opposing retrograde neuronal and astrocytic CB_1 signaling systems in the regulation of LHb glutamatergic transmission.

DISCUSSION

Increased LHb activity drives aversion, increases depressive-like behavioral phenotypes, and has been posited to contribute to the pathophysiology of psychiatric disorders including depression [84]. Elucidating neuromodulator mechanisms that influence LHb activity could reveal effective approaches for the treatment of mood and anxiety disorders. Here we identify a novel astrocyte-dependent mechanism by which tonic 2-AG-CB_1 signaling potentiates spontaneous glutamatergic transmission onto LHb neurons. In contrast, eCB-CB_1-mediated suppression of evoked release and spontaneous GABAergic transmission occur via canonical retrograde synaptic mechanisms [3]. At a population level, CB_1 appears to shunt LHb spontaneous synaptic E/I ratio towards greater net excitation via simultaneous reductions in spontaneous GABAergic and potentiation of spontaneous glutamatergic transmission. These CB_1-induced synaptic effects

are predicted to increase LHb output, enhancing aversion and increasing anxiety- and depressive-like phenotypes. These data could thus explain the antidepressant- and anxiolytic-like effects of intra-LHb CB_1 receptor blockade [158] which could reduce spontaneous excitatory drive onto LHb neurons via impairment in astrocytic 2-AG-CB_1 signaling. It is also well known that high doses of exogenous cannabinoids [204], and 2-AG augmentation under some conditions [246], can produce aversive and anxiogenic phenotypes in rodents and humans, and it is tempting to speculate potentiation of LHb glutamatergic transmission via astrocytic CB_1 could contribute to these phenomena, particularly given recent evidence that astrocytic CB_1 receptors may contribute to the aversive properties of cannabinoids [247]. These data provide new mechanistic insight into the how eCB signaling within the LHb could produce aversive-like phenotypes and potentially contribute to dose-dependent subjective experiences of exogenous cannabinoids, which have been thus far unexplained from a synaptic perspective [168].

Astrocytic eCB signaling is a rapidly emerging area of interest [35], spearheaded by seminal studies from Navarrete and Araque (2008, 2010) that first identified functional CB_1 receptors on astrocytes in the hippocampus that coupled to intracellular Ca^{2+} mobilization and modulated local synaptic transmission. These findings have since been extended to numerous other brain areas [38,60,245]. Preceding our findings was the observation that the highest density of CB_1 receptor immunoreactivity in the rodent LHb is on astrocyte membranes [158], although their functionality had not been determined. Our data demonstrate astrocyte CB_1 receptor functionality in the LHb and ascribe to them a function in the tonic potentiation of glutamate release. Additionally, to our knowledge, this is the first report in any brain area of a tonic eCB mechanism involving astrocytic CB_1 receptors that maintains physiological synaptic release probability. The mechanistic link between astrocytic CB_1 activation in the LHb and the potentiation of glutamate remains an open question. It is presumed that CB_1 mobilizes Ca^{2+} in astrocytes via coupling to G_q rather than canonical $G_{i/o}$ proteins due to a requirement for phospholipase C signaling and insensitivity to

pertussis toxin [36], although this remains to be definitively shown. CB_1-linked Ca^{2+} mobilization then leads to gliotransmitter release, and these mechanisms vary greatly by both brain region and synapse type under study, and may involve multiple subcellular pools of CB_1 [43]. For example, astrocytic CB_1 can potentiate synapses in the amygdala or hippocampus via stimulating astrocytic release of adenosine or glutamate, which facilitates synaptic release via presynaptic adenosine 2A or mGluR1, respectively [37,38]. Future studies should aim to identify whether similar or distinct molecular signaling mechanisms are recruited downstream of astrocytic CB_1 activation in the LHb.

Using optogenetic approaches, we also addressed whether eCB signaling in the LHb exhibits afferent specificity. Our studies reveal differential regulation of two inputs by eCBs, with the LPO synapses exhibiting depression by CB_1 activation and EPN synapses appearing insensitive to eCB modulation. Another important observation was the discrepancy between our circuit-specific evoked and spontaneous EPSC data with regards to the effects of CB_1 blockade. There are several potential explanations for this discrepancy: Firstly, it is possible that the LPO and EPN are not the target inputs for regulation via astrocytic eCB mechanisms or are not major contributors to the spontaneously active synapse pool; secondly, studies reporting astrocytic CB_1 regulation of synaptic strength, including our own data, have relied on minimal stimulation or spontaneous transmission approaches [37,38,60,245]. Astrocytic eCB potentiation of glutamate release in the hippocampus is observed using minimal stimulation techniques, but is not detectable when bulk stimulating larger numbers of synapses [248], suggesting there may be synaptic subpopulations amenable to astrocytic regulation and that are “lost in the noise” of our bulk stimulation methods; lastly, there may be differential mechanisms regulating evoked and spontaneous neurotransmitter release in the LHb, as these modes of neurotransmission can exhibit molecularly-distinct properties [249] and may be subject to regulation by differential eCB mechanisms. The degree to which highly synchronous release in the manner elicited by optogenetic approaches occurs *in vivo* is unknown, and thus the eCB signaling mechanisms that would predominate in a whole

animal model are difficult to predict conclusively. Future studies should address the relative contributions of canonical retrograde vs. astrocyte eCB signaling to LHb output and determine the causal relationship between astrocytic CB_1-induced potentiation of glutamate release and the aversive nature of cannabinoids in the LHb.

In summary, we provide a framework for how eCBs modulate excitatory and inhibitory transmission in distinct cellular and synaptic contexts, and provide a potential functional explanation for the aversive nature of CB_1 activation in the LHb [158], which could occur via simultaneous depression of GABA and potentiation of glutamate via astrocytic CB_1 to enhance net synaptic excitation and promote LHb activity and depressive-like phenotypes. Supporting this, chronically stressed rodents exhibit enhanced LHb neuron firing and elevated 2-AG content [158], although acute stress may disrupt some forms of 2-AG mobilization at LHb glutamatergic synapses [161]. Selective targeting of LHb eCB signaling or astrocytic function could present new therapeutic targets for depression as well as substance use disorders, as LHb eCB signaling can also influence drug intake in a manner opposite to systemic modulation in some cases [163,164]. Finally, given the association between chronic cannabinoid use and depression [239] and the aversive effects of high dose cannabinoids (e.g., THC) [204], these mechanisms may inform the importance of considering specific disease etiology for the application of cannabinoid-based therapeutics.

LIMITATIONS OF THE STUDY

With regards to astrocytic CB_1 activation, our agonist incubation approach results in a high degree of variability (see **Figures 2-3D**, **2-S3B**), potentially originating from competition between presynaptic and astrocytic CB_1, so alternative methods for stimulating this mechanism may be appropriate for future studies. Importantly, given the time course of our incubation experiments, it cannot be ruled out that other non-gliotransmitter-mediated astrocyte mechanisms not yet linked

to CB_1 activation may be involved, such as alterations in astrocyte glutamate clearance machinery, which can alter glutamate signaling in the LHb [250].

We demonstrated that cannabinoid receptor-mediated reduction of sIPSC frequency was intact following astrocytic CB_1 deletion (**Figure 2-S3G**) but did not explore basal phenotypes of astrocytic CB_1 receptor deletion on broader GABAergic transmission. We cannot rule out an interaction between astrocytic eCB signaling and inhibitory transmission, presenting a limitation in our model for the LHb eCB system.

Another limitation in our proposed model for the LHb eCB system is the unknown source for the tonic 2-AG tone that signals onto astrocyte CB_1. DO34 incubation terminates all DAGL activity in the slice, and astrocytes may produce 2-AG and signal onto local CB_1 receptors in an autocrine manner in culture [251]. Delineation of neuronal vs. astrocytic 2-AG production in distinct contexts will strengthen the model for interplay between these distinct eCB system components.

ACKNOWLEDGEMENTS

These studies were supported by NIH grants MH107435 (S.P.) and MH119817 (S.P.). The *Cnr1* floxed mouse generation was supported by the Integrative Neuroscience Initiative on Alcoholism (INIA stress) grant AA9013514 (E.D.). Confocal imaging for histology were performed in part through the use of the Vanderbilt Cell Imaging Shared Resource (supported by NIH grants CA68485, DK20593, DK58404, DK59637 and EY08126) and the Northwestern University Center for Advanced Microscopy generously supported by NCI CCSG P30 CA060553 awarded to the Robert H Lurie Comprehensive Cancer Center. The graphical abstract and schematic in Figure 2-3B were created with BioRender.com.

AUTHOR CONTRIBUTIONS

N.D.W., V.K., and N.L. conducted all experiments and analyzed the data in the laboratories of B.A.G and S.P. N.D.W, B.A.G, and S.P. contributed to experimental design. E.D. generated *Cnr1*

floxed mice. N.D.W. and S.P are responsible for study conception and data interpretation. N.D.W., B.A.G., and S.P wrote the manuscript.

DECLARATION OF INTERESTS

S.P. is a scientific consultant for Psy Therapeutics, Janssen Pharmaceuticals, and Jazz Pharmaceuticals unrelated to the present work. All other authors declare no conflicts of interest.

MATERIALS AND METHODS

LEAD CONTACT AND MATERIALS AVAILABILITY

Further information and requests for resources and reagents should be directed to and will be fulfilled by the Lead Contact, Sachin Patel (sachin.patel@northwestern.edu).

EXPERIMENTAL MODEL AND SUBJECT DETAILS

All experiments were approved by the Vanderbilt University Institutional Animal Care and Use Committees and were conducted in accordance with the National Institute of Health guidelines for the Care and Use of Laboratory Animals. 5-16 week-old male and female C57BL/6J mice obtained from Jackson Labs or bred in-house and were used for experiments throughout the manuscript. 10-18 week-old male and female *Cnr1*$^{flx/flx}$ mice bred in-house were used for experiments in Figure 2. Aldh1l1-Cre/ERT2 mice and Ai95D mice were obtained from Jackson Labs and crossed in-house to obtain Aldh1l1-Cre::Ai95D mice. 10-18 week-old male and female Aldh1l1-Cre::Ai95D mice were used for experiments in Figure 2. SOM-IRES-Cre mice and Ai14 mice were obtained from Jackson labs and crossed in-house to obtain SOM::Ai14 mice. 10-20 week-old male and female SOM::Ai14 mice were used for experiments in Figure 3. SOM::Ai14 mice were used over SOM-IRES-Cre mice due to the phenotype observed in homozygous SOM-IRES-Cre mice [252] and the availability of this line within our laboratory, as the Ai14 reporter construct should not interfere with our experimental strategy. Sex differences were not a primary

analysis variable in this study and no overt sex differences were observed, thus all data are pooled from both sexes.

Generation of *Cnr1*$^{flx/flx}$ mice

See [79].

METHOD DETAILS

Surgeries

Mice were initially anesthetized with 5% isoflurane and then transferred to the stereotax (Kopf Instruments, Tujunga, CA) and kept under 2-3% isoflurane anesthesia. The hair over the incision cite was trimmed and the skin was prepped with alcohol and iodine scrub. The skull was exposed via a midline sagittal incision and treated with the local anesthetic, benzocaine (Medline Industries, Brentwood, TN), and a hole drilled in the skull above the injection site. For all surgeries, we used a motorized digital software (NeuroStar; Stoelting Co., Wood Dale, IL) to guide a 10 µL microinjection syringe (Hamilton Co., Reno, NV) driven by a Micropump Controller (World Precision Instruments, Sarasota, FL). Virus was delivered bilaterally into the LHb (AP –1.10, ML ±0.55, DV +2.95); LPO (AP +0.65, ML ±0.52, DV +5.20) or EPN (AP -1.20, ML ±1.75, DV +4.70). All subjects received a 10mg/kg ketoprofen (AlliVet, St. Hialeah, FL) injection as a perioperative analgesic, and additional post-operative treatment with ketoprofen was maintained for 48 hours post-surgery.

Ex vivo electrophysiology

For acute *ex vivo* brain slice preparation, mice were anesthetized using isoflurane, and transcardially perfused with ice-cold and oxygenated cutting solution consisting of (in mM): 93 N-Methyl-D-glucamine (NMDG), 2.5 KCl, 20 HEPES, 10 $MgSO_4 \cdot 7H_20$, 1.2 NaH_2PO_4, 0.5 $CaCl_2 \cdot 2H_20$, 25 glucose, 3 Na-pyruvate, 5 Na-ascorbate, and 5 N-acetylcysteine. Mice were then

decapitated and brains collected. 200 µm coronal slices containing the lateral habenula were prepared on a vibrating Leica VT1000S microtome using standard procedures. Following collection of coronal sections, the brain slices were transferred to a 34°C chamber containing oxygenated cutting solution for a 10-20 minute recovery period. Slices were then transferred to a 25°C holding chamber with solution consisting of (in mM): 92 NaCl, 2.5 KCl, 20 HEPES, 2 $MgSO_4 \cdot 7H_20$, 1.2 NaH_2PO4, 30 $NaHCO_3$, 2 $CaCl_2 \cdot 2H_20$, 25 glucose, 3 Na-pyruvate, 5 Na-ascorbate, 5 N-acetylcysteine and were allowed to recover for ≥30 min. For recording, slices were placed in a perfusion chamber and continuously perfused with oxygenated artificial cerebrospinal fluid (ACSF; 31-33°C) consisting of (in mM): 113 NaCl, 2.5 KCl, 1.2 $MgSO_4 \cdot 7H_20$, 2.5 $CaCl_2 \cdot 2H_20$, 1 NaH_2PO_4, 26 $NaHCO_3$, 20 glucose, 3 Na-pyruvate, 1 Na-ascorbate, at a flow rate of 2-3 mL/min. All drugs (except CNQX, D-AP5, and strychnine) were dissolved in DMSO and included in ACSF and holding/incubation chambers also containing 0.1-0.5 mg/mL bovine serum albumin (except DO34). Drug concentrations for electrophysiology experiments (unless noted otherwise in figure legends) were (in µM): 5 CP55,940, 5 Rimonabant, 2.5 DO34, 1 JZL-184, 1 strychnine. Drug incubations were for a minimum of 30 minutes. For drug bath application experiments, cells were included in as data points in time course graphs provided they remained stable for a minimum of 15 minutes post-drug application, but were excluded from all other metrics if they did not remain stable the full time course. Slices incubated in CP55,940 or JZL-184 were used for < 120 min so as to minimize potential effects of CB_1 desensitization. Equal volumes of DMSO were added to all vehicle solutions.

Lateral habenula neurons were identified at 40X magnification with an immersion objective with differential interference contrast microscopy. The majority of cells patched were in the medial ~2/3 of the lateral habenula due to the greater visibility and number of healthy cells in the slice, similar as previously reported [253]. All recordings (except cell-attached) were carried out in whole-cell configuration with borosilicate glass pipettes (2-6 MΩ). For spontaneous synaptic recordings,

cells were voltage clamped at -70 or +20 mV with an intracellular solution containing (in mM): 120 Cs-gluconate, 2.9 NaCl, 5 tetraethylammonium-Cl, 20 HEPES, 2.5 Mg-ATP, 0.25 Na-GTP, 0.4 EGTA. Pharmacologically-isolated sIPSCs were recorded at -70 mV with an intracellular solution containing (in mM): 125 KCl, 4 NaCl, 10 HEPES, 4 Mg-ATP, 0.3 Na-GTP, and 10 Na-phosphocreatine. For evoked synaptic recordings cells were voltage clamped between -70-60 mV with an intracellular solution containing (in mM): 75 K-gluconate, 50 KCl, 4 NaCl, 10 HEPES, 4 Mg-ATP, 0.3 Na-GTP, 10 Na-phosphocreatine. 5 mM QX-314-Br was added fresh to internal aliquots for all voltage clamp experiments. Evoked or isolated spontaneous glutamate recordings were carried out in the presence of the $GABA_A$ receptor blocker picrotoxin (50 µM). Evoked or isolated spontaneous GABA recordings were carried out in the presence of the AMPA receptor antagonist CNQX (10-20 µM) and NMDA receptor antagonist D-AP5 (50 µM). Electrical stimulation of synaptic currents was achieved by placing a stimulating electrode in the stria medullaris. Electrically-evoked postsynaptic currents were adjusted for a stable response baseline between ~100-500 pA. For current clamp recordings, baseline current was adjust to hold cells at -65 mV with an intracellular solution containing (in mM): 125 K-gluconate, 4 NaCl, 10 HEPES, 4 Mg-ATP, 0.3 Na-GTP, and 10 Na-phosphocreatine. For cell-attached recordings, pipettes were filled with extracellular ACSF solution. Silent neurons were not included in cell-attached data sets. Liquid junction potentials were not corrected for. For all experiments, cells were allowed to stabilize for ≥3 minutes following break-in and cells with a series resistance of ≤30 MΩ were included in analyses for voltage clamp experiments.

***Ex vivo* optogenetics**

For electrophysiological interrogation of the LPO-LHb circuit, WT C57 mice were bilaterally injected with 175-200 nL of AAV5-CaMKIIaChR2(H134R)-eYFP into the LPO. For the EPN circuit, SOM::Ai14 mice were bilaterally injected with 175-250 nL of AAV5-EF1a-DIO-hChR2(H134R)-EYFP-WPRE into the EPN. Optogenetic recordings of synaptic currents were obtained via 473

nm light stimulation (1-2 ms pulse width) using a Thorlabs LEDD1B T-Cube driver or CoolLED stimulation system. Light intensity was adjusted to achieve a stable response at submaximal (~40-80%) amplitude between ~100-2000 pA.

Ex vivo Ca^{2+} imaging

Aldh1l1::Ai95D mice aged 5-10 weeks received 5 tamoxifen injections (75 mg/kg) 24 hr apart. A minimum of 2 weeks for Cre induction and GCaMP6f expression was allowed before sacrificing for imaging experiments. *Ex vivo* brain slice preparation, recovery, and holding for Ca^{2+} imaging was performed as detailed above for electrophysiological experiments. Following recovery, 200 µm coronal slices containing the lateral habenula were transferred to the electrophysiology rig and perfused with ACSF (described above; 31-33°C) containing 0.5 mg/mL bovine serum albumin (BSA) to assist with drug solubility. Slices were imaged at 40X using a standard DIC widefield microscope and a Nikon DS-Qi2 camera. GCaMP6f fluorescence was imaged via excitation with a 473 nm LED using a Thorlabs LEDD1B T-Cube driver. Videos were recorded using NIS-Elements software (Nikon, Melville, NY) with constant illumination and a video frame rate of 1 frame per second. Pseudocolored heat map images were generated from individual video frames in ImageJ.

Astrocytes in the lateral habenula were identified by their weak baseline GCaMP6f fluorescence and/or spontaneous Ca^{2+} activity. For local agonist application, CP55,940 was dissolved as an initial stock of 50 mM in DMSO, then diluted in ACSF containing 0.5 mg/mL BSA, for a final concentration of 100 µM CP55,940. This solution was loaded into patch pipettes connected to a Picospritzer III (Parker, Hollis, NH). For recordings, pipettes were maneuvered near identified cells at a distance of ~30-50 µm. A 30 second baseline was recorded before a 10 second pulse of CP55,940 was delivered (8-12 psi), followed by an additional 20 seconds of recovery. Mechanical agitation of visible blood vessels was avoided. For antagonist experiments,

the CB_1 receptor neutral antagonist NESS-0327 was used to negate the possibility of altered Ca^{2+} dynamics due to the inverse agonist properties of Rimonabant.

Immunohistochemistry and imaging

Mice were anesthetized using isoflurane and transcardially perfused with ice-cold phosphate buffered saline (PBS) followed by 4% paraformaldehyde (PFA) solution in PBS. Brains were dissected and stored overnight in 4% PFA and transferred to a 30% sucrose solution until tissue density reached equilibrium and brains sank to the bottom of their holding tubes. 40 µm brain sections were taken using a Leica CM3050 S cryostat (Leica Microsystem, Weitzlar, Germany). Brain sections were then washed in Tris-Buffered Saline (TBS) 3X for 10 minutes, followed by 30 minutes of block in TBS with 40% normal goat serum and 0.2% Triton X-100 (TBS+). Sections were then incubated in primary antibody diluted 1:500 in TBS+ overnight at room temperature with gentle agitation. The next day, sections were rinsed 3X in TBS+ then incubated in fluorescent secondary antibody diluted 1:1000 in TBS+ at room temperature for 2-3 hours with gentle agitation. Tissue was rinsed 3X with TBS, stained with DAPI, and mounted on slides in 0.15% porcine gelatin and allowed to dry in the dark overnight. Slides were then coverslipped with DPX mountant and imaged at 20X on a Zeiss LSM880 Airyscan Confocal Microscope or Nikon AX R confocal microscope. Quantification of cell marker overlap with GFAP-Cre-mCherry construct was conducted manually using the Colocalization plugin in Fiji (Version 2.9.0).

QUANTIFICATION AND STATISTICAL ANALYSIS

Statistics

Electrophysiological data was initially analyzed using ClampFit 10 software (Molecular Devices, San Jose, CA). Ca^{2+} imaging data was collected and videos were analyzed for changes in bulk astrocyte fluorescence at the target site using Inscopix Data Processing Software (Inscopix Inc., Mountain View, CA) and $\Delta F/F_{baseline}$ was calculated relative to the 30 second baseline. Datasets

were organized and quantified in Microsoft Excel and then transferred to GraphPad Prism 7 for generation of graphs and statistical analyses. For analysis of two groups, an unpaired or paired Student's t test was used, unless variance between groups was found to be significantly different as determined by an F test for equal variances, in which case a non-parametric Mann-Whitney U test was used. For analysis of three or more groups across a single independent variable, a one-way ANOVA was used with a Holm-Sidak posthoc multiple comparisons test between groups as noted in the figure legends. For analysis between two or more groups across two or more independent variables, a two-way ANOVA was used with a Holm-Sidak posthoc multiple comparisons test between groups as noted in the figure legends. Area under the curve data was quantified using the AUC calculation in Graphpad Prism 7. ROUT outlier test was applied to all individual datasets with a Q = 1%. When multiple measures were taken from an identified outlier, measures were treated independently and the corresponding cell was removed from only from that dataset. Sample sizes were derived empirically and based on our previous experience with these assays. Significance was determined as $p<0.05$ in all datasets. Data are represented as mean ± SEM excepted paired data showing individual values.

SUPPLEMENTAL INFORMATION

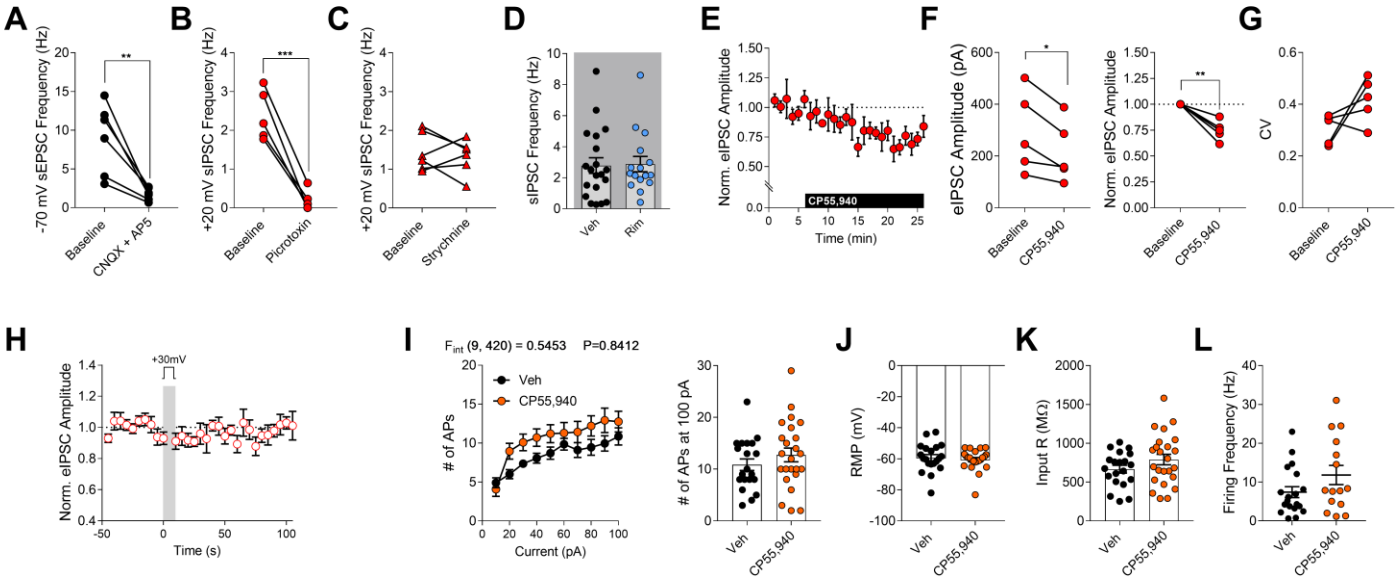

Figure 2-S1, Related to Figure 2-1

(A-C) Effects of synaptic blockers on electrically-isolated sEPSCs and sIPSCs in the lateral habenula (LHb). (A) Effect of CNQX + AP5 on sEPSCs recorded at -70 mV (n = 6 cells, 3 mice). (B) Effect of picrotoxin on sIPSCs recorded at +20 mV (n = 5, 2 mice). (C) Effect of strychnine on sIPSCs recorded at +20 mV (n = 6, 3 mice).

(D) Effect of Rim on pharmacologically-isolated sIPSCs recorded at -70 mV (Vehicle n = 20, 4 mice; Rim n = 16 cells, 4 mice).

(E-G) Effect of 10 μm CP55,940 bath application on electrically-evoked IPSCs in the LHb. (D) Time course of normalized eIPSC amplitude. (E) CP55,940 effects eIPSC amplitude. (F) CP55,950 effect on the eIPSC release probability metric coefficient of variation (CV) (n = 5, 3 mice).

(H) Time course for depolarization-induced suppression of inhibition in the presence of Rimonabant (GABA + Rim, quantified in Fig. 1H; n = 8, 3 mice).

(I) Effect of CP55,940 on LHb cellular excitability. Left: Number of action potentials (APs) fired in response to a series of 600 ms square wave current injections. Right: Direct quantification of number of APs at the max (100 pA) current injection (Vehicle n = 20, 7 mice; CP55,940 n = 24, 7 mice).

(J) Effect of CP55,940 on resting membrane potential of LHb neurons (Vehicle n = 20, 7 mice; CP55,940 n = 23, 7 mice).

(K) Effect of CP55,940 on input resistance in LHb neurons (Vehicle n = 20, 7 mice; CP55,940 n = 24, 7 mice).

(L) Effect of CP55,940 on tonic firing frequency of LHb neurons in cell-attached configuration (Vehicle n = 19, 4 mice; CP55,940 n = 15, 4 mice).

Data are mean ± SEM except paired data; n = number of cells. Data analyzed by (A-C, F-G) two-tailed paired t-test, (I, left) two-way ANOVA with Holm-Sidak multiple comparisons between Veh and CP55,940, or (D; I, right; J-L) two-tailed t-test. Significance for t-tests, ANOVA F and P values for drug x current interaction, and significance for post-hoc multiple comparisons shown on relevant panels (*p<.05, **p<0.01, ***p<0.001).

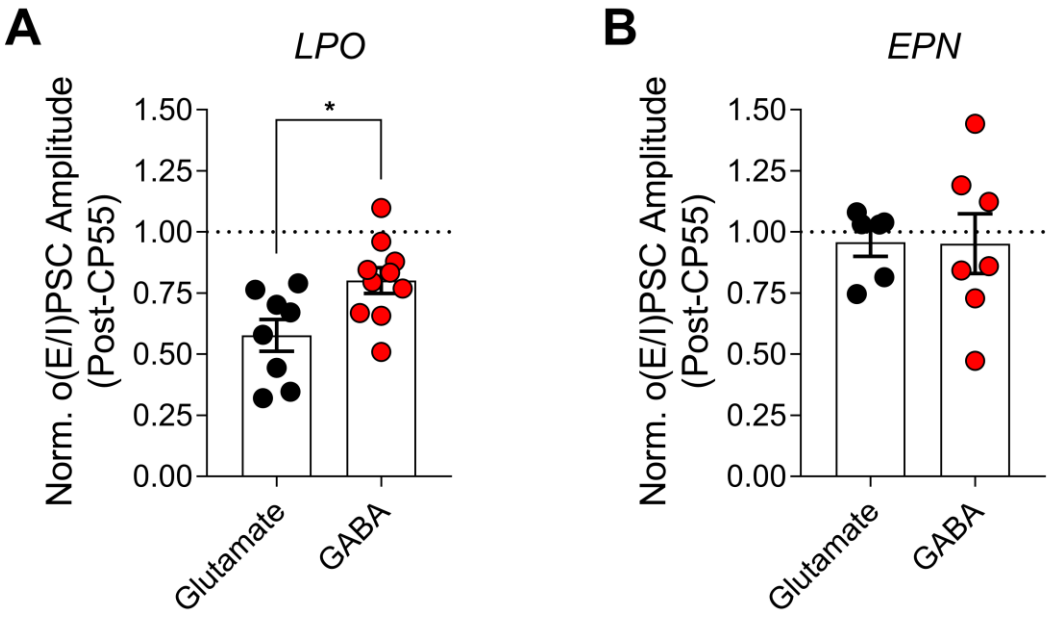

Figure 2-S2, Related to Figure 2-2

(A) Relative effects of CP55,940 on optically-evoked excitatory/inhibitory postsynaptic current amplitudes at LPO-LHb synapses. Data extracted from Figures 2C and 2E for direct comparison (Glutamate n = 8, 6 mice; GABA n = 10, 6 mice).

(B) Relative effects of CP55,940 on optically evoked excitatory/inhibitory postsynaptic current amplitudes at EPN-LHb synapses. Data extracted from Figures 2M and 2O for direct comparison (Glutamate n = 6, 5 mice; GABA n = 7, 5 mice).

Data are mean ± SEM; n = number of cells. Data in (A) and (B) analyzed by two-tailed t-test. Significance for t-tests shown on relevant panels (*p<0.05).

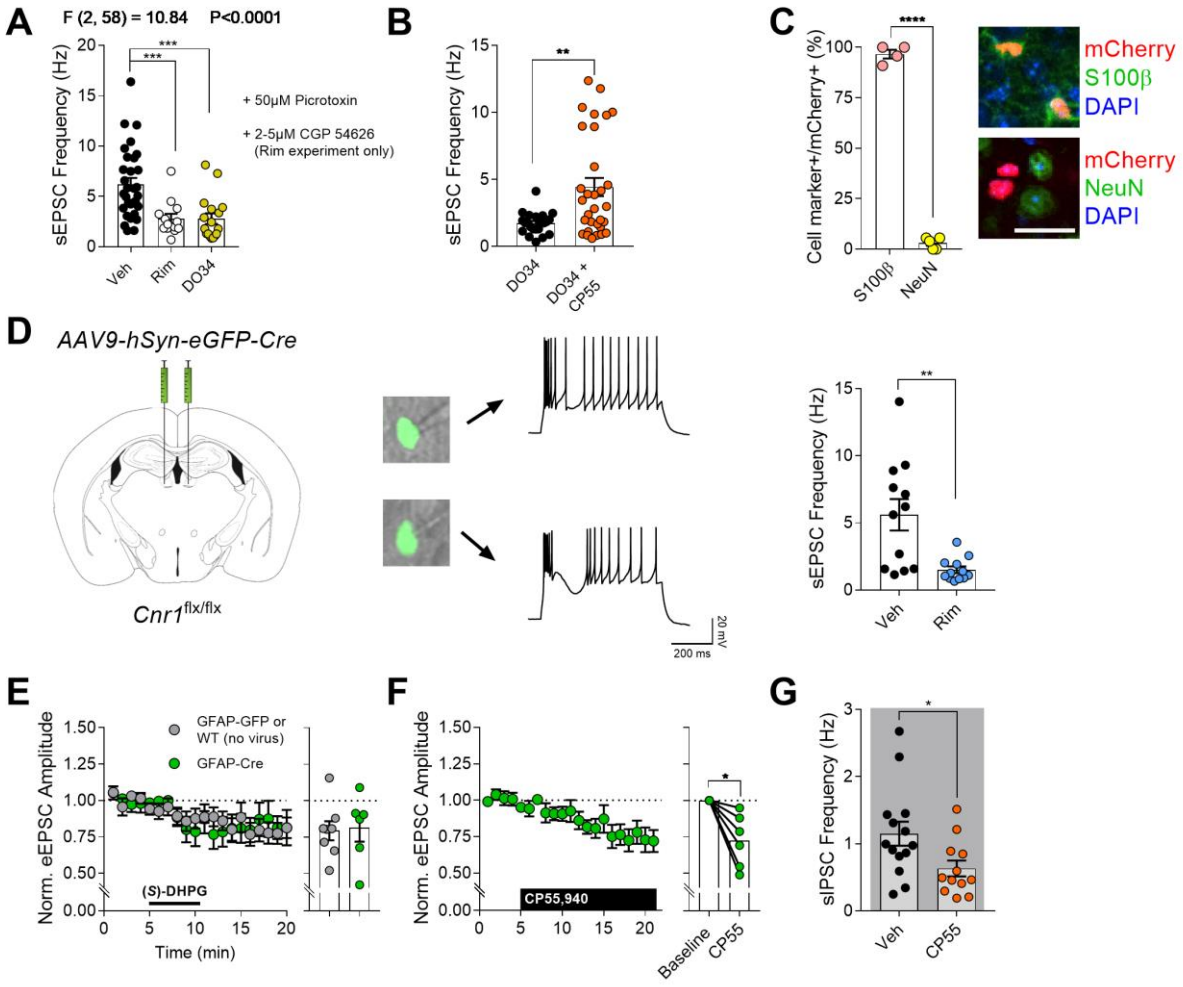

Figure 2-S3, Related to Figure 2-3

(A) Effects of Rimonabant and DO34 on pharmacologically-isolated sEPSC frequency (Veh n = 31, 8 mice; Rim n = 13, 4 mice; DO34 n = 17, 4 mice).

(B) Effect of CP55,940 on sEPSC frequency in the presence of DO34 (DO34 n = 22, 9 mice; DO34 + CP55 n = 31, 9 mice).

(C) Left: Quantification of GFAP-Cre-mCherry+ cell overlap with S100β or NeuN. Both *Cnr1*$^{flx/flx}$ and WT mice were included in analysis. Right: Staining for canonical astrocyte and neuron markers against expression of GFAP-Cre-mCherry; high zoom images supplementary to images from Figure 3D. Scale bar = 25 μm. (S100β n = 4 sections, 3 mice; NeuN n = 5 sections, 4 mice).

(D) Left: Schematic for viral injections in the LHb. Middle: Photomicrographs depicting recording from GFP-Cre+ cells and electrophysiological validation that Cre-GFP+ cells were predominantly neurons. Right: Effect of Rim on sEPSC frequency after CB_1 receptor deletion from LHb neurons.

Both GFP+ and GFP- neurons were recorded from to emulate the network effects of astrocyte CB_1 deletion in Figure 3 (Veh n = 12, 3 mice; Rim n = 12; 3 mice).

(E) Effects of DHPG and astrocytic CB_1 deletion on eEPSC amplitude. Viral strategy in *Cnr1*$^{flx/flx}$ mice was the same as in Figure 3D, except one uninjected WT mouse added to the control condition. Quantification on Right represents the last 2 minutes of the time course (GFAP-GFP or WT (no virus) n = 8, 4 mice; GFAP-Cre n = 6, 3 mice).

(F) Effects of CP55,940 bath application on eEPSC amplitude after astrocytic CB_1 receptor deletion. Viral strategy in *Cnr1*$^{flx/flx}$ mice was the same as in Figure 3D (Cre only). Quantification on Right represents the last 2 minutes of drug application (n = 6, 2 mice).

(G) Effects of CP55,940 on pharmacologically-isolated sIPSC frequency after astrocytic CB_1 receptor deletion. Viral strategy in *Cnr1*$^{flx/flx}$ mice was the same as in Figure 3D (Cre only; Veh n =14, 2 mice; CP55 n = 12, 2 mice).

Data are mean ± SEM; n = number of cells. Data analyzed by (A) one-way ANOVA with Holm-Sidak multiple comparisons relative to Veh, (B, D) Mann-Whitney U test, (C, E, G) two-tailed t-test, or (F) two-tailed paired t-test. ANOVA F and P value, significance for post-hoc multiple comparisons, and significance for U- and t-tests shown on relevant panels (*p<.05, **p<0.01, ***p<0.001, ****p<0.0001).

CHAPTER III

CANNABIDIOL DIFFERENTIALLY MODULATES SYNAPTIC RELEASE AND CELLULAR EXCITABILITY IN THE CENTRAL AND BASOLATERAL AMYGDALA

Nathan D. Winters[1,2], Farhana Yasmin[3], Veronika Kondev[2,4], Brad A. Grueter[1,2,4,5,6], and Sachin Patel[3,7*]

[1]Department of Pharmacology, Vanderbilt University School of Medicine, Nashville, TN, USA.

[2]Vanderbilt Center for Addiction Research, Vanderbilt University School of Medicine, Nashville, TN, USA.

[3]Northwestern Center for Psychiatric Neuroscience, Department of Psychiatry and Behavioral Sciences, Feinberg School of Medicine, Northwestern University, Chicago, IL, USA.

[4]Vanderbilt Brain Institute, Vanderbilt University School of Medicine, Nashville, TN, USA.

[5]Department of Anesthesiology, Vanderbilt University School of Medicine, Nashville, TN, USA.

[6]Department of Molecular Physiology and Biophysics, Vanderbilt University School of Medicine, Nashville, TN, USA.

[7]Lead contact.

*Correspondence: sachin.patel@northwestern.edu

ABSTRACT

Cannabidiol (CBD) is a non-psychoactive constituent of the *Cannabis* plant that has purported effectiveness in treating an array of stress-related neuropsychiatric disorders. The pharmacology of CBD is complex and contributes to a broad lack of understanding of the neurophysiological effects of the drug and a dearth of quality clinical data to support its medicinal use. The amygdala is a subcortical brain structure that regulates emotional behavior, and its dysfunction shares numerous overlapping implications with CBD, including links to anxiety and posttraumatic stress disorder. Despite this, the direct effects of CBD on amygdala physiology are not known. Using electrophysiology and pharmacology, we report that CBD reduces presynaptic neurotransmitter release in the amygdala, and these effects are dependent on subnucleus and cell type. Furthermore, CBD broadly decreases cellular excitability across amygdala neurons. These data present mechanisms by which CBD may act to decrease amygdala activity to potentially produce stress-mitigating therapeutic effects.

INTRODUCTION

Cannabidiol (CBD) is a major phytocannabinoid constituent of the *Cannabis* plant that has seen substantial increases in commercialization and interest in its therapeutic utility for a variety of conditions[255,256]. In contrast to Δ^9-tetrahydrocannabinol (THC), the major psychoactive -*Cannabis*-derived cannabinoid that acts as a $CB_{1/2}$ receptor partial agonist, CBD is non-psychoactive and exhibits relatively complex polypharmacology in the central nervous system[177,178]. Given the pleiotropic nature of CBD actions in the brain, the mechanisms subserving its purported therapeutic effects remain largely unknown. One series of indications for CBD that have gained a particularly strong degree of interest is the reported mitigation of stress-related neuropsychiatric disorders, such as anxiety[206,219] and posttraumatic stress disorder (PTSD)[205]. However, mechanistic studies of the effects of CBD on the limbic brain circuitry implicated in the etiology of these disorders are lacking.

A major integrative hub in the brain's stress response network that may serve as a locus for the effects of CBD on anxiety and fear is the amygdala, a subcortical brain structure that heavily regulates emotional behavior[257]. Amygdala plasticity is heavily implicated in anxiety and in fear learning and extinction[258,259], and human studies have demonstrated positive correlations between amygdala reactivity and stress susceptibility[260]. CBD can reduce basal activity in portions of the rodent amygdala, as measured by expression of the immediate early gene c-Fos[261]. Behaviorally, CBD has been shown to reduce conditioned fear expression in rodents[237,262], as well as facilitate fear extinction in both rodents[263] and humans[264]. Furthermore, direct cannulation of CBD into the amygdala can produce an anxiolytic effect in rodents[265] and multiple studies have reported that CBD decreases amygdala activity in human patients[266,267], supporting the hypothesis that CBD may directly modulate amygdala physiology.

The amygdala is divided into numerous subnuclei, each with unique circuitry, cell types, and relative functions[257]. The central and basolateral nuclei of the amygdala (CeA; BLA) are both critical in the integration of environmental information to guide optimal behavioral output and dysregulation of these structures is linked to numerous affective disorders[257,268,269]. Here we utilized electrophysiological and pharmacological approaches to examine the effects of CBD on CeA and BLA neurophysiology and report the CBD exhibits inhibitory pharmacodynamic effects on amygdala synaptic transmission and cellular excitability that depend on subnucleus and cell type, collectively suggesting that CBD may reduce amygdala activity. These findings could have mechanistic implications for the purported anxiolytic effects of CBD and provide insight for more targeted studies aimed at elucidating the mechanisms and efficacy of CBD for treating neuropsychiatric disorders.

RESULTS AND DISCUSSION

Cannabidiol reduces GABAergic synaptic transmission in the CeA with no effect on BLA synapses. To examine the effects of CBD on synaptic transmission in the CeA, we utilized patch clamp electrophysiology in acute *ex vivo* brain slices and recorded from neurons in the lateral subdivision of the CeA, which is comprised of GABAergic medium spiny-like neurons. Using a protocol that allows for the electrical isolation and of both spontaneous excitatory and inhibitory postsynaptic currents (sEPSCs; sIPSCS) onto single CeA neurons (**Figure 3-1A**), we incubated slices in a series of concentrations of CBD (2-20μM) to examine its influence on synaptic activity. CBD incubation had no effect on sEPSC frequency or amplitude at any concentration tested (**Figure 3-1B**). In contrast, CBD exerted a dose-dependent decrease in sIPSC frequency, with a small but significant reduction in sIPSC amplitude at 20μM (**Figure 3-1C**). Transformation of the data found a relative IC_{50} of 4.07μM CBD for the reduction of sIPSC frequency. When taking the ratio of sEPSCs and sIPSCs within single cells, we found a significant increase in the excitation-inhibition (E/I) ratio at 10 and 20μM CBD (**Figure 3-1D**). Given that we

saw maximal effects at 20µM CBD and comparable brain and plasma levels of CBD have been observed in rodents after *in vivo* administration[233], we utilized 20µM CBD for the remainder of the experiments.

We next examined synaptic transmission onto principal neurons in the BLA (**Figure 3-2A**), largely comprised of glutamatergic pyramidal neurons, using the same electrophysiological protocol as in **Figure 3-1A**. In contrast to the CeA, 20µM CBD had no effect on sEPSC frequency or amplitude, sIPSC frequency or amplitude, or E/I ratio onto BLA neurons (**Figure 3-2B-D**). These data indicate that CBD selectively dampens inhibitory transmission onto CeA neurons while leaving synaptic transmission in the BLA unaffected, revealing subnucleus-specific pharmacology of CBD in the amygdala.

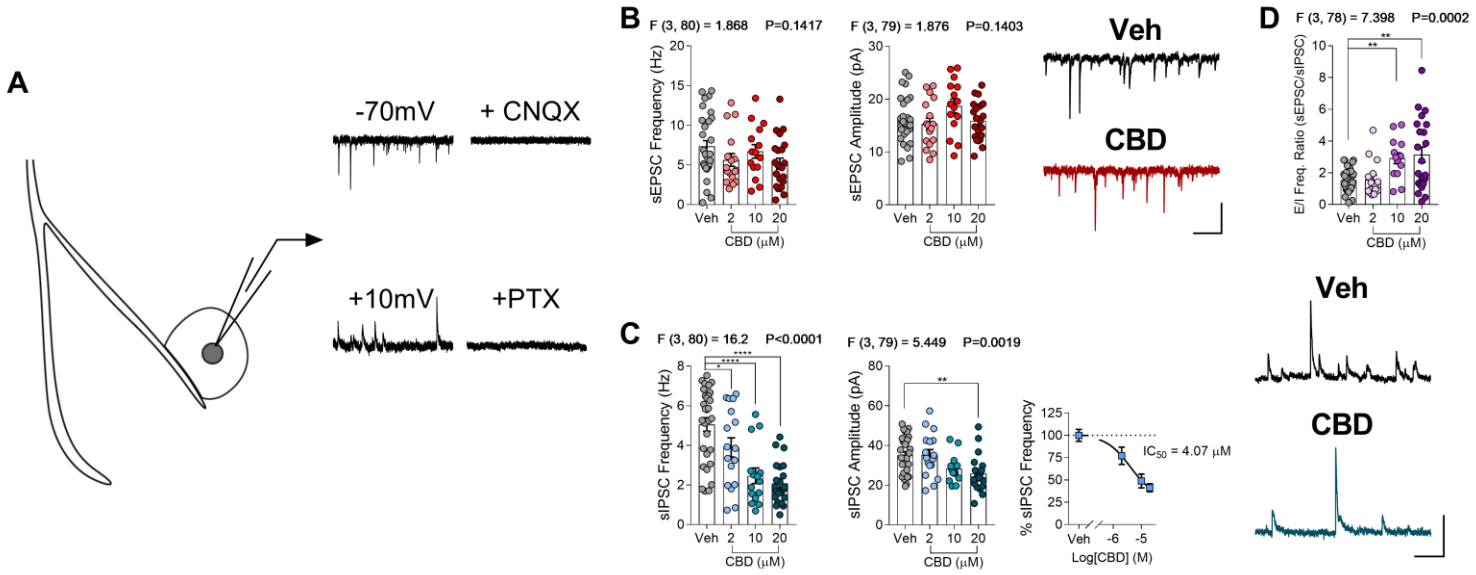

Figure 3-1: Cannabidiol reduces GABAergic synaptic transmission in the CeA. (A) Schematic depicting recording strategy for dual spontaneous excitatory and inhibitory postsynaptic currents; pharmacological validation of current identities (CNQX = AMPAR antagonist, Picrotoxin = $GABA_AR$ antagonist). **(B)** CBD concentration series effects on sEPSC frequency and amplitude (Scale = 20pA, 250ms). **(C)** CBD concentration series effects on sIPSC frequency and amplitude (Scale = 20pA, 250ms); concentration-response curve for the reduction

in sIPSC frequency. **(D)** CBD concentration-response series effects on excitation-inhibition ratio onto CeA neurons. (Veh n = 30, 5 mice; 2µM n = 17, 3 mice; 10µM n = 15, 3 mice; 20µM n = 21-22, 4 mice). Data are mean ± SEM; n = number of cells. Data analyzed by one-way ANOVA with Holm-Sidak multiple comparisons relative to Vehicle. ANOVA F and P values and significance for post-hoc multiple comparisons shown on relevant panels (*p<.05, **p<0.01, ****p<0.0001).

Cannabidiol exhibits cell type-specific modulation of CeA synaptic transmission. The CeA is comprised of a number of genetically distinct cell types, the most notable identified by their largely non-overlapping expression of somatostatin (SOM+), corticotropin-releasing factor (CRF+), or protein kinase C-δ (PKCδ+)[270-272]. Each of these cell types exhibit distinct physiological and behavioral properties[273] and can vary in the relative strength of specific presynaptic inputs[259,270,271]. To probe for potential cell type differences in the modulation of synaptic release by CBD, we utilized genetic reporter lines for each of these cell populations. This was achieved by crossing mice expressing Cre recombinase under the SST, CRF, or PKCδ promoters with Ai14 mice, which express a Cre-dependent tdTomato construct. This approach allows for the visual identification of genetically-defined neurons based on their fluorescence (**Figure 3-3A, E, I**). First examining SOM+ neurons, we found that 20µM CBD had no effect on sEPSC frequency or amplitude but decreased sIPSC frequency, with no effect on amplitude (**Figure 3-3B-C**). This resulted in a non-significant increase (p=0.0627) in E/I ratio onto SOM+ neurons (**Figure 3-3D**). Next examining CRF+ neurons, we found that 20µM CBD reduced sEPSC frequency with no effect on amplitude (**Figure 3-3F**), revealing an effect of CBD on glutamatergic transmission that was absent in SOM+ and unlabeled CeA neurons. CBD also reduced sIPSC frequency and amplitude and increased E/I ratio onto CRF+ neurons (**Figure 3-3G-H**). These findings demonstrate a degree of cell type specificity for CBD in modulating CeA synaptic transmission, suggesting that CBD may differentially engage subsets of synapses with distinct molecular properties. Lastly, examining PKCδ+ neurons, 20µM CBD had no effect on sEPSC frequency or amplitude (**Figure 3J**), but significantly reduced sIPSC frequency and had no effect on sIPSC

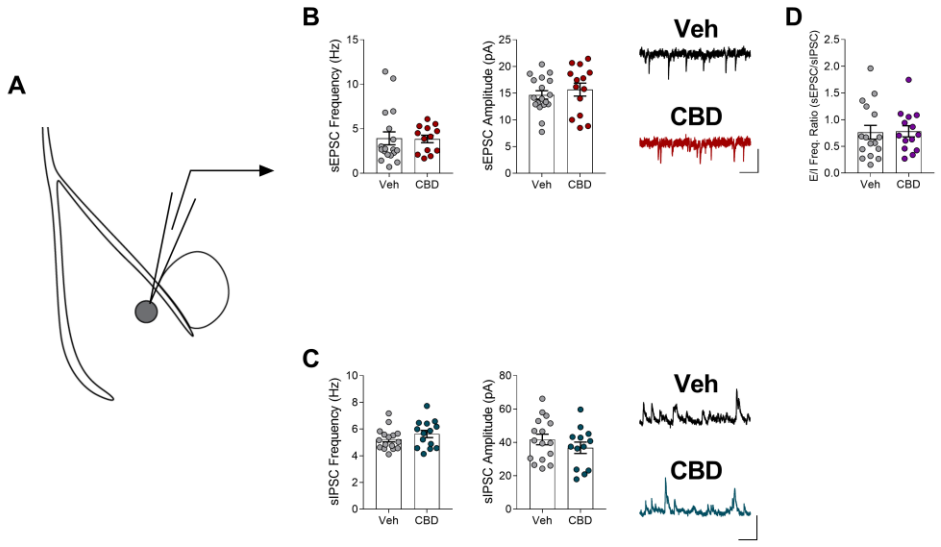

Figure 3-2: Cannabidiol has no effect on synaptic transmission in the BLA. (A) Schematic depicting recordings from BLA neurons. **(B)** Effects of 20µM CBD on sEPSC frequency and amplitude (Scale = 20pA, 250ms). **(C)** Effects of 20µM CBD on sIPSC frequency and amplitude (Scale = 50pA, 250ms). **(D)** Effect of 20µM CBD on excitation-inhibition ratio onto BLA neurons. (Veh n = 16-18, 5 mice; CBD n = 13-14, 5 mice). Data are mean ± SEM; n = number of cells. Data analyzed by two-tailed t-tests.

amplitude (**Figure 3-3K**). CBD significantly increased E/I ratio onto PKCδ+ neurons (**Figure 3-3L**). While the effects of CBD on SOM+ and PKCδ+ synapses were similar, the selective reduction of glutamate release onto CRF+ neurons is intriguing. It has been demonstrated that the BLA projection to the CeA exhibits a bias onto CRF+ neurons, relative to CRF- neurons[259], and it is tempting to speculate that the BLA-CeA circuit may be a potential target for CBD to dampen intra-amygdala communication. Plasticity in this circuit is highly relevant for amydala-dependent learning mechanisms such as Pavlovian fear conditioning[259], and could have important mechanistic implications for the studies that have reported CBD-mediated reductions in the expression of conditioned fear behaviors[237]. This would lend translational credibility to the application of CBD for the treatment of stress-related neuropsychiatric disorders, such as PTSD[205].

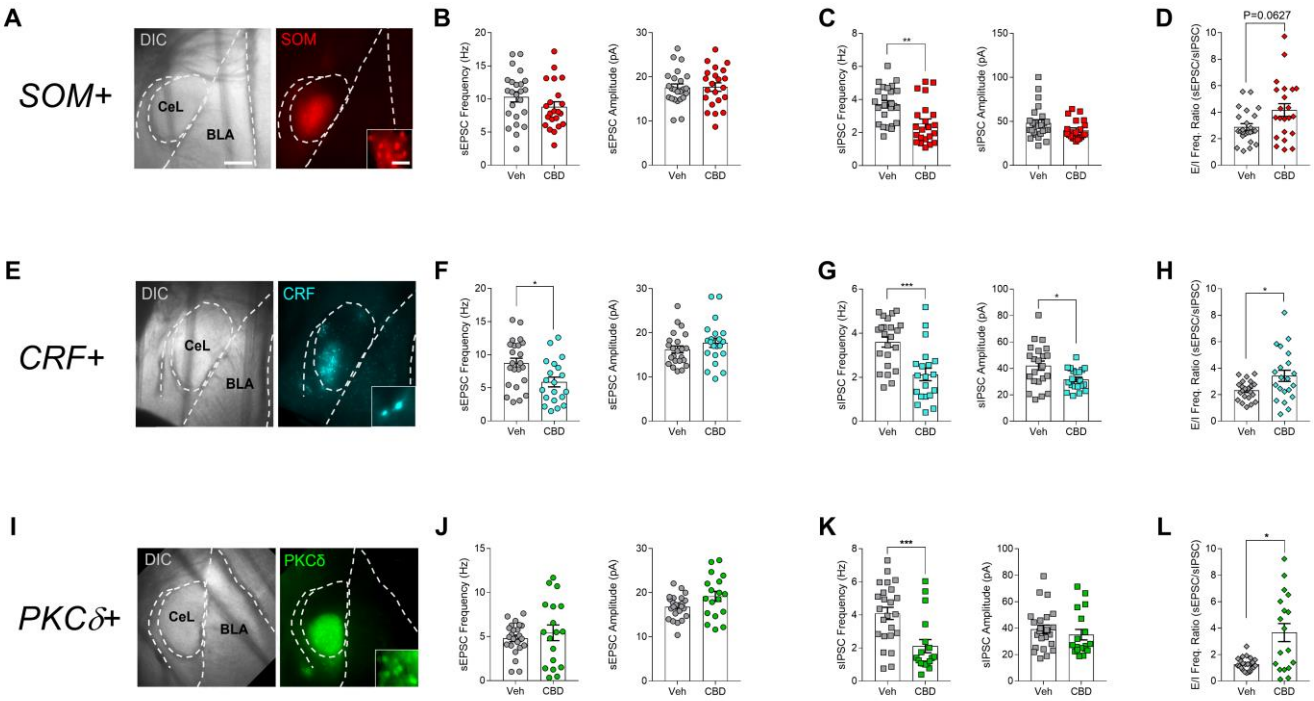

Figure 3-3: Cannabidiol exhibits cell type-specific modulation of CeA synaptic transmission. (A) DIC and fluorescence 4x images of the amygdala from a SOM::Ai14 reporter mouse. Inset: 40x image of fluorescent SOM+ cells. Scale bars = 250 µm, 25 µm for inset; scale derived from Allen Brain Atlas. **(B)** Effects of 20µM CBD on SOM+ sEPSC frequency and amplitude. **(C)** Effects of 20µM CBD on SOM+ sIPSC frequency and amplitude. **(D)** Effect of 20µM CBD on SOM+ E/I ratio (SOM+ Veh n = 24-25, 6 mice; SOM+ CBD n = 21-22, 6 mice). **(E-H)** Same as **A-D** for CRF+ cells (CRF+ Veh n = 22-23, 6 mice; CRF+ CBD n = 20-21, 6 mice). **(I-L)** Same as **A-D** for PKCδ+ cells (PKCδ+ Veh n = 23-24, 6 mice; PKCδ+ CBD n = 18, 6 mice). Data are mean ± SEM; n = number of cells. Data analyzed by **(B, C** left**, F, G** left**, K)** two-tailed t-test or **(C** right**, D, G** right**, H, J, L)** Mann-Whitney U-test. Significance for t- and U-tests shown on relevant panels (*p<.05, **p<0.01, ***p>.001, ****p<0.0001).

Cannabidiol decreases the cellular excitability of CeA and BLA neurons. CBD engages a number of targets that can influence cellular excitability, including various ion channels and GPCRs[177]. To determine if CBD modulates the excitability of amygdala neurons, we incubated slices in 20µM CBD and measured action potential firing and basal membrane properties of CeA and BLA neurons. In the CeA, CBD caused a significant reduction in the number of action potentials fired in response to square wave current injections, suggesting a reduction in intrinsic

excitability (**Figure 3-4A-B**). CBD had no effect on resting membrane potential (RMP) or input resistance of CeA neurons (**Figure 3-4C-D**).

We next repeated these experiments in principal BLA neurons. Similar to the effect on CeA neurons, CBD caused a significant reduction in the number of action potentials fired by BLA neurons in response to square wave current injections (**Figure 3-4E-F**). CBD also caused a small but significant hyperpolarization of the RMP of BLA neurons (**Figure 3-4G**). While this effect on RMP logically agrees with the reduction in cellular excitability, it is unclear what contribution this effect may have given the normalization of all cells to -70 mV for current injection experiments. CBD had no effect on the input resistance of BLA neurons (**Figure 3-4D**). Collectively, these broad CBD-mediated reductions in amygdala neuron excitability across the BLA and CeA could be highly applicable to the effects of CBD on amygdala physiology and related behaviors. For example, these effects could be relevant for the reports of CBD reducing fear expression (CITE) and CeA c-Fos expression[261] in rodents and potentially the reductions in human amygdala reactivity in patients treated with CBD[266,267].

Cannabidiol requires action potentials to modulate CeA GABAergic transmission.

CBD engages a variety of molecular targets in the CNS[177], and thus the effects of CBD on synaptic GABA release in the CeA may be explained by multiple potential mechanisms. Two potential examples include 1) mechanisms relating to metabotropic signaling at the presynaptic terminal to directly reduce neurotransmitter release probability or 2) cellular excitability effects that reduce presynaptic action potentials in local inhibitory networks and subsequent GABA release. To gain insight into which of these mechanisms likely mediates these effects, we examined CBD modulation of CeA synaptic transmission while blocking all action potential generation. To do this, we measured miniature excitatory and inhibitory postsynaptic currents (mEPSCs; mIPSCs) in the presence of the voltage-gated sodium channel blocker tetrodotoxin (TTX, 1µm) (**Figure 3-5A**). As seen with sEPSCs, CBD had no effect on mEPSC frequency or

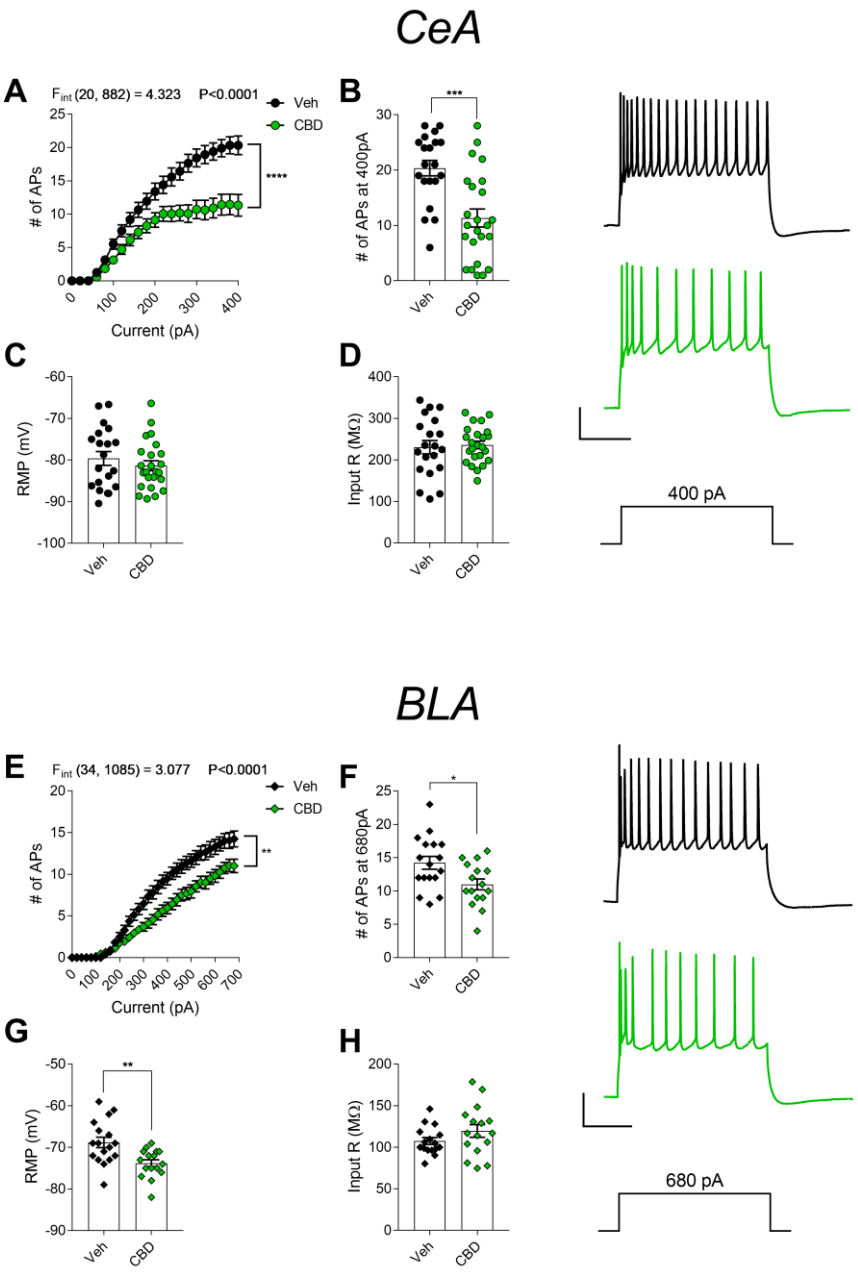

Figure 3-4: Cannabidiol decreases the cellular excitability of BLA and CeA neurons. (A) Effect of 20µM CBD on square wave current-evoked action potential firing in CeA neurons. **(B)** Direct quantification of max current injection from **A** (Scale = 25mV, 200ms). **(C-D)** Effects of 20µM CBD on **(C)** RMP and **(D)** Input R of CeA neurons (CeA Veh n = 20, 5 mice; CeA CBD n = 24, 5 mice). **(E)** Same as **A** for BLA neurons. **(F)** Same as **B** for BLA neurons (Scale = 25mV, 200ms). **(G-H)** Same as **C-D** for BLA neurons (BLA Veh n = 16-17, 5 mice; BLA CBD n = 16, 5 mice). Data are mean ± SEM; n = number of cells. Data analyzed by 2-way ANOVA with Holm-Sidak multiple comparisons **(A, E)** or two-tailed t-test **(B-D, F-H)**. ANOVA F and P values and significance for post-hoc multiple comparisons and t-tests shown on relevant panels (*p<.05, **p<0.01, ***p>.001, ****p<0.0001).

amplitude (**Figure 3-5B**). Interestingly, CBD had no effect on mIPSC frequency or amplitude and no effect on E/I ratio (**Figure 3-5C-D**). This directly contrasts the CBD-mediated reduction in sIPSCs observed throughout the study and suggests that CBD selectively inhibits action potential-dependent GABA release. The action potential dependency for CBD in reducing synaptic GABA

release is particularly interesting considering the effect of CBD on reducing CeA neuron excitability (**Figure 3-4A-B**) and high degree of recurrent inhibitory connectivity within the CeA[270,273]. It is interesting to speculate that CBD may reduce local GABA release in the CeA as a result of inhibiting tonic firing activity in local microcircuits, which would be predicted to override the enhanced E/I ratio onto these cells and cause a net reduction in CeA output.

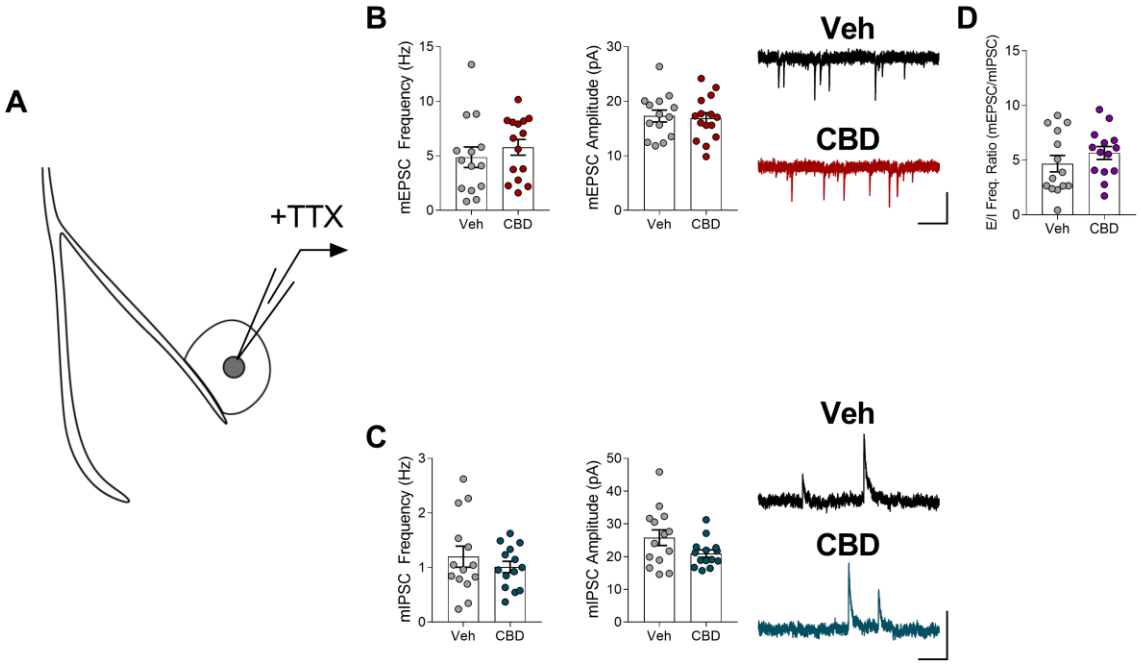

Figure 3-5: Cannabidiol requires action potentials to modulate CeA GABAergic transmission. (A) Schematic depicting recordings from CeA neurons in the presence of TTX. **(B)** Effects of 20µM CBD on mEPSC frequency and amplitude (Scale = 20pA, 250ms). **(C)** Effects of 20µM CBD on mIPSC frequency and amplitude (Scale = 40pA, 250ms). **(D)** Effect of 20µM CBD on excitation-inhibition ratio onto CeA neurons. (Veh n = 14, 4 mice; CBD n = 14-15, 4 mice). Data are mean ± SEM; n = number of cells. Data analyzed by (B, D) two-tailed t-test or (C) Mann-Whitney U-test.

Conclusions

The neurophysiological mechanisms of CBD are poorly understood and thus present a significant barrier to designing systematic clinical investigations into this drug for treating

neuropsychiatric disorders. Our data collectively provide, to our knowledge, the first direct mechanistic evidence for CBD in modulating amygdala physiology and propose cellular mechanisms by which CBD may reduce amygdala activity. Low micromolar plasma concentrations of CBD have been observed in human trials[234] and we observed significant alterations in amygdala synaptic transmission at 2 µM CBD, suggesting these findings could feasibly have high translational relevance. Given the implications of amygdala dysfunction across numerous neuropsychiatric conditions[257,268,269], this work could have significant implications for understanding the mechanisms subserving the reported but poorly understood effects of CBD in treating these conditions[205,206,219]. Future studies should aim to draw causal links between these mechanisms and the effects of CBD on amygdala-related behaviors and pathophysiology. This line of research will likely establish a framework for more targeted clinical studies that will more effectively illuminate the therapeutic potential of CBD in treating neuropsychiatric disorders.

MATERIALS AND METHODS

Subjects

All experiments were approved by the Vanderbilt University Institutional Animal Care and Use Committees and were conducted in accordance with the National Institute of Health guidelines for the Care and Use of Laboratory Animals. Male and female mice age 5-16 weeks were used for all experiments. C56BL6/J mice were obtained from Jackson Laboratories (Cat. # 000664) or bred in-house. SST-IRES-Cre (Jackson Laboratories, Cat. # 013044), CRF-IRES-Cre (Jackson laboratories Cat. # 012704), and Ai14 (The Jackson Laboratory, Cat. # 007914) were purchased and crossed in-house to generate SST::Ai14 and CRF::Ai14 mice. PKCδ-Cre mice were obtained from Danny Winder at Vanderbilt University, where they were bred in house following in-vitro fertilization of female mice with sperm from the Mutant Mouse Resource and Research Centers (MMRRC) at UC-Davis (# 011559-UCD, STOCK Tg(Prkcd-glc-1/CFP,-cre)EH124Gsat/Mmucd). PKCδ-Cre mice were then crossed with Ai14 mice in-house to generate PCKδ::Ai14 mice. Sex

was not a primary analysis factor and no overt sex differences were observed, thus all data are pooled from both sexes.

Ex vivo electrophysiology

For acute *ex vivo* brain slice preparation, mice were anesthetized using isoflurane, and transcardially perfused with ice-cold and oxygenated cutting solution consisting of (in mM): 93 N-Methyl-D-glucamine (NMDG), 2.5 KCl, 20 HEPES, 10 $MgSO_4 \cdot 7H_20$, 1.2 NaH_2PO_4, 0.5 $CaCl_2 \cdot 2H_20$, 25 glucose, 3 Na-pyruvate, 5 Na-ascorbate, and 5 N-acetylcysteine. Mice were then decapitated and brains collected. 250 µm coronal slices containing the amygdala were prepared on a vibrating microtome using standard procedures. Following collection of coronal sections, the brain slices were transferred to a 34°C chamber containing oxygenated cutting solution for a 10-20 minute recovery period. Slices were then transferred to a 25°C holding chamber with solution consisting of (in mM): 92 NaCl, 2.5 KCl, 20 HEPES, 2 $MgSO_4 \cdot 7H_20$, 1.2 NaH_2PO4, 30 $NaHCO_3$, 2 $CaCl_2 \cdot 2H_20$, 25 glucose, 3 Na-pyruvate, 5 Na-ascorbate, 5 N-acetylcysteine and were allowed to recover for ≥30 min. For recording, slices were placed in a perfusion chamber and continuously perfused with oxygenated artificial cerebrospinal fluid (ACSF; 31-33°C) consisting of (in mM): 113 NaCl, 2.5 KCl, 1.2 $MgSO_4 \cdot 7H_20$, 2.5 $CaCl_2 \cdot 2H_20$, 1 NaH_2PO_4, 26 $NaHCO_3$, 20 glucose, 3 Na-pyruvate, 1 Na-ascorbate, at a flow rate of 2-3 mL/min. Cannabidiol was dissolved in DMSO at a stock concentration of 50mM and added to ACSF and holding/incubation chambers containing 0.5 mg/mL bovine serum albumin. Equivalent volumes of DMSO were added to vehicle ACSF. CBD incubation was ≥30 min prior to recordings.

Amygdala neurons were identified at 40X magnification with an immersion objective with differential interference contrast microscopy. All recordings (except cell-attached) were carried out in whole-cell configuration with borosilicate glass pipettes (2-6 MΩ). For spontaneous synaptic recordings, cells were voltage clamped at -70 or +10 mV with an intracellular solution containing (in mM): 120 Cs-gluconate, 2.9 NaCl, 5 tetraethylammonium-Cl, 20 HEPES, 2.5 Mg-ATP, 0.25

Na-GTP. For current clamp recordings, baseline current was adjusted to hold cells at -70 mV with an intracellular solution containing (in mM): 125 K-gluconate, 4 NaCl, 10 HEPES, 4 Mg-ATP, 0.3 Na-GTP, and 10 Na-phosphocreatine. For cell-attached recordings, pipettes were filled with extracellular ACSF solution. Liquid junction potentials were not corrected for. For all experiments, cells were allowed to stabilize for ≥3 minutes following break-in and cells with a series resistance of ≤30 MΩ were included in analyses for voltage clamp experiments.

Quantification and Statistical Analysis

Electrophysiological data was initially analyzed using ClampFit 10 software (Molecular Devices, San Jose, CA). Datasets were organized and quantified in Microsoft Excel and then transferred to GraphPad Prism 7 for generation of graphs and statistical analyses. For analysis of two groups, an unpaired or paired Student's t test was used, unless variance between groups was found to be significantly different as determined by an F test for equal variances, in which case a non-parametric Mann-Whitney U test was used. For analysis of three or more groups across a single independent variable, a one-way ANOVA was used with a Holm-Sidak posthoc multiple comparisons test between groups as noted in the figure legends. For analysis between two or more groups across two or more independent variables, a two-way ANOVA was used with a Holm-Sidak posthoc multiple comparisons test between groups. Grubbs' outlier test was applied to all individual datasets with $\alpha = 0.05$. When multiple measures were taken from an identified outlier, measures were treated independently and the corresponding cell was removed from only from that dataset. Sample sizes were derived empirically and based on our previous experience with these assays. Significance was determined as $p<0.05$ in all datasets. Data are represented as mean ± SEM excepted paired data showing individual values.

LEAD CONTACT AND DATA AVAILABILITY

Further information and requests for resources and reagents should be directed to and will be

fulfilled by the Lead Contact, Sachin Patel (sachin.patel@northwestern.edu).

AUTHOR CONTRIBUTIONS

N.D.W., F.Y., and V.K. conducted all experiments and analyzed the data in the laboratories of B.A.G and S.P. N.D.W and S.P. contributed to experimental design and are responsible for study conception and data interpretation. N.D.W. and S.P. wrote the manuscript.

FUNDING AND ACKNOWLEDGEMENTS

These studies were supported by NIH grants MH107435 (S.P.) and MH119817 (S.P.). PCKδ-Cre mice were generously supplied by Danny Winder at Vanderbilt University, as noted in the methods.

DECLARATION OF INTERESTS

S.P. is a scientific consultant for Psy Therapeutics, Janssen Pharmaceuticals, and Jazz Pharmaceuticals unrelated to the present work. All other authors declare no conflicts of interest.

CHAPTER IV

CONCLUSIONS, LIMITATIONS, AND FUTURE DIRECTIONS

Physiology and Functions of the Multicellular Endocannabinoid System in the Lateral Habenula

The research presented in Chapter II of this thesis presents a foundational framework for the basic cellular and molecular functions of the eCB system in regulating synaptic physiology in the LHb. In summary, we identify that canonical cannabinoid-mediated synaptic suppression occurs at both glutamatergic and GABAergic terminals, in agreement with a small number of previous reports[140,160,161]. We also uncovered a novel astrocyte-dependent eCB mechanism that tonically potentiates spontaneous glutamate release. This adds to a growing body of literature demonstrating astrocytic eCB signaling as an effective synaptic neuromodulatory mechanism[35]. The figure below presents a graphical summary of our current understanding of the LHb eCB system, based on our data.

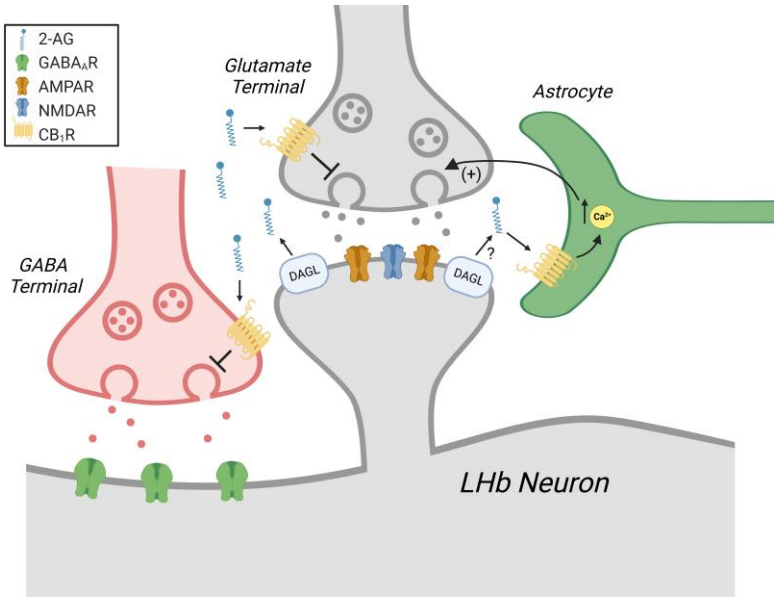

Figure 4-1: Current model for synaptic functions of the eCB system in the LHb.

Although much work remains to be done in identifying the functional relevance of these mechanisms, they do provide an intriguing level of logical agreement with previous speculation that eCBs may engage an activity-promoting, aversive-like cellular mechanism in the LHb based on the pro-depressive nature of local CB1 activation[158]. Although the observation that intra-LHb CB1 blockade produces antidepressant-like effects is surprising given the broad stress buffering functions of eCB signaling (detailed in Chapter I), similar paradoxical observations have been reported previously[274,275]. It has also been reported that CB1 antagonism increased central monoaminergic transmission[276]. Given the strong negative control the LHb exerts over monoaminergic activity, it is tempting to hypothesize that CB1 blockade-induced reductions in excitatory transmission onto LHb neurons may be one potential mechanism for this observation. It remains to be shown whether there exists a causal relationship between our reported mechanisms and these observations.

A major question that remains unanswered is, what are the relative contributions of neuronal vs. astrocytic eCB signaling mechanisms in the LHb? Similar questions remain where similar functionally opposing mechanisms have been identified, such as in the hippocampus[37,248]. One potential speculative explanation is that neuronal CB1 may act canonically as a negative feedback mechanism in response to enhanced activity at the level of a single LHb neuron, whereas the potentiating astrocyte mechanism may act as a regulator of the broader local glutamatergic network. This idea is supported by observations from other brain regions that demonstrate that astrocytes tend to couple together via gap junctions, allowing eCB signals to be laterally transduced to sites distal from the initial CB1 receptor activation, whereas at proximal sites CB1 activation on presynaptic terminals tends to predominate[37,38]. Another alternative explanation, though perhaps less likely, is that different synapses may be under the control of either neuronal *or* astrocyte CB1 signaling, and these systems exist in parallel to modulate distinct populations of

synapses. To this end, our study presents the first circuit-specific investigation of eCB function in the LHb and given the number of inputs not screened in our study, the uncovering of divergent eCB modulation across distinct LHb afferent circuits is a likely outcome of future research. It remains to be determined whether the LPO and EPN are definitively *not* regulated by astrocytic CB1, or if bulk stimulation methods override this potentially subtle neuromodulation[248], as discussed in Chapter II. Circuit-specific manipulations will be a likely necessity to uncover a cohesive understanding of neuronal vs. astrocytic CB1 control over LHb glutamatergic transmission.

Given the robust modulation of LHb glutamatergic transmission by astrocytic CB1 transmission observed in our data, it is interesting to speculate if astrocytic eCB signaling in the LHb contributes to the numerous reported contexts in which presynaptic glutamatergic plasticity is observed. For example, inescapable stress exposure potentiates presynaptic glutamate release onto LHb neurons[111], and the LHb exhibits broad temporal variations in presynaptic glutamate release across the light-dark cycle[277], in line with the known circadian activity patterns of the LHb[278,279]. Given that stress can drive long-lasting increases in LHb neuron firing[111,158] and elevated 2-AG content[158], and that 2-AG levels show basal diurnal fluctuations[56], there is logical plausibility for the involvement of astrocytic eCB signaling in both of these observations, among others. Future research will be needed to determine which aspects of LHb physiology eCB signaling mechanisms may be involved in. The case for the relevance of 2-AG-CB1 signaling in LHb astrocytes is made more compelling by its tonic nature – disruption of this signaling axis reduced basal glutamate release. It will be intriguing to determine if baseline 2-AG or astrocytic CB1 receptor availability presents a method by which the LHb adjusts baseline excitatory drive.

With regard to neuronal CB1 in the LHb, its function remains equally elusive. Data from our lab and others have identified that synaptic depression occurs at both glutamatergic and GABAergic terminals, and we provide evidence that this system is independent of astrocytic CB1.

However, the contexts in which these mechanisms are engaged *in vivo* remains unexplored. There is data in the literature that demonstrates intra-LHb eCB signaling may modulate stress coping strategies[158], alcohol intake[163], pain[163], and impulsive drug-seeking behaviors[165]. Our data presented in Chapter II complicate the interpretation of these observations, as our identification of an active astrocytic eCB signaling mechanism suggest that the mechanisms subserving these effects may extend beyond canonical CB1 signaling at neuronal axon terminals. Our data do, however, present an interesting case for a potential role of CB1 receptors on LPO glutamatergic terminals in the regulation of pain – it has been demonstrated that mu opioid receptor activation constrains glutamatergic transmission in the LPO-LHb circuit, and this produces a form of non-reinforcing analgesia[153]. Similarly, intra-LHb cannabinoid receptor activation or augmentation of AEA or 2-AG can produce analgesia[163]. Given that we demonstrated that glutamate release from the LPO is inhibited by CB1 receptors to similar extent as by the mu opioid receptor[153], it suggests that the LPO-LHb glutamatergic circuit may be a novel target for supraspinal cannabinoid analgesia. Genetic approaches including circuit-specific neuronal CB1 deletions will be key for future studies to test this hypothesis and delineate the broader functions of presynaptic CB1 in the LHb.

While we propose compelling evidence for an astrocytic CB1 signaling mechanism in the LHb, there are key components to this system that we did not address that may have functional importance. Firstly, we did not explore basal effects of astrocytic CB1 receptor deletion on GABAergic transmission. Our experiments determined that cannabinoid receptor-mediated inhibition of spontaneous GABA release was intact following astrocytic CB1 deletion, indicating that synaptic depression does not require local astrocytic CB1. However, although not reported in Chapter II, a preliminary analysis of basal GABAergic transmission in WT mice vs. following astrocytic CB1 deletion suggests that there may be a positive modulatory function on GABA release, similar as to was observed for glutamate release, as evidenced by a significantly lower

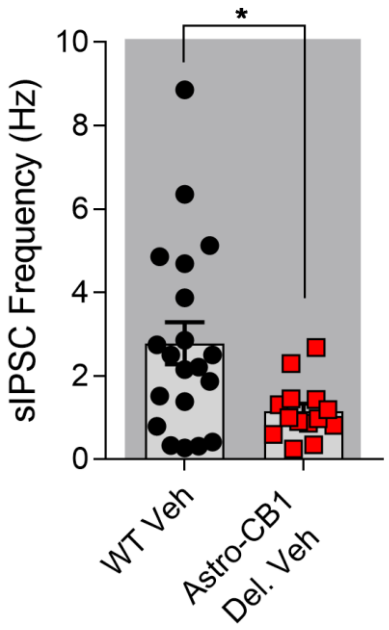

Figure 4-2: Astrocytic CB1 Receptor Deletion Reduces Presynaptic GABA release. Effects of astrocytic CB1 deletion (via GFAP-Cre-mCherry injected into LHb of *Cnr1*$^{flx/flx}$ mice) on pharmacologically-isolated sIPSC frequency measured at -70 mV (WT veh n = 20, 4 mice; Astro-CB1 Del. Veh n = 14, 2 mice). Data extracted from the Vehicle condition in **Figure 2-S1D** and **Figure 2-S3G**. Data are mean ± SEM; n = number of cells. Data analyzed by Mann-Whitney U test. Significance for U-test shown on panel (*p<0.05).

sIPSC frequency in the astrocyte CB1 deletion condition (**Figure 4-2**). While it is important to consider that these data are preliminary and require validation with the proper controls (i.e., all in virally-injected *Cnr1*$^{flx/flx}$ mice), they do pose an intriguing concept if validated. If astrocytic CB1 in the LHb exerts a similar potentiating effect of GABAergic transmission as seen with glutamate, it posits a much broader role for astrocyte eCB signaling in synaptic homeostasis within the LHb. This opens up many additional questions, such as – is the relative weight for neuronal vs. astrocytic CB1 control of glutamate vs. GABA different? Our data speculatively suggest that this may be the case, as evidenced by robust CP55,940 depression of sIPSC frequency and the lack of an effect of Rimonabant on sIPSCs. Furthermore, are the molecular mechanisms the same between astrocytic CB1 activation and glutamate vs. GABA synapses? This preliminary data

should be validated and these questions pursued for a more holistic understanding of this system. Another lingering unknown with regards to the cellular mechanisms proposed here is the source of the tonically-produced 2-AG that signals onto astrocytic CB1 receptors. Conventional models based off the literature would lead to the hypothesis that neuronally-produced 2-AG signals onto astrocytes to mediate a positive feedback loop to maintain excitatory drive. The logic behind this hypothesis is strengthened by the high degree of tonic firing of LHb neurons observed in *ex vivo* slices[102,111]; see also our data, **Figure 2-S1L**). Another set of preliminary data not included in Chapter II contests this hypothesis. We aimed to address this by injecting AAV9-CAMKIIA-GFP-Cre into the LHb of diacylglycerol lipase α (DAGLα) floxed (*DAGLA*$^{flx/flx}$) mice to delete DAGLα from local neurons, which would be predicted to occlude the effect of the DALG inhibitor DO34 on reducing spontaneous glutamate release. Interestingly, Cre expression had no effect on the ability of DO34 to reduce sEPSC frequency (**Figure 4-3**). The DAGL deletion from this experiment

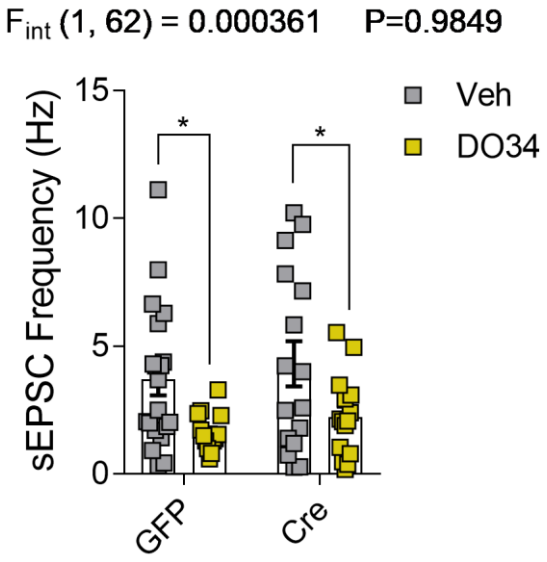

Figure 4-3: Neuronal DAGLα deletion does not occlude the effect of DAGL inhibition on sEPSC frequency. Effects of neuronal DAGLα deletion (via CaMKII-GFP-GFP injected into LHb of *DAGLA*$^{flx/flx}$ mice; CaMKII-GFP virus was used as a control) on sEPSC frequency. (GFP Veh n = 20, 4 mice; GFP DO34 n = 15, 4 mice; Cre Veh n = 16, 4 mice; Cre DO34 n = 15, 5 mice). Data

are mean ± SEM; n = number of cells. Data analyzed by one-way ANOVA with Holm-Sidak multiple comparisons between Veh and DO34 within each viral genotype. F and P values for ANOVA and significance for post-hoc multiple comparisons shown on panel (*p<.05).

has not been validated experimentally and thus *these data should be interpreted with caution until followed up and validated*, although the lab has previously shown that a similar approach results in functional DAGL deletion[79]. This finding suggests that neurons may not be the source of tonic 2-AG that signals onto astrocytic CB1 in the LHb. Astrocytes have been shown to express functional DAGLα in close proximity to CB1 receptors in culture[251], lending plausibility to a mechanism wherein LHb astrocytes engage an autocrine 2-AG-CB1 signaling system. Further investigations should aim to validate these preliminary findings and disentangle the details surrounding astrocytic eCB signaling in the LHb.

The eCB system within the LHb clearly exhibits complex and multicomponent neuromodulatory functions. These mechanisms are likely to have substantial influence over LHb output and the myriad physiological and behavioral functions under its control. Important translational applications that may be relevant to our work include LHb control over affective pathology, pain, and the subjective effects of high-dose exogenous cannabinoids (discussed in Chapter II). Taken together, our research in Chapter II and preliminary findings (to be interpreted with caution) may provide mechanistic insight for several outstanding questions in the field and lay the framework for future lines of research aimed at understanding the molecular details and broader physiological functions of eCB signaling within the LHb.

Stress Plasticity in the Lateral Habenula Endocannabinoid System

As highlighted in Chapter I, the LHb is highly responsive to noxious or stressful stimuli[94]. Stress exposure causes profound neural circuit plasticity across the brain, including in the LHb[84]. Indeed, rodent models of learned helplessness show enhanced LHb neuronal firing[102,111] and increased presynaptic glutamate release probability[111]. Some sparse but intriguing data has indicated that

the eCB system within the LHb is subject to stress-induced plasticity. The first report of stress-induced alterations in LHb eCB signaling demonstrated that a single acute stress exposure resulted in a disruption of eCB-mediated long-term depression (LTD) of glutamatergic synapses, and this was shown to be mediated by upregulation of postsynaptic Ca2+/calmodulin-dependent protein kinase II (CaMKII)[161], predicted to inhibit DAGL function and impair 2-AG synthesis[162]. This report aligns with broader canonical models of disrupted eCB signaling contributing to affective pathology, as the authors pose this loss of eCB control over glutamatergic drive as a potential mechanism contributing to stress-induced LHb hyperactivity[161], which has been implicated in depression[102,107]. In contrast to these data, another study reported elevated 2-AG content in the rodent LHb after *chronic* unpredictable stress, accompanied by an increase in LHb neuronal firing rates[158]. It is unclear whether different modes or durations of stress have differential effects on 2-AG production in the LHb, or if perhaps the elevated firing rates of LHb neurons overcome partially inhibited 2-AG synthetic machinery. In light of our data, an alternative interpretation of these data could be that reduced 2-AG synthesis following *acute* stress exposure could serve as a protective mechanism against enhanced glutamatergic drive and LHb activity (although the functional importance of LTD of evoked glutamate release remains to be determined), and repeated stress exposure could override this effect and lead to enhanced 2-AG produced and thus synaptic excitation. Further investigations into the effects of stress on the LHb eCB system across different models of stress exposure will be informative in resolving these outstanding questions.

Chronic unpredictable stress exposure has also been shown to elicit a number of interesting biochemical alterations in the LHb eCB system based on data from *in vitro* assays with LHb membrane preparations[158]. This study reported that, relative to controls, LHb membranes from chronically stressed rodents exhibited reduced CB1 receptor binding availability (reduced B_{max}), increased CB1 receptor binding *affinity* (reduced K_D), increased enzymatic capacity for MAGL

activity (increased V_{max}), and an increased K_m for MAGL activity. In the context of our data from Chapter II, these data are particularly intriguing given the multiple functional pools of CB1 in the regulation of LHb synaptic transmission. Reduced CB1 receptor binding availability could be a result of reductions in presynaptic, astrocytic, or postsynaptic CB1 receptors in the LHb[158], or a combination thereof. It is also interesting to consider if the enhancements in CB1 binding affinity are due to a broad biochemical change in all local CB1 receptor populations or a downregulation of lower-affinity CB1 receptor populations. It is not known whether neuronal or astrocytic CB1 receptors in the LHb would exhibit differential affinity for cannabinoid ligands, and this is technically challenging to experimentally address in a complex tissue preparation. However, functional interrogation of astrocytic vs. neuronal CB1 receptor function following chronic stress is a feasible line of investigation, and our data provide an experimental framework for how the effects of stress may differentially influence these opposing eCB signaling systems in the LHb. Given the elevated 2-AG content and LHb firing observed following chronic stress[158], addressing these and related questions could provide insight on the role of eCBs in stress-induced affective pathology within the LHb and potentially illuminate novel therapeutic strategies for neuropsychiatric disorders, such as depression[84,107].

Cannabidiol as a Therapeutic for Stress-Related Neuropsychiatric Disease

Cannabidiol (CBD) remains enigmatic as a therapeutic tool, despite the recent and rapid expansion of its use and availability by the public. As highlighted in Chapter I, the doses ingested by commercial CBD products likely do not produce drug plasma concentrations that are relevant for CBD's engagement with its purported targets based on the *in vitro* literature[177]. However, high doses of CBD are generally well tolerated[232,234], which suggests that at least some of the proposed targets for CBD may be therapeutically relevant in a high-dose context and the clinical utility of CBD should be investigated systematically, especially as novel formulations of CBD designed to enhance its bioavailability are under development[280]. Given the improving feasibility of

therapeutically relevant dosing of CBD, the next major challenge to understanding its utility is the dearth of mechanistic information regarding the pharmacodynamics of CBD. The aims of the research presented here in Chapter III were to begin bridging this gap by exploring mechanistic interactions between CBD and the amygdala. The intersections between amygdala physiology and purported use cases for CBD, such relevance to the biology and treatment of anxiety and PTSD[1,205,258,281,282], were central to the rationale underlying this study.

Preclinical literature has firmly established a role for the amygdala in regulating the central response to stress[70,283] and in gating fear-[259,284] and anxiety-related behaviors[78,282]. Human neuroimaging studies have demonstrated that the amygdala is central to emotional processing and reactive to fearful stimuli[285], and conditions such as PTSD are associated with heightened reactivity[286]. Interestingly, amygdala reactivity in humans is reduced by CBD[266,267]. Our data demonstrating that CBD reduces neuronal excitability across multiple subregions of the amygdala provides a potential mechanism to explain these observations. Surprisingly, relatively few preclinical reports describe interactions between CBD in the amygdala. One study reported reduced c-Fos expression in the central nucleus of the amygdala (CeA)[261], which strongly aligns with our data demonstrating that CBD reduces CeA neuron excitability. Another study reported anxiolytic effects produced by amygdala cannulation of CBD[265], which could also be explained by our data. One caveat to our neuronal excitability data is that we utilized 20 µM CBD for all of these experiments, which may exceed physiologically relevant drug concentrations. We chose this concentration based off of our dose-response data with regard to the effect of CBD on GABA release in the CeA. Notably, however, we saw significant effects at 2 µM, which is near the plausible plasma concentration range based on human pharmacokinetic data[234], and well within the range achievable in rodent models[233]. Based on our observations that blockade of action potentials by tetrodotoxin abolishes the effect of CBD on reducing GABA release and the known high degree of interconnectivity within the CeA[270,273], we have reason to expect that the CBD

reductions in CeA GABA release and excitability are related phenomena. Therefore, it is plausible and likely that CBD will reduce CeA excitability at lower concentrations (2 μM or lower), and this should be directly tested. Of note, our data may also have implications for the anticonvulsant properties of CBD in some contexts, as CBD has been shown to mitigate seizures in an amygdala-kindling model of epilepsy[287]. Future preclinical studies should apply these findings to form more directed hypothesis examining the effects of CBD on amygdala physiology and amygdala-related behaviors.

The effects that CBD exerts on CeA synaptic transmission may have translational relevance as well. Of particular interest was the selective reduction of glutamate release onto CRF+ neurons. This could have direct physiological relevance for treating PTSD symptomology and for the preclinical observations that CBD can reduce fear expression in fear conditioning paradigms[205]. Fear conditioning and extinction models actively involve amygdala-dependent learning processes and exaggerated fear responses or disrupted extinction are often posed as preclinical models for PTSD symptomology[258]. The basolateral amygdala (BLA) sends excitatory projections to the CeA that in a naïve, unconditioned rodent are biased onto CRF+ neurons, relative to CRF- neurons[259]. After fear conditioning, BLA synapses bias off of CRF+ neurons and exhibit equal synaptic strength onto CRF+/- neurons, and this bias is restored to CRF+ neurons after fear extinction[259]. Many CRF- neurons in the CeA are SOM+, and synaptic potentiation onto SOM+ neurons is a critical plasticity component of fear conditioning[288]. Based on this, it would be interesting to test if fear conditioning unmasks an inhibitory effect of CBD on glutamatergic drive onto SOM+ CeA cells. If this is confirmed, it is possible that BLA-CeA connectivity could be diminished by CBD, and this could impact anxiety and fear expression, particularly by inhibiting BLA-CeA(SOM+) connectivity. Of note, it is possible that other inputs may be involved as well, and other circuits are actively remodeled by fear conditioning, such as the insular cortex projection to the CeA exhibiting bias onto CRF+ neurons after fear conditioning[259]. Furthermore, it is also

possible that afferent synapses onto specific CeA cell types (CRF+ or otherwise) are molecularly distinct and thus differentially sensitive to CBD (thus not dependent on specific input biases). Collectively, our data lay the framework for numerous hypotheses to be tested regarding the effects of CBD on amygdalar plasticity in the context of fear conditioning. Future studies will likely provide mechanistic information relevant to the use of CBD in the treatment of stress-related neuropsychiatric disorders, such as PTSD.

Further studies are needed to verify the connection between our data and previous observations in the literature, such as the connection between CBD-mediated reductions in amygdala neuron excitability in *ex vivo* rodent brain slices and in amygdala reactivity in humans[266,267]. If validated, these findings could have broad implications for clinical investigations of CBD as a therapeutic for stress-related neuropsychiatric disease. For example, as CBD has purported efficacy in ameliorating symptomology associated with anxiety[206] and PTSD[205], one could speculate that functional neuroimaging of amygdala reactivity could be used as a biomarker for human clinical trials examining the effectiveness of CBD in treating these conditions. Systematic approaches and validated biomarkers would greatly facilitate studies aimed at advancing our clinical understanding of CBD as a regulator of neural physiology and a tool for treating brain disease.

Summary

In conclusion, the body of work presented in this thesis presents novel insights into two distinct lines of investigation that intersect under the theme of the central actions of cannabinoids. Although seemingly divergent, historically the studies of endogenous cannabinoid signaling and phytocannabinoid pharmacology are intimately connected. The endogenous cannabinoid system was discovered during efforts to understand the biology subserving the psychotropic effects of *Cannabis*, and today these fields of study function in parallel with regular intersections in brain biology and therapeutic intervention for brain disorders. In Chapter II, we present evidence for

canonical retrograde and opposing, astrocyte-dependent endogenous cannabinoid signaling systems that function in tandem to regulate synaptic transmission in the lateral habenula. In Chapter III, we describe robust pharmacodynamic effects of cannabidiol on amygdala physiology in the form of altered synaptic transmission and neuronal excitability. Collectively, these lines of research describe novel biological phenomena related to central cannabinoid functions that significantly advance our understanding of cannabinoid biology and could have compelling translational potential for advancing our understanding and treatment of neuropsychiatric disorders.

APPENDIX

The work in this chapter was published in The Journal of Clinical Investigation[164].

TARGETING DIACYLGLYCEROL LIPASE REDUCES ALCOHOL CONSUMPTION IN PRECLINICAL MODELS

Nathan D. Winters[1,2,3*], Gaurav Bedse[1,2*], Anastasia Astafyev[1], Toni A. Patrick[1], Megan Altemus[1], Amanda J. Morgan[1], Snigdha Mukerjee[2,3], Keenan D. Johnson[1], Vikrant R. Mahajan[1], Md. Jashim Uddin[4], Philip J. Kingsley[4], Samuel W. Centanni[2,5,6], Cody A. Siciliano[2,3,6], David C. Samuels[5,7], Lawrence J. Marnett[3,4], Danny G. Winder[2,5,6], and Sachin Patel[1,2,3,5,6]

[1]Department of Psychiatry and Behavioral Sciences, Vanderbilt University School of Medicine, Nashville, TN, USA.

[2]Vanderbilt Center for Addiction Research, Vanderbilt University School of Medicine, Nashville, TN, USA.

[3]Department of Pharmacology, Vanderbilt University School of Medicine, Nashville, TN, USA.

[4]Departments of Biochemistry and Chemistry, A.B. Hancock Jr. Memorial Laboratory for Cancer Research, Vanderbilt Institute of Chemical Biology, Vanderbilt University School of Medicine, Nashville, TN, USA.

[5]Department of Molecular Physiology and Biophysics, Vanderbilt University School of Medicine, Nashville, TN, USA.

[6]Vanderbilt Brain Institute, Vanderbilt University School of Medicine, Nashville, TN, USA.

[7]Vanderbilt Genetics Institute, Vanderbilt University School of Medicine, Nashville, TN, USA.

*These authors contributed equally to this work.

ABSTRACT

Alcohol use disorder (AUD) is associated with substantial morbidity, mortality, and societal cost, and pharmacological treatment options for AUD are limited. The endogenous cannabinoid (eCB) signaling system is critically involved in reward processing and alcohol intake is positively correlated with release of the eCB ligand 2-Arachidonoylglycerol (2-AG) within reward neurocircuitry. Here we show that genetic and pharmacological inhibition of diacylglycerol lipase (DAGL), the rate limiting enzyme in the synthesis of 2-AG, reduces alcohol consumption in a variety of preclinical models ranging from a voluntary free-access model to aversion resistant-drinking and dependence-like drinking induced via chronic intermittent ethanol vapor exposure in mice. DAGL inhibition during either chronic alcohol consumption or protracted withdrawal was devoid of anxiogenic and depressive-like behavioral effects. Lastly, DAGL inhibition also prevented ethanol-induced suppression of GABAergic transmission onto midbrain dopamine neurons, providing mechanistic insight into how DAGL inhibition could affect alcohol reward. These data suggest reducing 2-AG signaling via inhibition of DAGL could represent an effective approach to reduce alcohol consumption across the spectrum of AUD severity.

INTRODUCTION

Alcohol use disorder (AUD) is a chronic relapsing substance abuse disorder that exhibits a lifetime prevalence of approximately 30% in the United States[289]. Like disordered use of other drugs, AUD can be conceptualized as a chronic disease quintessentially characterized by lack of control over alcohol drinking behaviors despite adverse consequences. Patients with AUD exhibit cravings and a compulsive drive to seek and use alcohol during abstinence, and may exhibit tolerance and withdrawal symptoms often leading to relapse[290]. Societal costs related to problematic drinking led to an estimated economic burden of $249 billion in the United States in 2010[291], emphasizing AUD as a critical public health concern. Current treatment approaches for AUD consist of limited pharmacological treatments combined with various forms of group and individual psychotherapy, often and most effectively in conjunction[290]. Despite this, efficacy is limited and relapse rates in AUD are high[290,292], highlighting the need for the elucidation of effective pharmacological targets for the advancement of AUD therapeutics development.

A growing body of work has implicated the endocannabinoid (eCB) system as a critical modulator of the effects of ethanol (see Ref. [293] and [294] for review), and the eCB system is heavily implicated in a variety of processes relevant to distinct stages of AUD including reward processing, stress-reactivity, and affect modulation[64,75,295], suggesting this system may serve as a promising target for AUD therapeutic development. The eCB system is a retrograde neuromodulator system wherein the lipid-derived eCB ligands, 2-arachidonoylglycerol (2-AG) and anandamide (AEA), are synthesized and released from the postsynaptic compartments of neurons and activate presynaptic cannabinoid-1 (CB_1) receptors to decrease neurotransmitter release probability. Ethanol (EtOH) mobilizes the major brain eCB 2-AG in the nucleus accumbens[296,297] and in some neuronal culture models[298,299]. Importantly, inhibition of CB1 receptors attenuates EtOH self-administration in rodents[300,301] and diminishes ethanol-stimulated

enhancements of dopamine neuron activity in midbrain reward circuits[302], collectively suggesting a necessity for intact eCB signaling for driving alcohol-seeking behaviors.

Inhibition of eCB signaling is posited as a potentially effective strategy to treat AUD, and a CB1 receptor inverse agonist (Rimonabant) has been explored in clinical trials for AUD[303] as well as other addiction-related disorders[304,305], but this compound was removed from the European Union market due to severe neuropsychiatric side effects[306]. Given that EtOH mobilizes 2-AG in the reward circuitry in a manner correlated with EtOH intake[296,297], we hypothesized targeted inhibition of 2-AG signaling (thereby leaving AEA-CB1 signaling intact) could be an effective approach to reducing EtOH drinking with a lower adverse effect liability. Here we implemented genetic and pharmacological strategies to test the hypothesis that inhibiting diacylglycerol lipase (DAGL), the rate-limiting enzyme in 2-AG synthesis, reduces EtOH drinking behaviors without facilitating the development of anxiety- and depression-like behaviors after chronic EtOH drinking. We found that genetic deletion of DAGLα, the primary DAGL isoform in the adult brain[307], or the pharmacological DAGL inhibitor DO34[308], decreased EtOH consumption across a range of clinically-relevant models and did not exacerbate negative affective behaviors in chronically drinking mice or during protracted abstinence. Collectively, our data suggest that DAGL inhibition could be a promising and broadly applicable therapeutic strategy to reduce alcohol drinking across the spectrum of AUD.

RESULTS

Genetic and pharmacological inhibition of DAGL decreases voluntary EtOH drinking

Having previously established that genetic deletion of DAGLα results in reduced brain 2-AG levels[75,77], we evaluated the effects of DAGLα deletion on EtOH drinking behavior. Separate cohorts of male and female DAGLα$^{-/-}$ mice and WT littermates were exposed to continuous access two-bottle choice (2BC) EtOH drinking paradigm (**Fig. A-1A**). Both male and female DAGLα$^{-/-}$

mice exhibited lower EtOH preference (**Fig. A-1B-C**) and consumption (**Fig. A-1D-E**) relative to their WT littermates. Of note, DAGLα$^{-/-}$ males maintained lower preference and consumption for the duration of the experiment (**Fig. A-1B, D**), whereas female DAGLα$^{-/-}$ mice reached WT levels by Week 4 (**Fig. A-1C, E**). DAGLα$^{-/-}$ mice exhibited no difference in total fluid consumption relative to WT controls (**Fig. A-1F-G**). We next evaluated the effects of pharmacological DAGL inhibition on alcohol drinking by using the DAGL inhibitor DO34[308]. Previously, we have demonstrated that DO34 (50 mg/kg) significantly decreases brain 2-AG levels 2 hours after administration[75]. Separate cohorts of male and female C57BL/6J mice were exposed to the 2BC EtOH drinking paradigm. After 6 weeks of stable drinking, DO34 (50 mg/kg) was administered for three consecutive days (**Fig. A-2A**). DO34 reduced EtOH preference non-significantly in males and significantly in females (**Fig. A-2B-C**) and significantly reduced consumption in both sexes (**Fig. A-2D-E**). DO34 did not significantly alter total fluid consumption in either sex at any timepoint (**Fig. A-2F-G**). Vehicle control injections had no effect on EtOH preference (**Fig. A-S2A, D**) or consumption (**Fig. A-S2B, E**). DO34 had no effect on body weight in female mice (**Fig. A-S2F**) but caused a small but significant decrease in body weight in males that recovered upon cessation of drug treatment (**Fig. A-S2C**). Due to their higher relative EtOH preference and consumption levels, female C57 mice were used for all drinking and behavioral experiments hereafter.

Although our convergent genetic and pharmacological studies indicate a role for DAGL in alcohol consumption, DO34 does exhibit some activity at other targets, such as alpha/beta hydrolase domain-containing 2 and 6 (ABHD2/6), platelet-activating factor acetylhydrolase 2 (PAFAH2), carboxylesterase 1C (CES1C), and phospholipase A2 group 7 (PLA2G7)[308]. To confirm that the DO34 effects on EtOH consumption and preference are specific to DAGL inhibition, we utilized the structural analog DO53, which retains the off-target activity profile of DO34 but does not inhibit DAGL[308]. A cohort of female mice stably drinking 10% EtOH on our

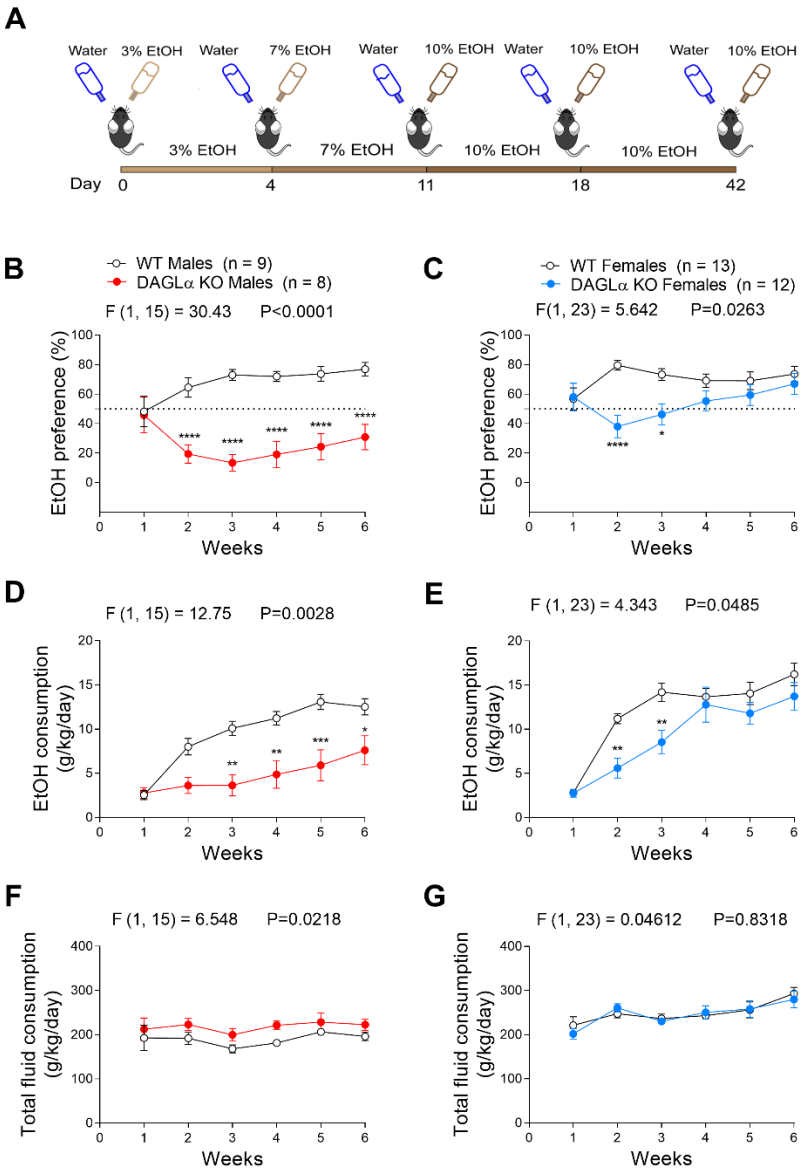

Figure A-1: Genetic deletion of DAGLα reduces voluntary alcohol intake. (A) Schematic of 2BC EtOH drinking paradigm for DAGLα$^{-/-}$ mice. **(B-C)** Male and female DAGLα$^{-/-}$ mice exhibited lower EtOH preference and **(D-E)** consumption relative to WT mice. Male DAGLα$^{-/-}$ maintained lower relative EtOH preference (B) and consumption **(D)** throughout the experiment, whereas females reached WT levels in both measures by Week 4 **(C, E)**. **(F-G)** Male and female DAGLα$^{-/-}$ mice exhibited no difference in total fluid consumption. Data analyzed by repeated measures two-way ANOVA followed by a Holm-Sidak test for multiple comparisons between genotypes. Sample size n, P and F values for main effects of genotype, and significance for post-hoc multiple comparisons reported on graphs. (*P<.05, **P<0.01, ***P<0.001, ****P<0.0001). Data are mean ± SEM.

2BC paradigm were administered DO53 (50 mg/kg) for 5 consecutive days. EtOH consumption was transiently reduced by DO53 treatment (**Fig. A-2I**), however, this was paralleled by a non-specific decrease in total fluid consumption (**Fig. A-2J**). Accordingly, there was no effect on EtOH preference (**Fig. A-2H**) and no change in body weight (**Fig. A-S3**) during the 5-day DO53 treatment. These effects are in contrast with the persistent decrease in EtOH preference and consumption (**Fig. A-2B-E**) and unchanged fluid consumption (**Fig. A-2F-G**) observed during DO34 treatment. Combined with our genetic studies using DAGL$\alpha^{-/-}$ mice, these control data suggest the effects of DO34 were mediated through DAGL inhibition, rather than off-target mechanisms.

DO34 depletes brain 2-AG levels similarly in naïve and chronically drinking mice and does not affect blood EtOH concentrations

Given that our results demonstrating DO34-mediated reductions in EtOH drinking were collected in mice that had been chronically drinking, we next verified that DO34 causes comparable reductions in brain 2-AG levels after prolonged alcohol exposure. To do this, we collected brains from naïve or chronically (6 weeks, 2BC 20% EtOH) drinking mice after 4 days of repeated DO34 injections (50 mg/kg). Brains were collected 2 hours after the final DO34 injection, hemisected, and half brain samples were prepared for mass spectrometric analysis of bulk tissue levels of endocannabinoids and related lipid metabolites. As expected, DO34 caused a strong depletion of 2-AG (**Fig. A-2K**) and its major metabolite, arachidonic acid (AA) (**Fig. A-2L**), in all mice, regardless of alcohol history. Levels of prostaglandins E2 (PGE2) and D2 (PGE2), which are derived downstream from AA[309], were also decreased in DO34-treated mice from both groups (**Fig. A-2M-N**). Furthermore, there was no significant effect on anandamide (AEA) levels in either group (**Fig. A-2O**).

A possible indirect mechanism we sought to rule out is potential pharmacokinetic interaction between DO34 and blood EtOH concentration. One study reported higher BECs in CB_1 receptor

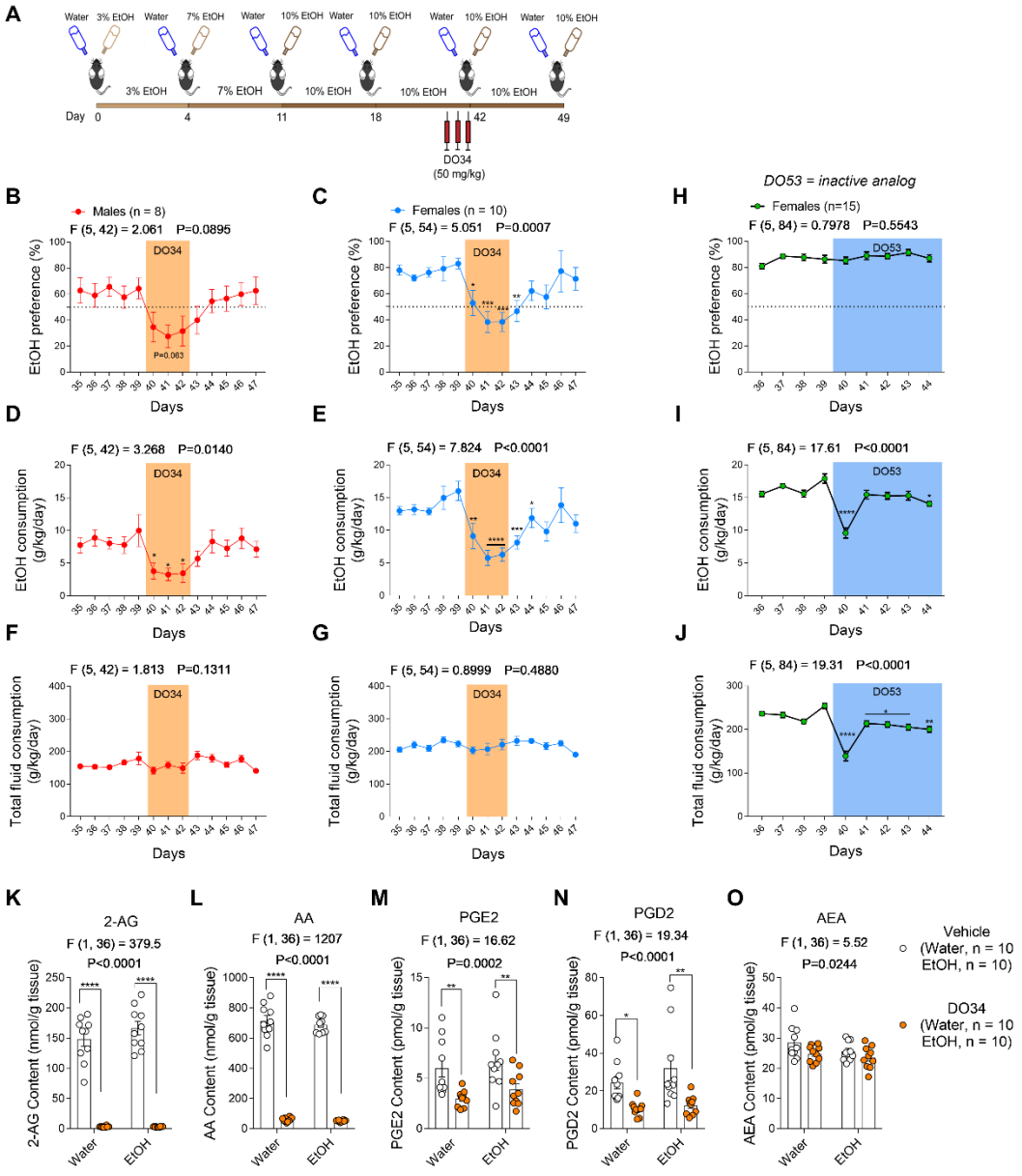

Figure A-2: Pharmacological inhibition of DAGL by DO34 reduces voluntary alcohol intake and produces similar brain lipid profiles in naïve and chronically drinking mice. (A) Schematic of 2BC EtOH drinking paradigm for mice receiving DO34 treatment. **(B)** DO34 (3 days) non-significantly reduced EtOH preference in male mice and **(C)** significantly reduced EtOH preference in female mice. **(D-E)** DO34 reduced EtOH consumption in both **(D)** male and **(E)** female mice. **(F-G)** DO34 had no effect on total fluid consumption in **(F)** male or **(G)** female WT mice. **(H)** Analog compound DO53 (5 days) had no effect on EtOH preference in female mice. **(I)** DO53 reduced EtOH consumption in female mice and this was paralleled by **(J)** a non-specific reduction in total fluid consumption. **(K-O)** DO34 (4 days) depletes brain **(K)** 2-AG, **(L)** AA, **(M)** PGE2, and **(N)** PGD2 levels similarly in naïve and chronically (6 weeks, 20% EtOH) drinking mice, with **(O)** no effect on AEA levels. **(B-G)** Data analyzed by one-way ANOVA on time points 39-44 followed by a Holm-Sidak test for multiple comparisons to baseline (Day 39) control. **(H-J)** Data analyzed by one-way ANOVA on averaged baseline (Days 36-39) and individual treatment days

followed by a Holm-Sidak test for multiple comparisons to averaged baseline. **(K-O)** Data analyzed by two-way ANOVA followed by a Holm-Sidak test for multiple comparisons between vehicle and DO34. All DO34/53 treatments were dosed at 50 mg/kg. Sample size n, P and F values for main effects of drug treatment, and significance for post-hoc multiple comparisons reported on graphs. (*P<.05, **P<0.01, ***P<0.001, ****P<0.0001). Data are mean ± SEM. 2-AG, 2-arachidonoylglycerol; AA, arachidonic acid; PGE2, prostaglandin E2; PGD2, prostaglandin D2; AEA, anandamide or N-arachidonoylethanolamine.

knockout mice after i.p. EtOH injection, albeit only at a high dose that exceeded clinically-relevant BECs[310]. To address this, we injected a cohort of EtOH-naïve mice with either vehicle or DO34 (50 mg/kg) for 3 consecutive days and 2 hours after the last injection delivered an i.p. bolus of EtOH (3 g/kg). 30 mins after EtOH injection, trunk blood was collected and BEC measurements were taken. We chose this method as the 30 min time point captures peak BEC according to previously reported pharmacokinetic data[311] and inherently reduces variability in EtOH exposure relative to voluntary drinking sessions. Repeated DO34 treatment had no effect on BEC at the 30 min time point (**Fig. A-S4**), suggesting that DO34 effects on alcohol drinking were not due to pharmacokinetic interactions leading to altered BECs or subsequent degrees of intoxication.

Effects of 2-AG modulation are specific to EtOH and not bidirectional

To confirm that DO34 effects are specific to EtOH and not generalized reward-seeking, we tested the effect of DO34 in a 2BC sucrose preference paradigm. DO34 had no effect on sucrose preference, suggesting a degree of specificity for EtOH over natural rewards (**Fig. A-S5A**). Furthermore, given that depletion of 2-AG reduces EtOH drinking, we next tested if augmentation of 2-AG would increase EtOH drinking. The monoacylglycerol lipase inhibitor JZL-184 (10 mg/kg) was administered for three consecutive days to mice drinking 10% EtOH in the 2BC drinking paradigm. JZL-184 had no significant effect on EtOH preference or consumption (**Fig. A-S5B-C**) and did not affect body weight (**Fig. A-S5D**), indicating the effects of 2-AG modulation on EtOH drinking are not bidirectional.

Pharmacological DAGL inhibition reduces aversion-resistant EtOH drinking

Alcohol seeking despite negative consequences is recognized as a key element of AUD and is a major obstacle to effective AUD treatment[290,312]. To determine whether DAGL inhibition could reduce EtOH consumption in a more clinically-relevant model, we utilized an aversion-resistant drinking model wherein animals actively consume EtOH that has been adulterated with the bitter tastant quinine[312]. First, we validated this model by adulterating quinine in one of the two bottles after 4 weeks of the 2BC paradigm and determined the preference and consumption for the quinine adulterated bottles. Quinine was adulterated at 0.01, 0.03 and 0.1g/L in water, 10% EtOH and 20% EtOH bottles. Mice receiving water + quinine (0.03 and 0.1 g/L) exhibited very low preference (<7 %) (**Fig. A-S6A**), however, EtOH (10 and 20%) + quinine maintained a higher preference relative to the Water + quinine condition. Mice drinking 20% EtOH + quinine showed higher EtOH consumption compared to mice drinking 10% EtOH + quinine (**Fig. A-S6B**), leading us to use 20% EtOH for examining DO34 effects on aversion-resistant drinking. 0.03 g/L quinine was selected for further experiments, as mice exhibited robust aversion resistant drinking at this concentration (**Fig. A-S6A**).

To test the effects of DO34 in this model, a separate cohort of 2BC mice was used and 0.03g/L quinine was added to either water bottles (control mice) or 20% EtOH bottles after 4 weeks of stable 2BC drinking. 20% EtOH + quinine showed higher preference compared to the water + quinine mice **(Fig. A-3A)**. DO34 (50 mg/kg, 3 days) treatment significantly reduced the EtOH preference (**Fig. A-3A**) and consumption (**Fig. A-3B**), although day 3 of treatment failed to reach statistical significance. DO34 treatment had no effect on total fluid consumption (**Fig. A-S6C**). These data suggest DAGL inhibition can reduce aversion-resistant alcohol consumption.

Efficacy of DAGL inhibition is maintained following chronic intermittent EtOH exposure and dependence-like drinking

AUD exists on a severity spectrum and involves a shift from problematic alcohol use to dependence[290,313]. This transition is driven by a shift from positive to negative reinforcement[313], and thus may involve differing neurobiological mechanisms in early vs. severe, late stages of

AUD. Critical to the development of pharmacotherapies for AUD is the examination of relative efficacy during varying stages of AUD. To address this, we examined the efficacy of DO34 in mitigating alcohol consumption following a model of chronic intermittent EtOH (CIE) exposure to develop escalation and dependence-like drinking. CIE models are widely used to develop EtOH dependence in rodents and generally result in more severe AUD symptomology and higher intoxication levels relative to continuous access models[312,314,315]. Mice were exposed to intermittent 2BC 15% EtOH drinking for 24hr periods, 3x per week on alternating days. On alternating weeks, mice were exposed to EtOH vapor inhalation for 16 hr/day, 4x per week (**Fig. A-3C**). Mice exhibited a clear escalation in EtOH preference and consumption following the first week of EtOH vapor exposure. Following 3 2BC-vapor chamber cycles and one additional week of baseline drinking, mice were treated daily with DO34 (50 mg/kg) for 6 days, starting the day before the first drinking session to maintain consistent DO34 exposure during the intermittent drinking period. DO34 caused a non-significant ($p=0.055$) reduction in EtOH preference, and EtOH preference was significantly lower during DO34 treatment when compared to the recovery week after an additional 2BC-vapor cycle (**Fig. A-3D-E**). DO34 treatment significantly reduced EtOH consumption during the treatment week and consumption recovered to baseline following an additional cycle of 2BC-vapor treatment (**Fig. A-3F-G**). DO34 treatment also caused a small but significant reduction in total fluid consumption during the treatment week, however, fluid intake remained significantly decreased compared to baseline after recovery (**Fig. A-S6D-E**). These data suggest that DAGL inhibition may be a broadly applicable therapeutic strategy for the treatment of varying stages of AUD, including late-stage dependence-like drinking modeled using the CIE exposure paradigm.

Pharmacological DAGL inhibition does not precipitate negative affective behaviors during late chronic EtOH drinking

2-AG signaling is an important modulator of anxiety- and depressive-related behaviors[64,75,78,295,316], and depletion of 2-AG produces anxiety-like phenotypes and exacerbates

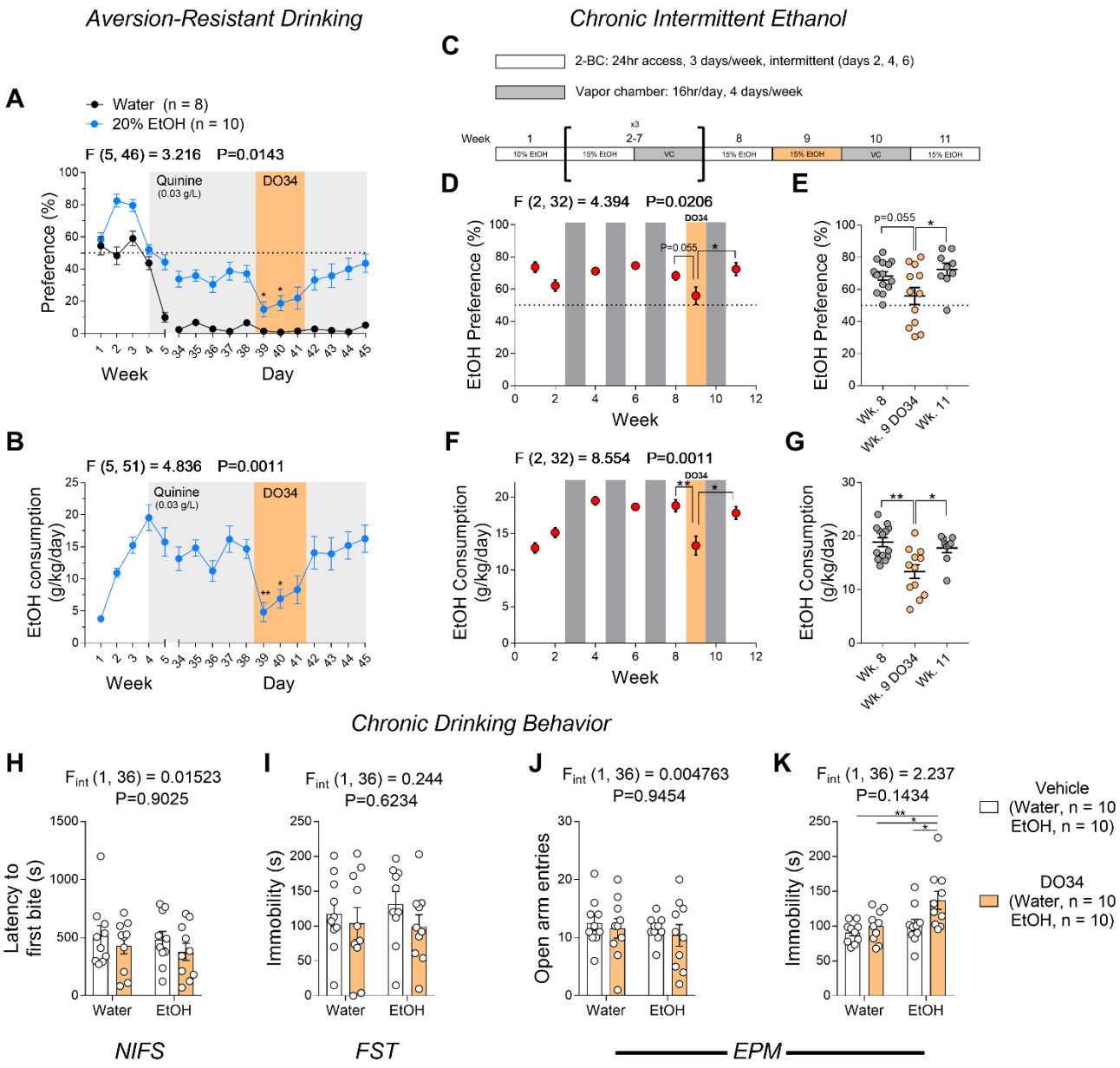

Figure A-3: DO34 decreases EtOH intake across aversion-resistant and chronic intermittent models of EtOH drinking and does not precipitate negative affective phenotypes after chronic EtOH drinking. (A) DO34 (3 days) decreased preference and **(B)** consumption of 20% EtOH + 0.03 g/L quinine (blue). Water + quinine control shown for reference (black). **(C)** Schematic depicting the chronic intermittent EtOH exposure (CIE) paradigm. **(D-E)** DO34 (6 days) caused a non-significant reduction in EtOH preference (P=.055) and **(F-G)** significantly decreased consumption of 15% EtOH in the CIE model. **E** and **G** depict individual mouse EtOH preference or consumption values from **D** and **F**, respectively. **(H-K)** DO34 had no effect on **(H)** latency to first bite in the NIFS test, **(I)** immobility time in the FST, or **(J)** open arm entries in the EPM in water control or chronically (6 weeks, 2BC, 20% EtOH) drinking mice. **(K)** DO34 treatment mildly increased immobility time in the EPM in EtOH drinking mice. **(A-B)** Data

were analyzed by one-way ANOVA on time points 38-43 followed by a Holm-Sidak test for multiple comparisons to baseline (Day 38). **(D-G)** Data analyzed by one-way ANOVA on Week 8, 9, and 11 followed by a Holm-Sidak test for multiple comparisons between these 3 time points. **(H-K)** Data analyzed by two-way ANOVA followed by a Holm-Sidak test for multiple comparisons between all groups. Female C57 mice were used in all experiments and DO34 was dosed at 50 mg/kg. Sample size n reported on graphs for experiments in **A-B** and **H-K**. n = 9-14 mice in **D-G**. P and F values for main effects of **(A-G)** drug treatment or **(H-K)** EtOH x DO34 interaction and significance for post-hoc multiple comparisons reported on graphs (*P<.05, **P<0.01). Data are mean ± SEM. NIFS, novelty-induced feeding suppression; FST, forced swim test; EPM, elevated plus maze.

the affective consequences of stress exposure[75,77-79]. Additionally, 2-AG augmentation has been shown to mitigate anxiety-like behaviors in a rodent model of EtOH withdrawal[80]. When considering these data in the context of DAGL inhibition for treating AUD, a potential problem with this therapeutic strategy is that pharmacological depletion of 2-AG may produce affective disturbances, similar to those previously observed with the CB_1 receptor inverse agonist Rimonabant[306]. We therefore wanted to examine the potential affective side effect profile of DAGL inhibition by examining the effects of DAGL inhibition on anxiety- and depressive-like behaviors in animals after chronic alcohol exposure. To test this, we exposed female mice to 6 weeks of 2BC drinking at 10% EtOH (or water as a control) and subjected them to a series of behavioral tests after treatment with vehicle or DO34 (50 mg/kg) 2 hours prior to each behavioral test. These mice were tested in the open field (OF), elevated zero maze (EZM), tail suspension test (TST), light-dark box, and 3-chamber social interaction assays **(Fig. A-S7A)**. DO34 treatment decreased OF % center distance in water control mice, but not in EtOH mice (**Fig. A-S7B**). Additionally, DO34 treatment increased EZM open arm entries in EtOH mice, but not in water control mice, and total distance in the EZM was increased by DO34 treatment in both water and EtOH mice (**Fig. A-S7C**). In the TST, DO34 increased immobility time in water control mice, but decreased immobility time in EtOH mice, supported by a strong EtOH x DO34 interaction (**Fig. A-S7D**). There was no effect of DO34 treatment or EtOH history on anxiety-like behaviors in the light-dark box or in social function as measured by the 3-chamber social interaction test (**Fig. A-S7E-F**).

We repeated this experiment in additional cohort of mice drinking at 20% EtOH for 6 weeks, followed by behavioral testing in the novelty-induced feeding suppression (NIFS) test, forced swim test (FST), and elevated plus maze (EPM) assays. There was no effect of DO34 treatment on latency to first bite in the NIFS test, immobility time in the FST, or open arm entries in the EPM in either water or EtOH mice (**Fig. A-3H-J**). DO34 caused a small but significant increase in the immobility time in the EPM in EtOH drinking mice (**Fig. A-3K**). These data agree with the 10% EtOH cohort behavioral data, collectively demonstrating a lack of anxiety- or depressive-like phenotypes in chronically drinking mice treated with DO34.

Pharmacological DAGL inhibition reduces reinstatement of EtOH drinking

Another major obstacle to effective AUD treatment is the susceptibility to relapse after abstinence[317]. We therefore used a model of EtOH reinstatement to test the effects of DO34 treatment on the potential for relapse after EtOH abstinence. Mice were subjected to our 2BC paradigm for 5 weeks (at 10% EtOH), followed by a 10-day withdrawal period where EtOH bottles were replaced with water. After the withdrawal period, mice were re-exposed to 10% EtOH for 9 days. Mice were treated with vehicle or DO34 (50 mg/kg) for 7 consecutive days, starting 2 days prior to the initiation of EtOH reinstatement. DO34-treated mice showed significantly lower EtOH preference (**Fig. A-4A**) and consumption (**Fig. A-4B**) compared to vehicle-treated mice upon EtOH re-exposure. DO34 treatment concomitantly increased total fluid consumption (**Fig. A-S8**), again demonstrating the DO34-driven decrease in EtOH consumption is not due to off-target reductions in fluid intake.

Pharmacological DAGL inhibition does not precipitate negative affective behaviors during protracted abstinence from EtOH drinking

Although DO34 effectively mitigates reinstatement of alcohol drinking after abstinence, affective disturbances are particularly problematic during protracted abstinence from alcohol drinking[317,318]. Accordingly, this timepoint may be of notable concern for potential affective side effects of DAGL inhibition. To examine the effects of DO34 treatment after protracted abstinence

from EtOH, female mice were exposed to our 2BC paradigm at 20% EtOH (or water as a control) for 6 weeks and placed into forced abstinence for 2 weeks (**Fig. A-4C-E**). Behavioral tests were matched to those performed on the previous cohort drinking 20% EtOH in **Fig. A-3H-K** (NIFS, FST, EPM). Mice were treated with vehicle or DO34 (50 mg/kg) on testing days two hours prior to each behavioral test. EtOH-withdrawn animals treated with vehicle exhibited a higher latency to first bite relative to water control mice in the NIFS assay, suggesting an anxious phenotype produced by withdrawal from EtOH (**Fig. A-4F**). DO34 reduced this latency in EtOH-withdrawn mice, with no effect on water mice and supported by an EtOH x DO34 interaction (**Fig. A-4F**). DO34 reduced immobility time in the FST in both water and EtOH mice (**Fig. A-4G**). In the EPM assay, DO34 increased open arm entries and decreased immobility time only in EtOH-withdrawn mice, again supported by an EtOH x DO34 interaction (**Fig. A-4H-I)**. These data suggest that DO34 does not produce an anxiety- or depressive-like phenotype during protracted alcohol withdrawal and, in contrast, may exhibit anxiolytic or antidepressant properties in some contexts. Although there was variability between the withdrawal and late drinking cohorts with regards to the DO34 effects on immobility time in the FST (**Fig. A-3I; Fig. A-4G**) and EPM (**Fig. A-3K; Fig. A-4I**), these may be due to inter-cohort and -experimenter variability, and nonetheless, these datasets collectively suggest no adverse affective side effect liability from DAGL inhibition after a history of EtOH consumption or protracted abstinence in these mouse models.

DO34 blocks EtOH-driven disinhibition of posterior VTA putative dopamine neurons

The mitigating effect of DO34 on alcohol consumption suggests a role for 2-AG mobilization in driving alcohol seeking. EtOH stimulates the activity of VTA dopamine neurons in a manner that requires eCB signaling[302]. It has been previously reported that inhibition of CB_1 receptors in the posterior (but not anterior) VTA reduces alcohol intake[319]. In line with these findings, EtOH reduces inhibitory GABA transmission onto putative dopamine neurons in the posterior VTA[320], and VTA GABA transmission is regulated by eCB signaling[321-324]. Furthermore, it has been reported that DAGL lipase signaling disinhibits dopamine neurons by suppressing GABA release

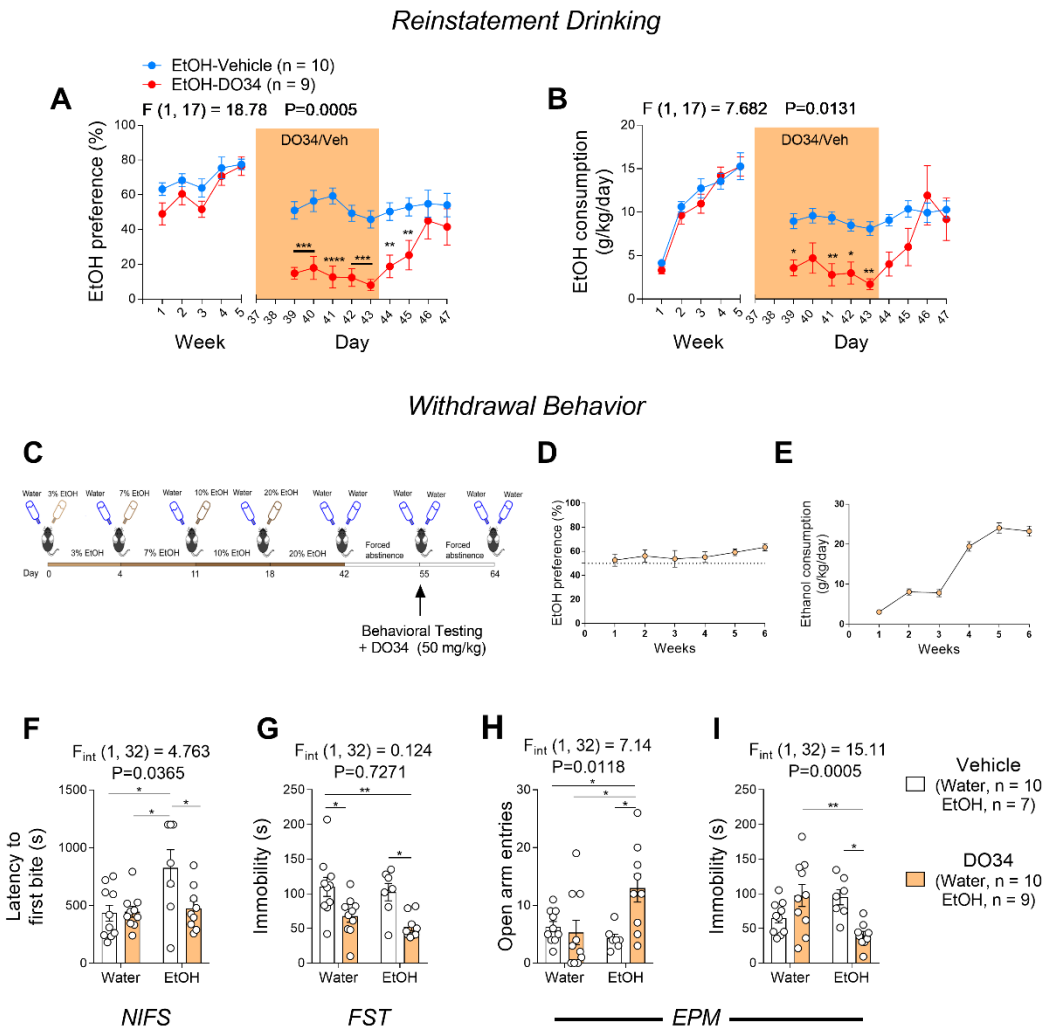

Figure A-4: DO34 reduces reinstatement of EtOH drinking and does not precipitate negative affective phenotypes during protracted abstinence. (A) DO34 (7 days) reduced preference and **(B)** consumption relative to vehicle upon reinstatement of 10% EtOH drinking after 5 weeks of drinking and 10 days of withdrawal. DO34 treatment was initiated 2 days before onset of reinstatement of EtOH access. **(C)** Schematic depicting 2BC drinking paradigm for behavioral testing in withdrawal. **(D)** EtOH preference and **(E)** consumption in mice tested in withdrawal cohort. **(F)** EtOH-withdrawn mice showed a higher latency to first bite in the NIFS test that was reduced back to baseline with DO34 treatment. **(G)** DO34 treatment decreased immobility time in the FST in both groups. **(H-I)** DO34 treatment increased number of **(H)** open arm entries and **(I)** decreased immobility time in the EPM only in EtOH-withdrawn mice. **(A-B)** Data analyzed by repeated measures two-way ANOVA followed by a Holm-Sidak test for multiple comparisons between treatment conditions. **(F-I)** Data analyzed by two-way ANOVA followed by a Holm-Sidak test for multiple comparisons between all groups. DO34 was dosed at 50 mg/kg. Sample size n, P and F values for main effects of **(A-B)** drug treatment or **(F-I)** EtOH x DO34 interaction, and significance for post-hoc multiple comparisons reported on graphs (*P<.05, **P<0.01, ***P<0.001,

****P<0.0001). Data are mean ± SEM. NIFS, novelty-induced feeding suppression; FST, forced swim test; EPM, elevated plus maze.

following chronic nicotine exposure[321], suggesting EtOH may stimulate a similar, eCB-mediated disinhibitory mechanism in these cells. To test whether DAGL regulates alcohol-induced inhibition of VTA GABAergic transmission, we utilized tyrosine hydroxylase (TH)::Ai14 mice that express Td-tomato in TH+ cells to conduct fluorescence-assisted electrophysiological recordings of spontaneous inhibitory postsynaptic currents (sIPSCs) from putative dopamine (TH+) neurons in posterior midbrain slices (**Fig. A-5A**). Acute bath application of EtOH (100mM) decreased the frequency of sIPSCs onto the majority of cells recorded, as previously reported[320] (**Fig. A-5B**). Incubation of slices in 2.5µM DO34 abolished this effect (**Fig. A-5B**) and significantly decreased the proportion of cells that exhibited a reduction in sIPSC frequency in response to EtOH application (**Fig. A-5C**). Additionally, EtOH induced a small but significant reduction in sIPSC amplitude in DO34-treated slices (**Fig. A-S9**).

Although these data suggest that EtOH mobilizes 2-AG at posterior VTA GABA synapses, direct evidence of EtOH-stimulated increases in VTA 2-AG levels has not been demonstrated, as has been shown in the nucleus accumbens[296,297]. To attempt to address this, we injected mice with an i.p. bolus of EtOH (3 g/kg) and 30 mins later collected acute midbrain tissue punches containing the VTA. Mass spectrometry analysis of midbrain punches showed no effect on midbrain 2-AG levels (**Fig. A-S10A**). We repeated this experiment in a separate cohort of voluntary, 2BC drinking mice after 6 weeks stable drinking at 10% EtOH. These punches were taken at the initiation of the dark cycle to attain maximal alcohol intake based on 2BC drinking time course measurements previously obtained from another cohort (**Fig. A-S10B**). This method again did not show any effect on midbrain 2-AG levels (**Fig. A-S10C**). This could be due to technical limitations and the lack of anatomical specificity afforded by bulk punches from mouse brain tissue, as our punches undoubtedly contained both anterior and posterior VTA (note specificity of posterior VTA in CB_1 effects on alcohol intake, see Ref. [319]) as well as portions of

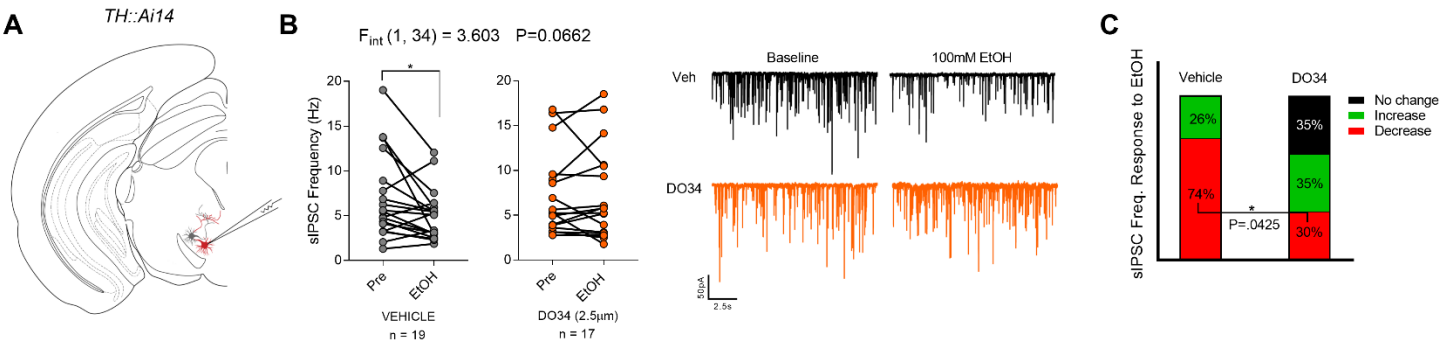

Figure A-5: DO34 prevents EtOH suppression of posterior VTA GABA transmission. (A) Schematic depicting recording strategy used to identify putative dopamine neurons exhibiting red fluorescence in the posterior VTA. **(B, left)** Bath application of 100mM EtOH reduced sIPSC frequency in vehicle-treated but not DO34-treated slices. **(B, right)** Example traces of sIPSC response to 100mM EtOH in vehicle- (black) or DO34-treated (orange) slices. **(C)** Relative proportions of sIPSC frequency response to 100mM EtOH (defined as ≥10% change). DO34 treatment reduced the proportion of cells that exhibited a reduction in sIPSC frequency. 1-3 cells per mouse included in analyses. Vehicle, 9 mice; DO34, 10 mice; from 15 mice total (both conditions sampled from a subset of 4 mice). **(B)** Data analyzed by two-way ANOVA followed by a Holm-Sidak test for multiple comparisons between baseline and EtOH application. **(C)** Data analyzed by Fisher's exact test for proportion of cells exhibiting reduced sIPSC frequency after EtOH application. Sample size n (cells), P and F values for EtOH x DO34 interaction, and significance for post-hoc multiple comparisons reported on graph (*P<.05). sIPSC, spontaneous inhibitory postsynaptic current.

other adjacent midbrain structures. This question could be better addressed in future studies with an alternative approach that offers greater spatial resolution, such as cannabinoid-sensitive biosensors. Despite these technical limitations, our electrophysiological data functionally suggest DO34 could decrease positive reinforcement-driven voluntary EtOH consumption via preventing EtOH-induced reductions in VTA GABA transmission and subsequent increases in VTA dopamine neuron activity.

DISCUSSION

Here we show that genetic and pharmacological inhibition of DAGL activity reduced alcohol consumption and preference across a range of distinct drinking models. Specifically,

pharmacological DAGL inhibition and DAGLα KO mice show reduced voluntary alcohol consumption and preference under a continuous access model. Importantly, pharmacological DAGL inhibition also reduced alcohol consumption and preference in an aversion-resistant drinking model, in a dependence-like model that leverages chronic intermittent vapor exposure to drive an escalation in voluntary alcohol consumption, and in a model of reinstatement drinking. In line with our data, DAGL inhibition by DO34 has been previously shown to reduce operant responding for alcohol[325]. The magnitude of effect on EtOH intake observed after DAGL inhibition is comparable to or greater than those observed with clinically available treatments such as Naltrexone[326-328] and Acomprasate[328,329] in similar rodent models. Moreover, pharmacological DAGL inhibition did not affect sucrose preference, suggesting a lack of generalized effect to natural reward, although female DAGLα KO mice do exhibit reductions in sucrose preference under some conditions[77]. Although DO34 inhibits both α and β isoforms of DAGL[308], the ability of DAGLα genetic knockout to reduce alcohol consumption suggests the α isoform may be the relevant molecular target contributing to the efficacy of DO34. Furthermore, we found a control compound DO53, which does not inhibit DAGL α or β, but does inhibit a number of off-targets also inhibited by DO34[308], produced a transient suppression of alcohol intake that was paralleled by a reduction in non-specific fluid intake and no effect on alcohol preference. This effect may be due to activity at shared off-targets or unique off-targets of DO53 such as ABHD3/6[308]. Regardless of the precise mechanisms by which DO53 transiently suppresses non-specific fluid intake, it did not affect alcohol preference or alcohol consumption after repeated injection, providing an additional degree of confidence that the effects of DO34 on alcohol consumption and preference were mediated via DAGL inhibition. Overall, these data suggest targeting DAGLα may represent an effective approach to the treatment of AUD across a spectrum of severity and development of potent and selective DAGLα inhibitors should remain a high priority. *DAGLA* transcript is known to be preferentially expressed within the human brain, while *DAGLB* is more ubiquitously

expressed (see **Fig. A-S11**). Accordingly, DAGLα$^{-/-}$ mice have been shown to have reduced brain 2-AG levels, with no difference in peripheral 2-AG relative to their WT littermates[77], collectively suggesting that selective targeting of DAGLα may have less somatic adverse effect liability, however this remains to be determined experimentally.

Another key finding of the present work is that DO34 did not increase anxiety or depressive-like behaviors in mice exposed to chronic alcohol or during protracted abstinence. In chronically drinking mice, DO34 reduced immobility in the TST, while it increased immobility in water drinking controls. These data exemplify the notion that the effects of DO34 are dependent on alcohol history and could explain, in part, the apparently contradictory results relative to previously published work that would predict an increase in affective behaviors[75,79]. For example, DO34 increases anxiety-like behaviors in mice exposed to acute stress[79] and impairs extinction of conditioned fear memories[330]. Moreover, DAGLα KO mice exhibit anxiety-like behaviors under some, but not all, conditions, and some reports are conflicting. For example, one report found a robust anxiety-like phenotype in DAGLα KO mice in the light-dark box assay[77], but this effect was absent in DAGLα mice in a later report using a similar light-dark box assay[331]. Furthermore, DO34 exerted mild anxiolytic effects during protracted abstinence, which was unexpected given the anxiogenic effects of DO34 observed after stress exposure[79]. These data again highlight the notion that behavioral function of 2-AG signaling (and thus the effects of DO34) on anxiety and depressive-like phenotypes is highly dependent upon context, such as alcohol use history. Interestingly, we recently showed that augmenting 2-AG levels via inhibition of the 2-AG degrading enzyme monoacylglycerol lipase (MAGL) also showed anxiolytic effects[75,79], and MAGL inhibition has exhibited anxiolytic effects in alcohol withdrawal as well[80]. This apparently paradoxical finding has also been observed in other models; for example, both inhibition[330] and augmentation[332] of 2-AG signaling can facilitate acute fear responses in conditioned fear paradigms. These data collectively suggest that bidirectional manipulations of 2-AG levels can

have overlapping effects in some cases, and the behavioral effects of pharmacological 2-AG modulation may be highly context-dependent. Furthermore, there are several genetics variants that strongly alter DAGLα expression in the brain (see **Fig. A-S12** for one example, rs11604261), demonstrating that the baseline expression of DAGLα can vary across individuals. This suggests that variation within the *DAGLA* gene may demonstrate correlations with susceptibility to AUD or other neuropsychiatric disorders or serve as a biomarker for predicting responsiveness to pharmacological DAGL inhibition. Large scale genetic studies are needed to test this hypothesis.

eCB signaling has been shown to regulate VTA dopamine neuron activity via suppression of afferent GABAergic drive[321-324]. For example, 2-AG mediated suppression of GABA transmission onto VTA DA neurons is weaker in alcohol Sardinian alcohol-preferring rats relative to non-preferring rats[322,324], an effect mediated by enhanced 2-AG degradation[322]. These data suggest that 2-AG can promote alcohol preference via activity-dependent suppression of GABAergic transmission onto VTA dopamine neurons. Based on these data we tested the hypothesis that pharmacological DAGL inhibition could affect alcohol modulation of GABAergic transmission onto VTA DA neurons, which have been shown to increase their firing rate in response to exogenous alcohol[302]. Consistent with these data, *ex vivo* alcohol application to VTA brain slices decreased IPSC frequency into posterior VTA dopamine neurons, as shown previously[320]. This effect was blocked by DO34, suggesting DAGL inhibition could reduce alcohol consumption and preference via reductions in alcohol-stimulated dopamine neuron activity via maintaining high relative levels of GABAergic inhibition. Similar mechanisms have been proposed to underlie the effects of DAGL signaling on nicotine activation of VTA dopamine neurons[321]. While these data suggest DAGL inhibition could reduce positive reinforcement-driven alcohol consumption by reducing alcohol-induced activation of VTA dopamine neurons, negative reinforcement driven mechanisms are thought to mediate alcohol seeking and drinking under dependent conditions[313]. Although DO34 was able to reduce alcohol consumption in a dependent-like drinking model, the underlying

synaptic mechanisms subserving these effects may indeed be different. Future studies should be aimed at elucidating the distinct mechanisms by which DAGL inhibition affects positive vs. negative reinforcement-driven alcohol drinking.

Alterations in other molecular targets that interact with DAGL have been implicated in the pathophysiology of AUD as well, most notably being metabotropic glutamate receptor 5 (mGlu5), which couples to DAGL function through the canonical G_q-phospholipase Cβ-DAGL pathway. mGlu5 has also been posited as a potential therapeutic target for AUD, as several studies have shown inhibition of mGlu5 to have similar effects to those of DAGL inhibition with regards to both alcohol consumption[333,334] and negative affect[335,336] (see Ref. [337] for review), and mGlu5 expression levels are altered by chronic drinking and abstinence[336,338]. Chronic alcohol exposure has also been shown to disrupt group I mGlu receptor mediated depression of glutamate release in the bed nucleus of the stria terminalis[339], the maximal magnitude of which has been shown to be CB_1 receptor dependent[340], although the specific role of 2-AG in this effect has not been experimentally demonstrated. The relationship between altered mGlu5 and DAGL function after chronic alcohol exposure and the mechanisms by which DO34 exerts unexpected anxiolytic effects remain to be determined.

In summary, our data present a key role for DAGL signaling in voluntary alcohol drinking, and posit targeting 2-AG synthesis as a promising pharmacotherapeutic mechanism for the treatment of AUD. The finding that DO34 does not produce affective phenotypes (and exhibits mild anxiolytic effects in some cases) further highlights the therapeutic potential of DAGL as a target for AUD and is especially pertinent given the neuropsychiatric side effects of CB_1 receptor blockade[306]. The variety of models in which we tested the effects of DO34 address several key hallmarks of AUD that serve as barriers to current treatments, including aversion-resistant, susceptibility to relapse, and dependence-like drinking. The ability of DO34 to reduce drinking in all these contexts suggest DAGL inhibition may exhibit therapeutic utility for treating the broad spectrum of early to late-stage, severe AUD, which could have broad implications. Future studies should be aimed at

determining the cellular and synaptic mechanisms underlying the effects of DO34 on early vs. late, dependence-like drinking, as well as on the development of more selective DAGLα inhibitors to further test this hypothesis and ultimately lead to the discovery of more safe and effective therapies for AUD.

MATERIALS AND METHODS

Subjects

C57BL/6J male and female mice between 6–8 weeks of age at the beginning of experiments were used. DAGLα$^{-/-}$ male and female mice were generated by disruption of exon 8 and were maintained on a C57Bl6/N background by interbreeding DAGLα+/− mice. Further details are described in Ref. [77]. Tyrosine hydroxylase (TH) reporter mice (TH::Ai14 mice) were generated by crossing TH-Cre mice (Jax Stock No: 008601) with Ai14 mice (Jax Stock No: 007914) for Cre-dependent Td-tomato expression in TH+ cells to label catecholaminergic neurons. All mice were group housed on a 12:12 light-dark cycle (lights on at 6:00 a.m.) with food and water available ad libitum. All behavioral testing was performed between 6:00 am and 6:00 pm.

Drugs and treatment

The DAGL inhibitor DO34 (50 mg/kg; Glixx Laboratories Inc., MA, USA), control compound DO53 (50 mg/kg; synthesized in-house, see **Fig. A-S1**), MAGL inhibitor JZL184 (10 mg/kg; Cayman Chemical, MI, USA), pyrazole (68 mg/kg; Sigma-Aldrich, WI, USA) and quinine hydrochloride (0.01, 0.03 and 0.1 g/L; Millipore, MA, USA) were used. DO34 and DO53 (or vehicle control) were administered by intraperitoneal (i.p.) injection at a volume of 10 ml/kg in a formulation containing ethanol (Pharmco, KY, USA): kolliphor (Sigma-Aldrich, WI,): saline (Hospira, IL, USA) (1:1:18). JZL184 (or vehicle control) was administered by i.p. injection at a volume of 1 ml/kg in DMSO (Sigma-Aldrich, WI, USA, Cat. No. D8414). EtOH + pyrazole solutions for vapor chamber experiments were prepared in saline and injected i.p. at a dose of 1.6 g/kg EtOH + 68 mg/kg pyrazole. Drug pretreatment times were two hours prior to behavioral testing or 30 minutes prior

to vapor chamber sessions. Drugs for EtOH drinking experiments were injected 2 hours before starting the dark cycle. Quinine hydrochloride (Millipore, MA, USA) was added to the drinking water or ethanol bottles at varying concentrations. 190 proof ACS/USP grade grain-derived EtOH was used to make EtOH solutions.

Two-bottle choice (2BC) EtOH drinking paradigm

Mice were singly housed and acclimatized for 5-7 days in 2BC cages. Mice had access to two sippers throughout the experiment. For EtOH drinking mice, EtOH concentration was slowly increased from 3% to 10% or 20% as shown in **Figure A-1A** and maintained on respective solutions for the duration of the experiment. Water and ethanol intake were monitored either daily, after 4 days, or weekly depending on the experimental timeline. For the intermittent access model (see **Fig. A-3C**), mice were given intermittent access to alcohol (10% on week one, 15% thereafter) 3 days per week for 24-hour periods on alternating days. Whenever mice were given pharmacological treatments, water intake, EtOH intake and body weights were measured daily. Food was provided *ad libitum* throughout the alcohol drinking paradigm. EtOH naive mice (control) were also housed in the same conditions, but two bottles of water remained in their cage until day of experiment. EtOH preference was determined as ((EtOH intake (g)/total fluid intake (g)) × 100). EtOH consumption was determined as [((EtOH intake (g)/mice body weight (kg)/number of days) × EtOH concentration × EtOH density (0.816 g/mL)]. Dummy cages were used to calculate water and EtOH drip and subtracted from intake values.

Aversion-Resistant EtOH drinking model

After 4 weeks of EtOH drinking in 2BC EtOH drinking paradigm, quinine was added to either water (control mice) or EtOH bottles (EtOH group) at varying concentration (0.01, 0.03 and 0.1 g/L). EtOH quinine and water quinine preference and consumptions were calculated as described above.

Ethanol vapor inhalation treatment for chronic intermittent EtOH (CIE) exposure

For chronic intermittent ethanol exposure, female C57Bl6/J were exposed to vapor inhalation for 16 hours per day, 4 days per week, on alternating weeks as shown in **Fig. A-4C**. Mice were given i.p. injections of EtOH (1.6 g/kg) + pyrazole (alcohol dehydrogenase inhibitor, 68 mg/kg) 30 minutes prior to the start of each session. Mice were then placed in a chamber with volatilized EtOH (18-22 mg/L) for 16 hours. Mice had *ad libitum* access to food and water for the duration of the session. These procedures were similar as done previously[341] which were able to produce blood EtOH levels of 150–185 mg/dl. Following 4 days of vapor treatment, mice went through 72 hours of abstinence before returning to the intermittent 2BC paradigm described above.

EtOH Reinstatement Drinking

After 5 weeks of EtOH drinking in 2BC EtOH drinking paradigm, EtOH bottles were replaced with water bottles for 10 days. After 10 days, EtOH was provided to study reinstatement of EtOH drinking behavior. EtOH preference and consumptions were calculated as described above.

Behavioral experiments

Novelty-induced feeding suppression (NIFS)

NIFS assay was performed as described previously[316]. Briefly, mice were deprived of food for a 48hr period, with brief access to food from 23-25hr. Following food deprivation, mice were acclimated to the testing room for at least 2hr prior to placement in a brightly lit (250-300 lux) 50 x 50cm arena with a single food pellet in the center of the arena. Mouse movement and behavior was tracked with an overhead camera using AnyMaze software (Stoelting, IL, USA). Mice remained in the arena until their first bite of the food pellet. Mice were given *ad libitum* access to food after testing.

Marble burying test

For the marble burying test, empty cages without food or water were filled with 5cm fresh Diamond Fresh Soft Bedding (Envigo, IN, USA) and 20 marbles (5 rows, 4 columns) placed on top of the bedding. Mice were placed in the cage for 30 minutes, then removed. Marbles were considered “buried” if 2/3 of the marble was covered by bedding. Marbles were counted manually by an

experimenter that was blinded to the treatment condition. Light intensity in the room was 200-250 lux.

Forced swim test (FST)

FST was performed as described previously[316]. Briefly, mice acclimated to the testing room for at least 2 hours then were placed in a cylinder containing water (23-25°C) at a level such that mice could not touch the bottom or the top. The test lasted for 6 minutes and filmed via overhead camera and later scored by an observer blinded to treatment. Immobility time was analyzed during the last 4 minutes of the test.

Elevated plus maze (EPM)

EPM assay was performed similar to as described previously[78]. The apparatus consisted of two open arms (30 × 10cm) and two closed arms (30 × 10 × 20cm) that met at a center junction (5 × 5cm) and was elevated 50cm above the floor. Light intensity in the open arms was 200-250 lux and <100 lux in the closed arms. Mice were placed in the center of the apparatus, facing an open arm and allowed to freely explore for 6 minutes. Movement and behavior were tracked via an overhead camera and AnyMaze software (Stoelting, IL, USA).

Open field

For open-field testing (OFT), exploration of a novel open field arena contained within a sound-attenuating chamber was monitored for 30 min (27.9 × 27.9 × 20.3 cm; MED-OFA-510; MED Associates, St. Albans, Vermont). The walls of the open field arena were made of clear plexiglass; this arena was contained within an opaque sound-attenuating chamber. Beam breaks from 16 infrared beams were recorded by Activity Monitor v5.10 (MED Associates) to monitor position and behavior.

3-chamber social interaction

Social behavior was tested in a 3-chamber acrylic arena with opaque outer walls and clear walls separating each 20 cm x 40 cm chamber, which contained 10 cm sliding doors for introduction of the test mouse into the middle chamber. Testing was performed under low lighting conditions

(~40 lux) and mice were acclimated to this lighting for at least 1 hour before testing began. The test mouse was allowed to explore the apparatus, which contained one empty inverted wire pencil cup in each outer chamber, for 10 minutes and was then coaxed back into the middle chamber and doors replaced. The target mouse (a female WT C57Bl6 mouse, which was aged matched and previously acclimated to the pencil cup for 30 min) was then placed under one of the pencil cups and the doors were removed allowing the test mouse to explore the entire apparatus for 5 minutes. The mouse was monitored by an overhead camera and AnyMaze software (Stoelting, IL, USA) and the time spent in each chamber was measured. Preference for the social target was determined within each group by comparing the time spent in the target-mouse chamber to the time spent in the empty pencil cup chamber using a paired two-tailed student t-test. Mice that did not spend significantly more time in the target-mouse chamber were considered deficient in sociability.

Elevated-zero maze

The elevated-zero maze (EZM, San Diego instruments, California, USA) is annular white platform and divided four equal quadrants. It consisted of two open arms and two closed arms. The outer and inner diameter of EZM was 60.9 cm and 50.8 cm, respectively. The apparatus was elevated 60.9 cm from the floor. Light levels in the open arms were approximately 200 lux, while the closed arms were <100 lux. Mice were placed in the closed arm of the maze and allowed to explore for 5 min. ANY-maze (Stoelting, Wood Dale, Illinois, USA) video-tracking software was used to monitor and analyze behavior during the test.

Brain Tissue Preparation and Mass Spectrometry

For acute brain tissue sample collection, mice were sacrificed by cervical dislocation and decapitation followed by rapid removal of the brain. For half brain samples, mice were treated with DO34 (50 mg/kg) for 4 days. 2 hours after the final treatment, whole brains were removed and snap frozen in 2-methylbutane (Sigma-Aldrich, WI, USA) on dry ice and quickly hemisected before storing at -80°C for further processing. Of note, brains collected for analysis in **Fig. A-2**

were from the mice that underwent behavioral testing in **Fig. A-3H-K**. For midbrain tissue punches, brains were blocked around the VTA (1mm thick section) and snap frozen by placing the blade and tissue on an aluminum block in dry ice. 1.5-2.0mm midbrain punches were then taken from the center of the section and stored at -80°C for further processing.

Liquid chromatography and mass spectrometry performed similarly to as previously reported[342]. Briefly, samples were sonicated in 300 µl of homogenization solution and placed in a bath sonicator for up to 2 minutes and incubated at -20°C overnight. The following day, samples were centrifuged at 3000 rpm for 12 minutes at 4°C. Supernatant was collected and dried under nitrogen. Afterwards, samples were reconstituted by the addition of 60 µl of methanol followed by 30 µl of distilled water and vortexing. Finally, samples were centrifuged at 3000 rpm for 12 minutes at 4°C if they were cloudy and/or had visible particulate matter. LC-MS/MS analysis was performed on Shimadzu Nexera X2 system in-line with SCIEX 6500 QTrap. Samples were analyzed using Analyst software program and then analyzed for significance with GraphPad Prism. Data was normalized to tissue mass and presented as either “pmol/g tissue” or “nmol/g tissue.” Detection methods for analytes and internal standards can be found in **Table A-S1**.

Blood Ethanol Concentration Measurements

Female WT mice were injected with DO34 (50 mg/kg) or vehicle and 2 hours later given an i.p. bolus of EtOH (3 g/kg). 30 mins after EtOH injection, mice were anesthetized under isoflurane and decapitated for trunk blood collection. Samples were allowed to coagulate at room temperature then placed on ice until centrifugation at 4500RPM for 15 mins at 4°C. Serum supernatant samples were extracted and used for evaluation of blood ethanol concentration per the protocol provided in the kit (Pointe Scientific, Cat. No. A7504-39). The standard EtOH concentrations were obtained from a calibration kit (Cerilliant, Cat. No. E-034) and the assay was run in a 96 well plate and read on a Glomax-Discover plate reader (Promega, Cat. No. GM3000).

Electrophysiology Experiments

Male and female TH::Ai14 mice (described above) were used for electrophysiological experiments. Acute slice preparation was performed as described previously[79]. Coronal midbrain slices were cut at 200µm. Following recovery, slices were transferred to a recording chamber and perfused at a rate of 2-3mL/minute with oxygenated artificial cerebrospinal fluid (ACSF; 31-33°C) recording solution consisting of (in mM): 113 NaCl, 2.5 KCl, 1.2 $MgSO_4 \cdot 7H_20$, 2.5 $CaCl_2 \cdot 6H_20$, 1 NaH_2PO_4, 26 $NaHCO_3$, 20 glucose, 3 Na-pyruvate, and 1 Na-ascorbate. TH+ cells were visually identified by their red fluorescence. Whole-cell recordings of spontaneous inhibitory post-synaptic currents (sIPSCs) were performed in voltage clamp configuration at -70mV in the presence of 10µM CNQX and 30µM D-AP5. 3–6 MΩ borosilicate glass pipettes were filled with the intracellular pipette solution consisting of (in mM): 125 KCl, 4 NaCl, 10 HEPES, 4 MgATP, 0.3 NaGTP, 10 Na-phosphocreatine, and 0.2 EGTA. Following break in, all cells were allowed to dialyze with the pipette solution for 3 minutes prior to recordings. Cells with an access resistance of ≤25 MΩ were included in analyses. DO34 was dissolved in DMSO stocks at 10mM and diluted in ACSF for a final concentration of 2.5µM. DO34-treated slices were incubated for a minimum of 45 minutes prior to recordings. sIPSC baselines were recorded for 2 minutes, followed by 10-minute bath application of 100 mM ethanol. Cells were then recorded for an additional 2 minutes in the continued presence of EtOH. Recordings were performed using a MultiClamp 700B amplifier (Molecular Devices, CA, USA), and Clampex software (Molecular Devices, CA, USA). Traces were analyzed using pCLAMP 10 software (Molecular Devices, CA, USA).

Statistics

Drinking time course experiments examining 2 groups (genotype or drug vs. vehicle) were analyzed via a repeated measures two-way ANOVA followed by a Holm-Sidak multiple comparisons test between groups at all time points. Single group drinking time course experiments were analyzed via a one-way ANOVA on time points noted in figure legends followed by a Holm-Sidak multiple comparisons test referenced to baseline before drug treatment. Behavioral data analyzed by t-test or two-way ANOVA followed by a Holm-Sidak multiple

comparisons test between all groups as noted in figure legends. Electrophysiology data analyzed by two-way ANOVA followed by a Holm-Sidak multiple comparisons test between baseline and EtOH application or by Fisher's exact test. All statistical analyses were conducted using GraphPad Prism 7 (GraphPad Software, CA, USA). For behavioral studies, all replicates (n values) represent biological replicates defined as data derived from a single mouse. Summary data are presented as mean ± S.E.M. unless otherwise noted. Significance was defined as $p<0.05$ throughout the manuscript. F and P values for ANOVA analyses are indicated within figure panels, while post-hoc significance level is indicated above individual bars or time points. Testing was counterbalanced, but no randomization was performed, and sample sizes were derived empirically during the course of the experiments and guided by our previous work using these assays.

Study Approval

All studies were carried out in accordance with the National Institutes of Health Guide for the Care and Use of Laboratory Animals and approved by the Vanderbilt University Institutional Animal Care and Use Committee (M1600213-01; M1800046; M1900114-00).

ACKNOWLEDGEMENTS

These studies were supported by NIH grants AA026186 (S.P.) and AA019455 (D.G.W.) and Brain Behavior Research Foundation NARSAD Young Investigator Awards 27172 (S.W.C.).

AUTHOR CONTRIBUTIONS

G.B., and N.D.W., and S.P. conceived the study, designed experiments, and co-wrote the manuscript.; S.W.C and D.G.W. assisted in alcohol drinking model development and optimization.; G.B., N.D.W., T.A.P., A.A., M.A., K.D.J, S.M., and V.R.M. performed experiments and acquired and analyzed data in the laboratories of S.P., D.J.W., and C.A.S.; J.U. synthesized

the control compound DO53 and P.J.K. and M.A. ran the mass spectrometry experiments in the laboratory of L.J.M.; D.C.S. acquired gene expression data.

SUPPLEMENTAL INFORMATION

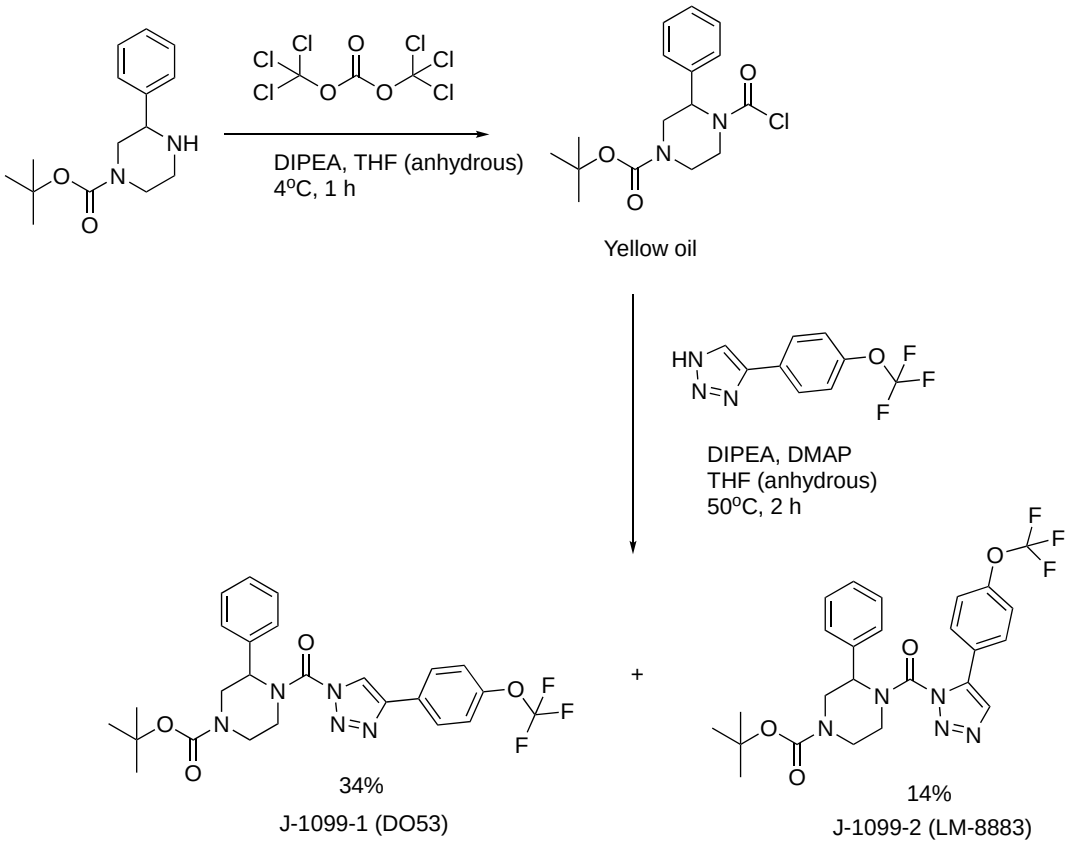

Figure A-S1: Chemical synthesis and spectroscopic characterization of (4-{[(2-Methyl-2-propanyl)oxy]carbonyl}-2-phenylpyperazinyl){4-[(4-trifluoromethoxy)phenyl]-1H-1,2,3-triazol-1-yl}metanone (DO53).

Synthetic Procedure: Diisopropylethylamine (275 mg, 2 mmol) followed by triphosgene (100 mg, 0.34 mmol) was added to a solution of 1-Boc-3-phenylpiperazine (175 mg, 0.65 mmol) dissolved in anhydrous tetrahydrofuran (5 mL), and the resultant reaction mixture was stirred 1 hour on ice. The reaction mixture was poured into water (5 mL) and extracted with ethyl acetate, and the organic layer was washed with water and brine, dried over anhydrous sodium sulfate and concentrated in vacuo. The residue was kept under vacuum overnight, then dissolved in anhydrous tetrahydrofuran (10 mL), to which diisopropylethylamine (275 mg, 2 mmol), 4-(dimethylamino)pyridine (80 mg, 0.65 mmol) and 4-(4- trifluoromethoxyphenyl)-1H-1,2,3-triazole (150 mg, 0.65 mmol) were added chronologically. The reaction mixture was wormed and stirred for 2 hours at 50 °C. The reaction mixture was cooled to ambient temperature and poured into saturated aqueous ammonium chloride solution and extracted with ethyl acetate. Combined organic layer was washed with water and brine, dried over anhydrous sodium sulfate and concentrated in vacuo. The crude product was purified by silica gel column chromatography (ethyl acetate: hexane = 1:8, v/v) to afford (4-{[(2-methyl-2-propanyl)oxy]carbonyl}-2-

phenylpyperazinyl){4-[(4- trifluoromethoxy)phenyl]-1H-1,2,3-triazol-1-yl}metanone (DO53) (119 mg, 34%).

Spectroscopic Characterization: ^{1}H NMR (DMSO-d_6 600 MHz): 1.33 (s, 9H), 3.03-3.20 (m, 1H), 3.21-3.42 (m, 1H), 3.45-3.59 (m, 1H), 3.69-3.89 (m, 1H), 3.95-4.10 (m, 1H), 4.45-4.55 (m, 1H), 5.58 (s, 1H), 7.25−7.35 (m, 1H), 7.36−7.42 (m, 4H), 7.48 (d, 2H, J = 8.6 Hz), 8.08 (d, 2H, J = 8.6 Hz), 8.19 (s, 1H). ESI MS calcd. C25H26F3N5O4 [M+H]+ 518.20, MS found 518.08.

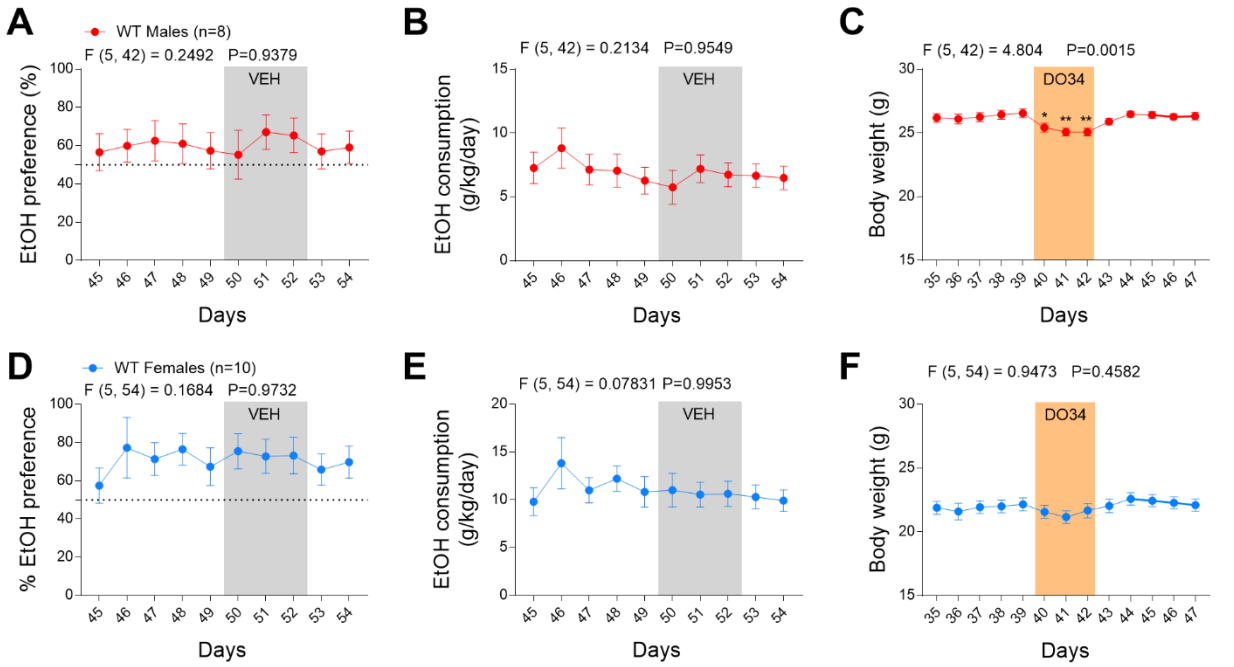

Figure A-S2: Vehicle treatment does not affect EtOH preference or consumption and DO34 reduces body weight only in male mice. Vehicle treatment had no effect on EtOH **(A, D)** preference or **(B, E)** consumption in either sex. **(c)** DO34 decreased body weight in male mice. Body weight recovered after cessation of DO34 treatment. **(F)** DO34 had no effect on body weight in female mice. All DO34 treatments were dosed at 50 mg/kg. Data were analyzed by one-way ANOVA on time points 49-54 **(A-B, D-E)** or 39-44 **(C, F)** (to include baseline, drug treatment, and two recovery points) followed by a Holm-Sidak test for multiple comparisons to baseline control. Sample size *n*, *P*, and *F* values for main effects of drug treatment reported on graphs. Significance for post-hoc multiple comparisons reported on graphs (*P<.05, **P<0.01, ***P<0.001, ****P<0.0001). Data are mean ± SEM.

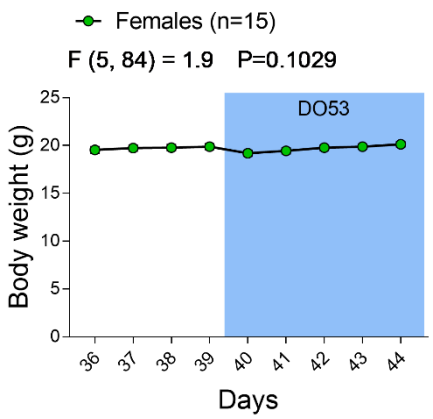

Figure A-S3: DO53 treatment has no effect on body weight in female mice. Treatment with the control compound DO53 (5 days) had no effect on body weight. Baseline data were averaged for analyses. Data analyzed by one-way ANOVA on averaged baseline (Days 36-39) and individual treatment days followed by a Holm-Sidak test for multiple comparisons to averaged baseline. Sample size *n* and *P* and *F* values for main effects of drug treatment reported on graph. All DO53 treatments were dosed at 50 mg/kg. Female mice were used for these experiments. Significance for post-hoc multiple comparisons reported on graphs (*P<.05, **P<0.01, ***P<0.001, ****P<0.0001). Data are mean ± SEM.

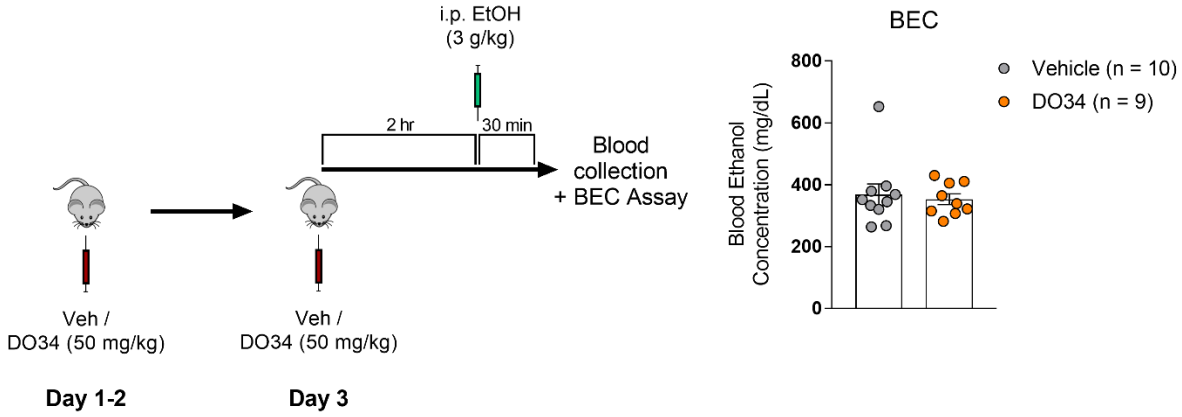

Figure A-S4: DO34 does not alter blood ethanol concentrations. (*left*) Schematic of experimental design for BEC measurements. **(*right*)** DO34 treatment had no effect on BEC 30 min after 3 g/kg i.p. EtOH injections. Sample size *n* reported on graph. Data analyzed by two-tailed student's t-test (P=0.7145). Data are mean ± SEM. BEC, blood ethanol concentration.

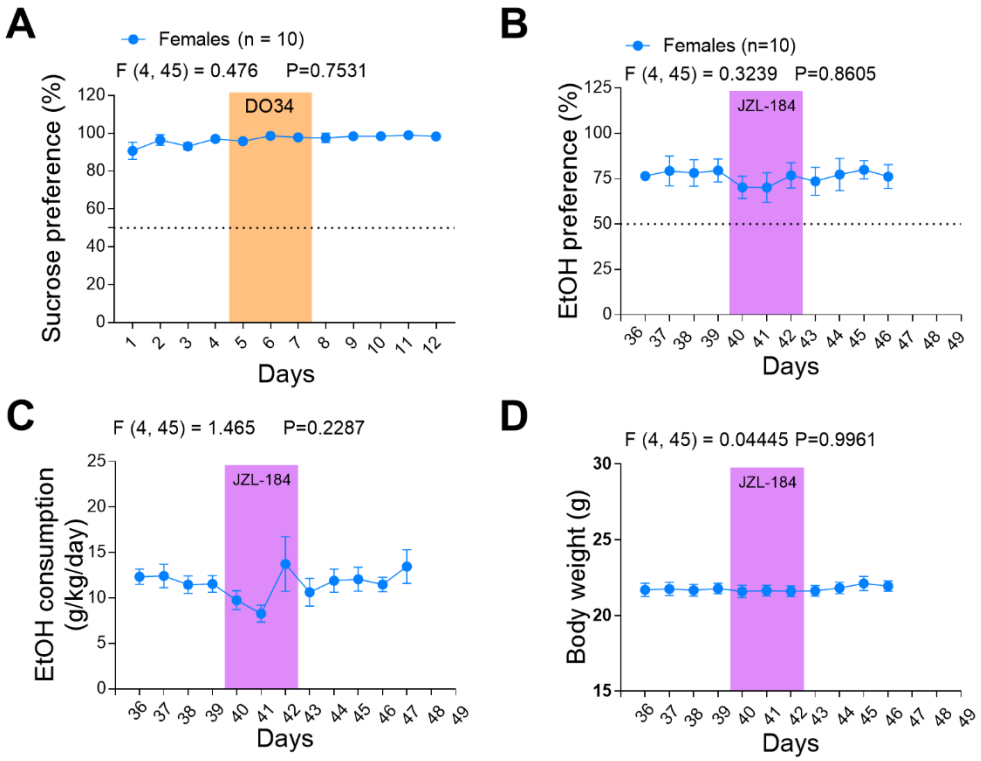

Figure A-S5: DO34 does not alter sucrose preference and 2-AG augmentation has no effect on EtOH drinking or body weight. (A) DO34 treatment had no effect on 2BC sucrose preference. **(B)** Treatment with the monoacylglycerol lipase inhibitor JZL-185 had no effect on EtOH preference, **(C)** EtOH consumption, or **(D)** body weight. Data were analyzed by one-way ANOVA on time points **(A)** 4-8 or **(B-D)** 39-41 (to include baseline, drug treatment, and one recovery point) followed by a Holm-Sidak test for multiple comparisons to baseline control. Sample size *n*, *P*, and *F* values for main effects of drug treatment reported on graphs. All DO34 treatments were dosed at 50 mg/kg. All JZL-184 treatments were dosed at 10 mg/kg. Female mice were used for these experiments. Data are mean ± SEM.

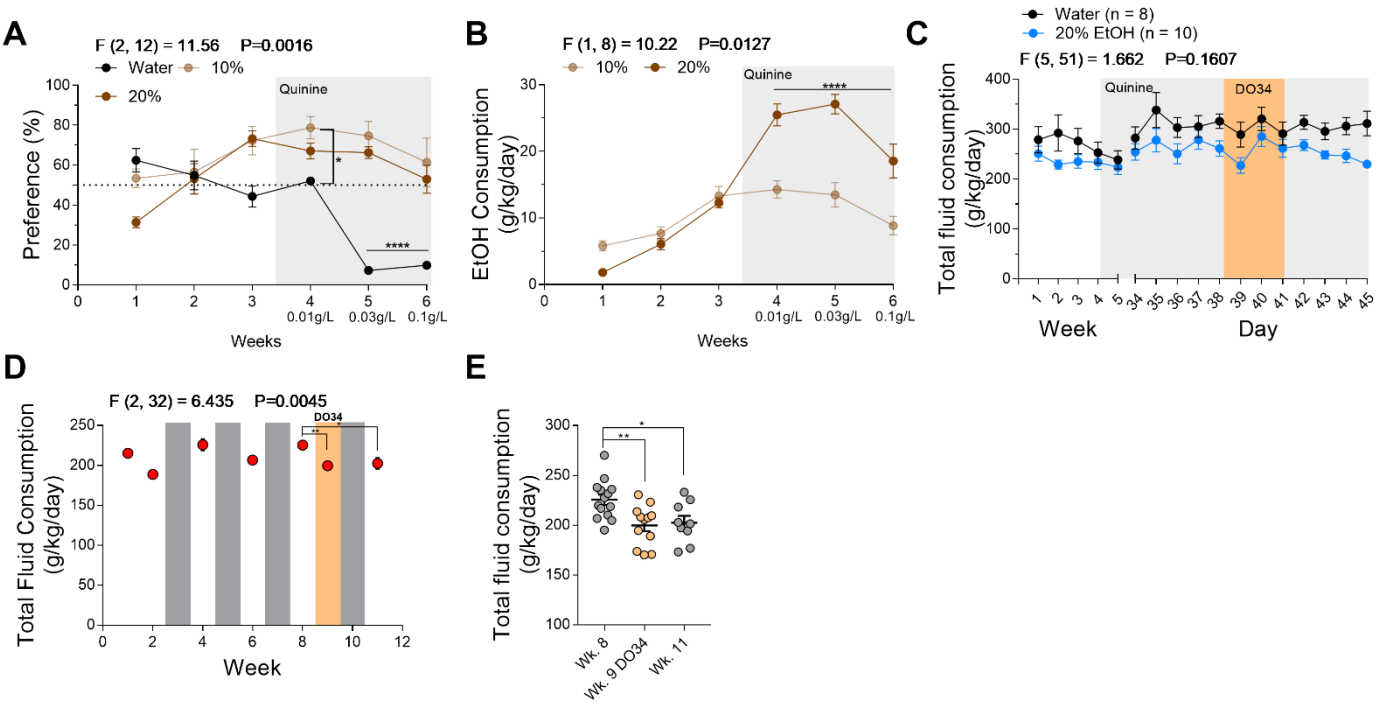

Figure A-S6: Mice reliably drink quinine-adulterated EtOH and DO34 has variable but minimal effects on total fluid consumption across EtOH drinking models. (A) Mice showed significantly higher preference for EtOH + quinine compared to water + quinine at 0.03 and 0.1 g/L quinine. **(B)** Mice drank significantly higher levels of 20% EtOH + quinine compared to 10% EtOH + quinine. **(C)** DO34 treatment had no effect on total fluid consumption in the aversion-resistant drinking model. **(D)** DO34 treatment reduced total fluid intake in the chronic intermittent ethanol model compared to the baseline week and fluid consumption remained decreased during the recovery week. **(E)** Graph depicting individual mouse total fluid consumption during baseline, treatment, and recovery weeks. Fluid consumption is lower in treatment and recovery weeks compared to baseline, but treatment and recovery consumption levels are not significantly different. **(A-C)** Data were analyzed by repeated measures two-way ANOVA during **(A-B)** quinine exposure or **(C)** time points 38-43 (to include baseline, drug treatment, and two recovery points), followed by a Holm-Sidak test for multiple comparisons. **(D-E)** Data were analyzed by one-way ANOVA on time points 8, 9, and 11, followed by a Holm-Sidak test for multiple comparisons between these 3 time points. *P* and *F* values for main effects of drug or quinine treatment reported on graphs. *n* = 5 mice per group in (**A-B**). Sample size *n* reported on graph in **(C)**. *n* = 9-14 mice in (**D-E**). Significance for post-hoc multiple comparisons reported on graphs (*P<.05, **P<0.01, ****P<0.0001). Data are mean ± SEM.

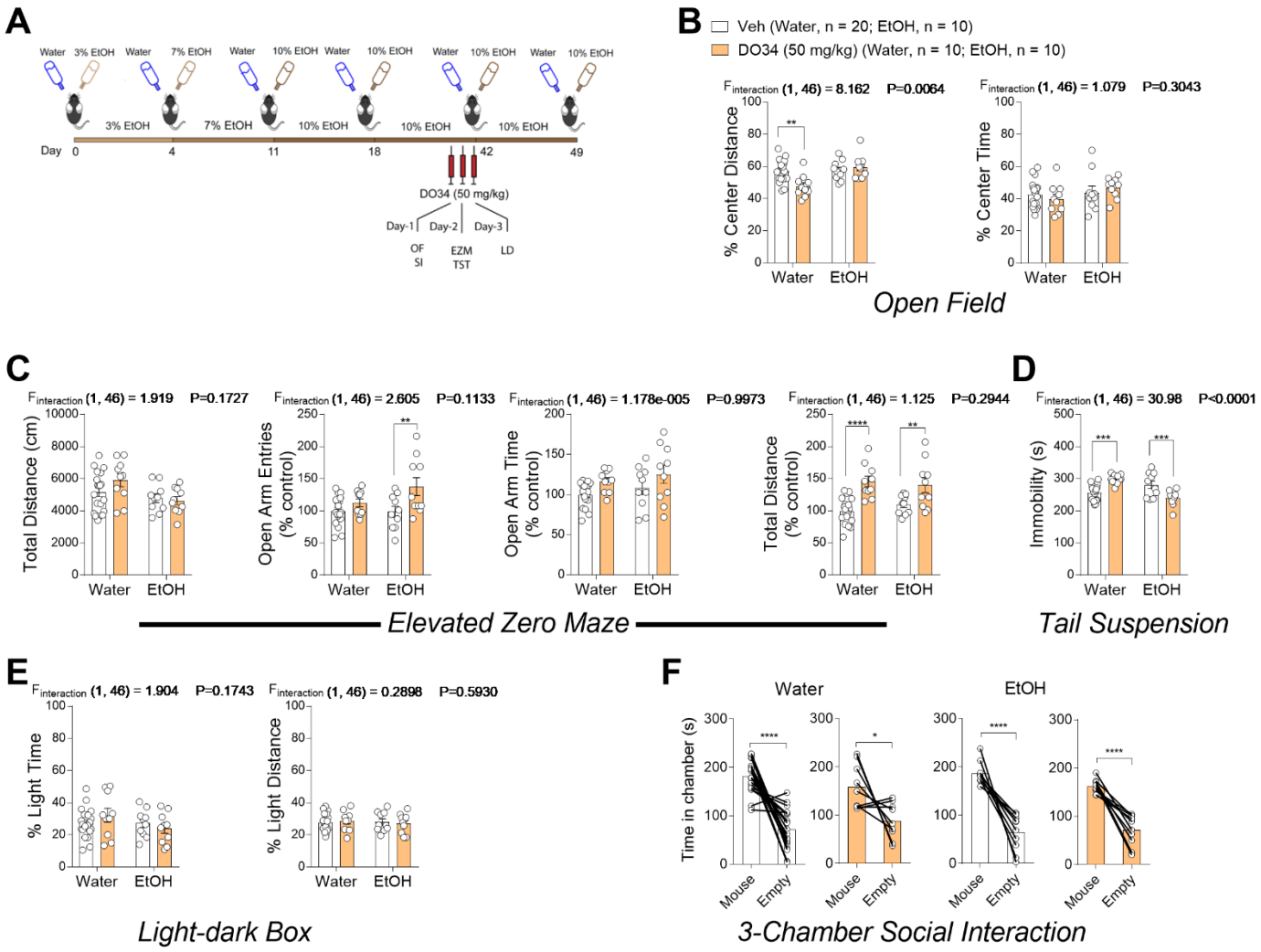

Figure A-S7: DO34 treatment does not precipitate negative affective phenotypes after chronic drinking at 10% EtOH. (A) Schematic depicting 2BC drinking paradigm and time course of behavioral testing. **(B)** DO34 treatment decreased open field test % center time in water control mice but not in EtOH drinking mice. **(C)** DO34 treatment increased % open arm entries in EtOH mice but not water control mice and increased total distance travelled in both water and EtOH dunking mice. **(D)** DO34 increased immobility time in the tail suspension test in water control mice but decreased immobility time in EtOH mice. **(E)** DO34 treatment had no effect on anxiety-like behaviors in the light-dark box assay. **(F)** DO34 treatment had no effect on social behaviors in the 3-chamber social interaction test. **(B-E)** Data were analyzed by two-way ANOVA or **(F)** paired t-test followed by a Holm-Sidak test for multiple comparisons between all groups. Female mice were used in all experiments. *P* and *F* values for EtOH x drug interaction reported on graphs. Significance for post-hoc multiple comparisons reported on graphs (*P<.05, **P<0.01, ***P<0.001, ****P<0.0001). Data are mean ± SEM.

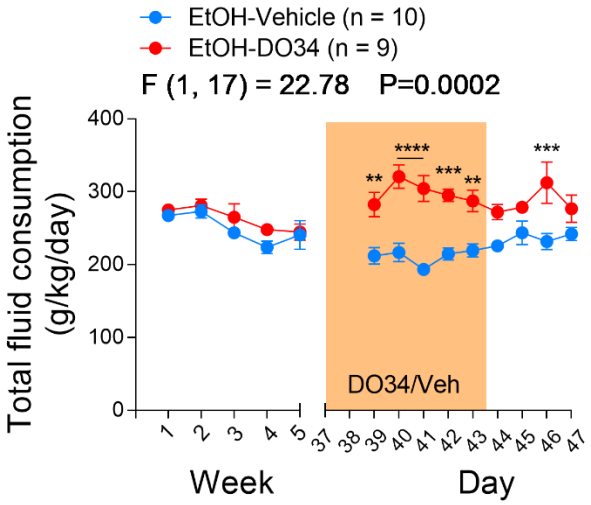

Figure A-S8: DO34 treatment does not precipitate negative affective phenotypes after chronic drinking at 10% EtOH. DO34 increased total fluid consumption in the relapse drinking model. Female mice were used in this experiment and DO34 was dosed at 50 mg/kg. Data analyzed by repeated measures two-way ANOVA followed by a Holm-Sidak test for multiple comparisons between treatment conditions. Sample size *n*, *P* and *F* values for main effects of drug treatment, significance for post-hoc multiple comparisons reported on graphs (**P<0.01, ***P<0.001, ****P<0.0001). Data are mean ± SEM.

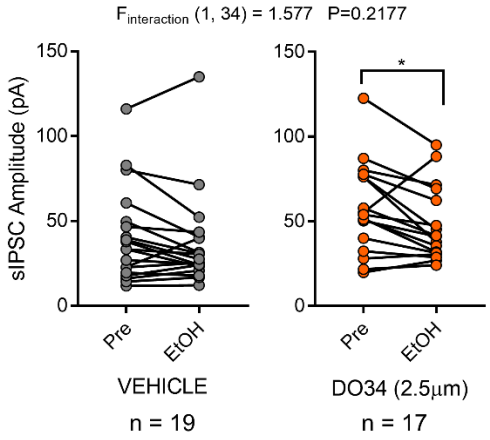

Figure A-S9: EtOH reduces sIPSC amplitude onto putative dopamine neurons in the posterior VTA of DO34-treated slices. Bath application of 100mM EtOH reduced sIPSC amplitude in DO34- but not vehicle-treated slices. All cells recorded were putative dopamine neurons visually-identified by their red fluorescence (see main text, **Fig. 5A**). Data were analyzed by repeated measures two-way followed by a Holm-Sidak test for multiple comparisons between baseline and EtOH treatment. Vehicle, *n* = 19 cells; DO34, *n* = 17 cells; from 13 mice. *P* and *F* value for EtOH x DO34 interaction reported on graph. Significance for post-hoc multiple comparisons reported on graph (*P<.05).

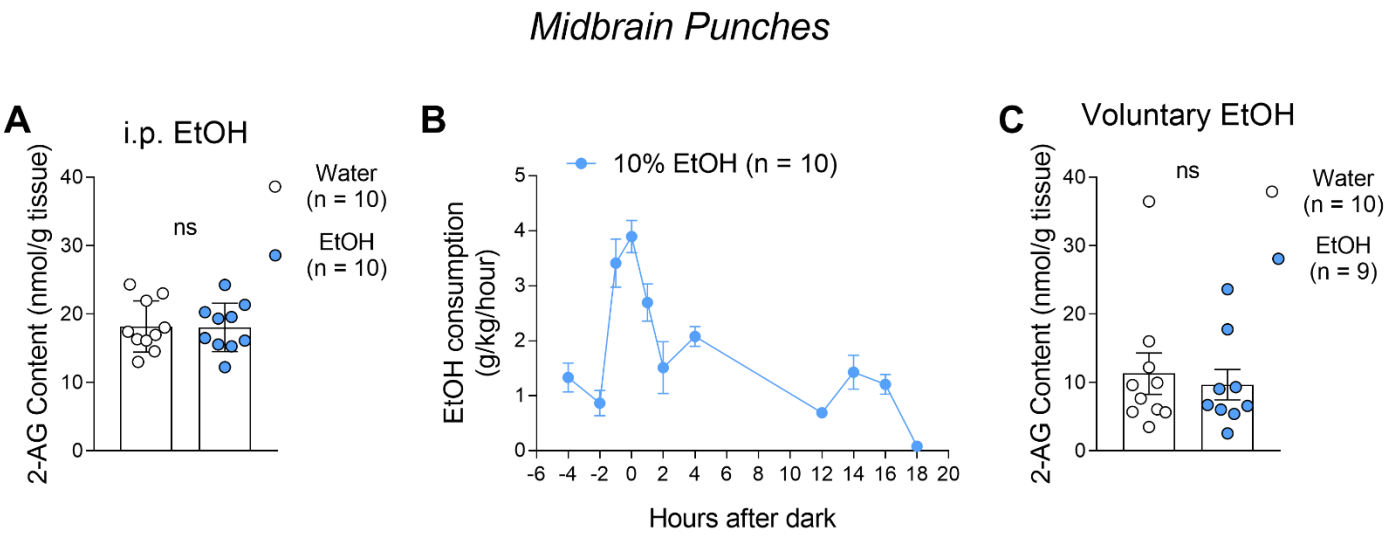

Figure A-S10: EtOH does not increase 2-AG levels measured by mass spectrometry in midbrain punches containing VTA. (A) Intraperitoneal (i.p.) EtOH injection (3 g/kg) had no effect on midbrain punch 2-AG levels 30 minutes after injection. **(B)** EtOH consumption time course of an independent cohort in our 2BC drinking paradigm. **(C)** Voluntary 2BC EtOH intake had no effect on midbrain punch 2-AG levels when collected between 0-2 hours after dark. **(A, C)** Data analyzed by two-tailed student's t-test. Sample size *n* reported on graphs. Data are mean ± SEM.

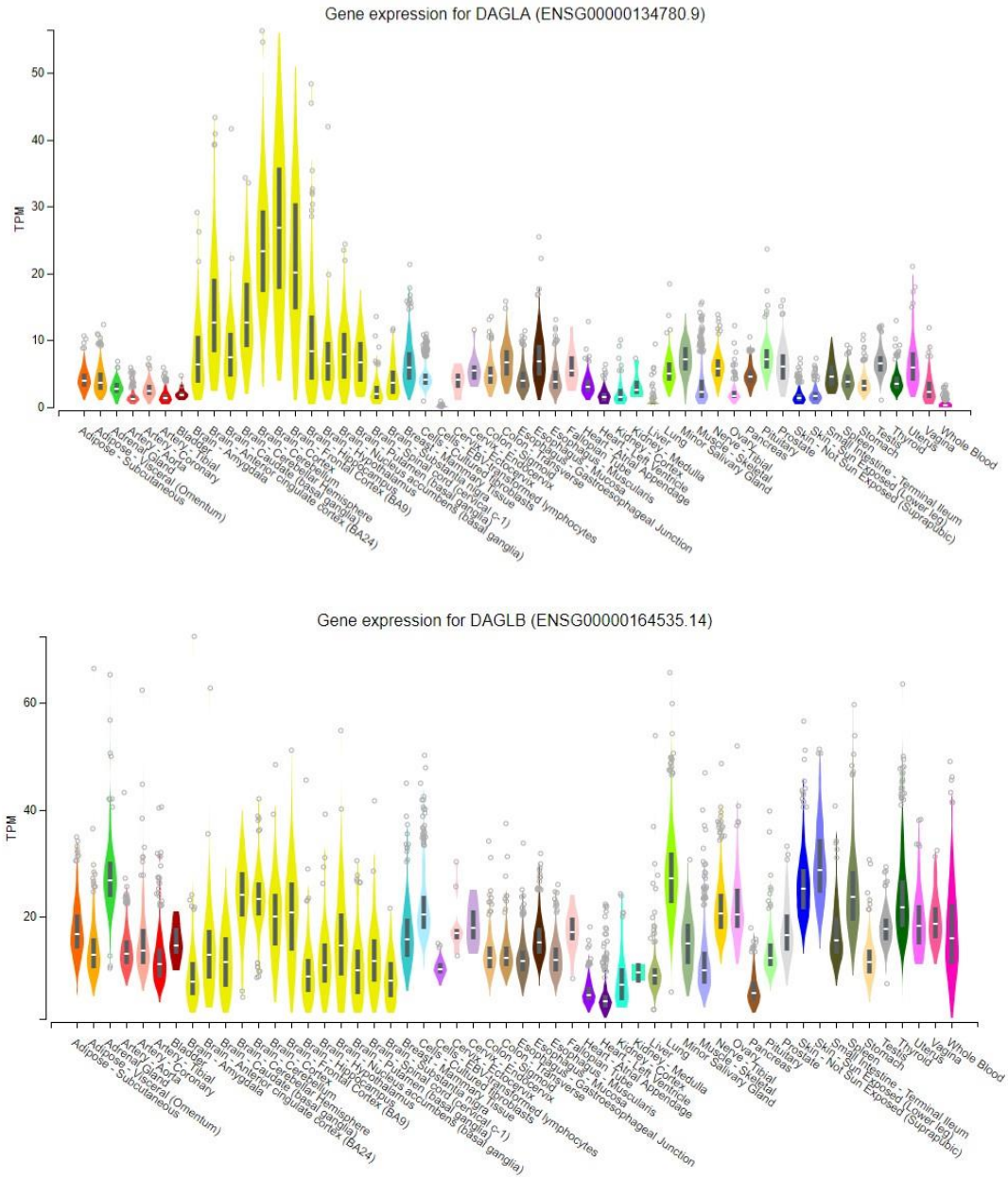

Figure A-S11: GTEx data on tissue-specific expression of *DAGLA* and *DAGLB* expression: (*top*) Expression profile for *DAGLA*, demonstrating highest expression in brain tissues (yellow). **(*bottom*)** Expression profile for *DAGLB*, demonstrating ubiquitous tissue distribution. Data are expressed as transcripts per million reads (TPM), and obtained from the GTEx Portal (dbGaP Accession phs000424.v8.p2; see https://gtexportal.org/home)

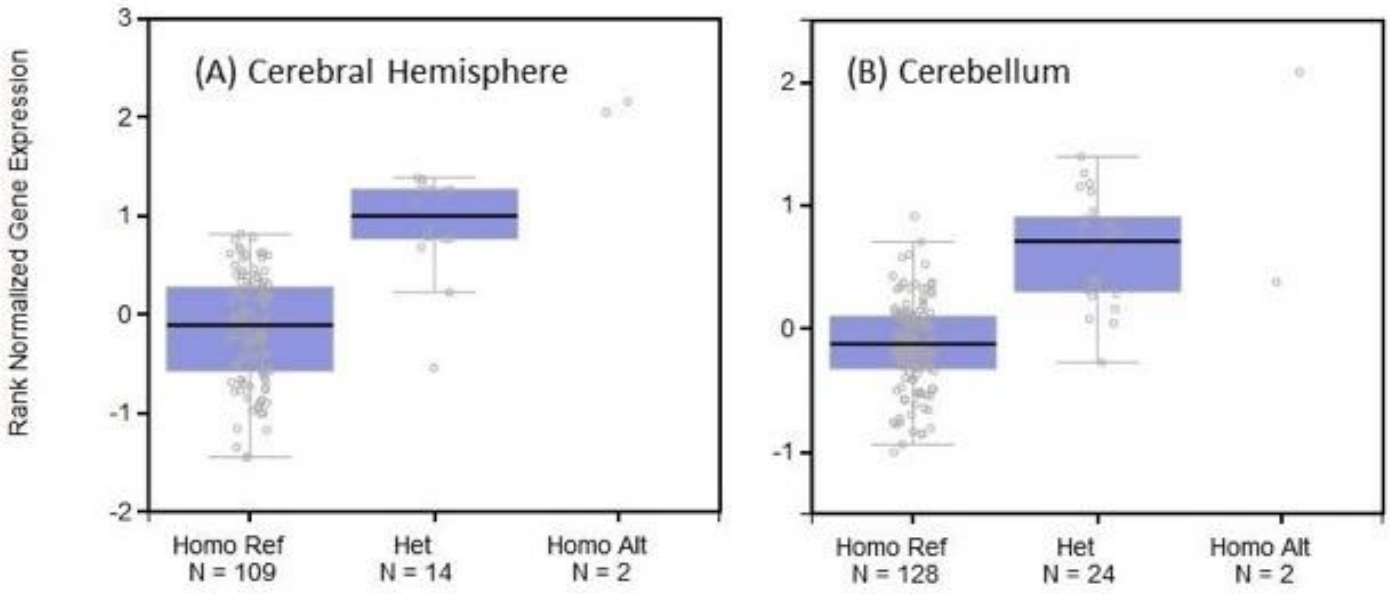

Figure A-S12: GTEx data on the effect of *DAGLA* genetic variant rs11604261 on relative gene expression: The effect of the common variant rs11604261 on DAGLα expression in two brain regions. Normalized expression values are plotted for the three genotypes: homozygous reference, heterozygous, and homozygous alternative allele. Data obtained from the GTEx Portal (dbGaP Accession phs000424.v8.p2; see https://gtexportal.org/home).

Analytes were detected by selected reaction monitoring (SRM) as [M + H] complexes in positive ion mode except for AA which was detected by SRM as in negative ion mode (as the [M – H] ion). The table below gives the Q1 and Q3 values for each analyte (mass in parentheses is the mass of the deuterated internal standard):

Analyte	Q1 (m/z)	Q3 (m/z)
2AG (-d5)	379.2 (384.2)	287.2 (287.1)
AEA (-d4)	348.2 (352.2)	62 (66)
AA (-d8)	303.2 (311.2)	259.1 (267.1)
PGE2_D2 (-d4)	351.2 (355.2)	271.1 (275.1)

The samples were chromatographed on a Acquity C18 column with a gradient elution scheme. The gradient profile was as follows: 0-0.25 min, 62%B, %B was then increased to 99% over 3 minutes, held at 99% for 2 more 5 minutes, and then returned to initial conditions at 5.25 minutes. Mobile phase A was water with 0.1% Formic Acid and 3%B and Mobile phase B was 4:1 acetonitrile:methanol with 0.1% formic acid and 1% of A.

Table A-S1: Detection methods for LC-MS/MS analysis of analytes and deuterated internal standards. 2-AG, 2-arachidonoylglycerol; AEA, anandamide or N-arachidonoylethanolamine; AA, arachidonic acid; PGE2_D2, prostaglandins E2 and D2.

References

1 Kondev, V., Winters, N. & Patel, S. Cannabis use and posttraumatic stress disorder comorbidity: Epidemiology, biology and the potential for novel treatment approaches. *Int Rev Neurobiol* **157**, 143-193, doi:10.1016/bs.irn.2020.09.007 (2021).

2 Winters, N. D. & Patel, S. in *Marijuana and Madness* (eds D. D'Souza, D. Castle, & R. Murray) In Review (Cambridge University Press, 2022).

3 Kano, M., Ohno-Shosaku, T., Hashimotodani, Y., Uchigashima, M. & Watanabe, M. Endocannabinoid-mediated control of synaptic transmission. *Physiol Rev* **89**, 309-380, doi:10.1152/physrev.00019.2008 (2009).

4 Mechoulam, R. & Shvo, Y. Hashish. I. The structure of cannabidiol. *Tetrahedron* **19**, 2073-2078, doi:10.1016/0040-4020(63)85022-x (1963).

5 Gaoni, Y. & Mechoulam, R. Isolation, Structure, and Partial Synthesis of an Active Constituent of Hashish. *J Am Chem Soc* **86**, 1646-+, doi:DOI 10.1021/ja01062a046 (1964).

6 Devane, W. A., Dysarz, F. A., 3rd, Johnson, M. R., Melvin, L. S. & Howlett, A. C. Determination and characterization of a cannabinoid receptor in rat brain. *Mol Pharmacol* **34**, 605-613 (1988).

7 Matsuda, L. A., Lolait, S. J., Brownstein, M. J., Young, A. C. & Bonner, T. I. Structure of a cannabinoid receptor and functional expression of the cloned cDNA. *Nature* **346**, 561-564, doi:10.1038/346561a0 (1990).

8 Lawrence, D. K. & Gill, E. W. The effects of delta1-tetrahydrocannabinol and other cannabinoids on spin-labeled liposomes and their relationship to mechanisms of general anesthesia. *Mol Pharmacol* **11**, 595-602 (1975).

9 Mechoulam, R. *et al.* Stereochemical requirements for cannabinoid activity. *J Med Chem* **23**, 1068-1072, doi:10.1021/jm00184a002 (1980).

10 Howlett, A. C. & Fleming, R. M. Cannabinoid inhibition of adenylate cyclase. Pharmacology of the response in neuroblastoma cell membranes. *Mol Pharmacol* **26**, 532-538 (1984).

11 Howlett, A. C., Qualy, J. M. & Khachatrian, L. L. Involvement of Gi in the inhibition of adenylate cyclase by cannabimimetic drugs. *Mol Pharmacol* **29**, 307-313 (1986).

12 Glass, M., Dragunow, M. & Faull, R. L. Cannabinoid receptors in the human brain: a detailed anatomical and quantitative autoradiographic study in the fetal, neonatal and adult human brain. *Neuroscience* **77**, 299-318, doi:10.1016/s0306-4522(96)00428-9 (1997).

13 Herkenham, M. *et al.* Cannabinoid receptor localization in brain. *Proc Natl Acad Sci U S A* **87**, 1932-1936, doi:10.1073/pnas.87.5.1932 (1990).

14 Howlett, A. C. The cannabinoid receptors. *Prostaglandins Other Lipid Mediat* **68-69**, 619-631, doi:10.1016/s0090-6980(02)00060-6 (2002).

15 Daniel, H., Rancillac, A. & Crepel, F. Mechanisms underlying cannabinoid inhibition of presynaptic Ca2+ influx at parallel fibre synapses of the rat cerebellum. *J Physiol* **557**, 159-174, doi:10.1113/jphysiol.2004.063263 (2004).

16 Katona, I. & Freund, T. F. Multiple functions of endocannabinoid signaling in the brain. *Annu Rev Neurosci* **35**, 529-558, doi:10.1146/annurev-neuro-062111-150420 (2012).

17 Eldeeb, K., Leone-Kabler, S. & Howlett, A. C. CB1 cannabinoid receptor-mediated increases in cyclic AMP accumulation are correlated with reduced Gi/o function. *J Basic Clin Physiol Pharmacol* **27**, 311-322, doi:10.1515/jbcpp-2015-0096 (2016).

18 Finlay, D. B. *et al.* Galphas signalling of the CB1 receptor and the influence of receptor number. *Br J Pharmacol* **174**, 2545-2562, doi:10.1111/bph.13866 (2017).

19 Lauckner, J. E., Hille, B. & Mackie, K. The cannabinoid agonist WIN55,212-2 increases intracellular calcium via CB1 receptor coupling to Gq/11 G proteins. *Proc Natl Acad Sci U S A* **102**, 19144-19149, doi:10.1073/pnas.0509588102 (2005).
20 Hojo, M. *et al.* mu-Opioid receptor forms a functional heterodimer with cannabinoid CB1 receptor: electrophysiological and FRET assay analysis. *J Pharmacol Sci* **108**, 308-319, doi:10.1254/jphs.08244fp (2008).
21 Khan, S. S. & Lee, F. J. Delineation of domains within the cannabinoid CB1 and dopamine D2 receptors that mediate the formation of the heterodimer complex. *J Mol Neurosci* **53**, 10-21, doi:10.1007/s12031-013-0181-7 (2014).
22 Moreno, E. *et al.* Singular Location and Signaling Profile of Adenosine A2A-Cannabinoid CB1 Receptor Heteromers in the Dorsal Striatum. *Neuropsychopharmacology* **43**, 964-977, doi:10.1038/npp.2017.12 (2018).
23 Carriba, P. *et al.* Striatal adenosine A2A and cannabinoid CB1 receptors form functional heteromeric complexes that mediate the motor effects of cannabinoids. *Neuropsychopharmacology* **32**, 2249-2259, doi:10.1038/sj.npp.1301375 (2007).
24 Niehaus, J. L. *et al.* CB1 cannabinoid receptor activity is modulated by the cannabinoid receptor interacting protein CRIP 1a. *Mol Pharmacol* **72**, 1557-1566, doi:10.1124/mol.107.039263 (2007).
25 Booth, W. T., Walker, N. B., Lowther, W. T. & Howlett, A. C. Cannabinoid Receptor Interacting Protein 1a (CRIP1a): Function and Structure. *Molecules* **24**, doi:10.3390/molecules24203672 (2019).
26 Marinelli, S. *et al.* The endocannabinoid 2-arachidonoylglycerol is responsible for the slow self-inhibition in neocortical interneurons. *J Neurosci* **28**, 13532-13541, doi:10.1523/JNEUROSCI.0847-08.2008 (2008).
27 Bacci, A., Huguenard, J. R. & Prince, D. A. Long-lasting self-inhibition of neocortical interneurons mediated by endocannabinoids. *Nature* **431**, 312-316, doi:10.1038/nature02913 (2004).
28 Marinelli, S., Pacioni, S., Cannich, A., Marsicano, G. & Bacci, A. Self-modulation of neocortical pyramidal neurons by endocannabinoids. *Nat Neurosci* **12**, 1488-1490, doi:10.1038/nn.2430 (2009).
29 Benard, G. *et al.* Mitochondrial CB(1) receptors regulate neuronal energy metabolism. *Nat Neurosci* **15**, 558-564, doi:10.1038/nn.3053 (2012).
30 Hebert-Chatelain, E. *et al.* A cannabinoid link between mitochondria and memory. *Nature* **539**, 555-559, doi:10.1038/nature20127 (2016).
31 Soria-Gomez, E. *et al.* Subcellular specificity of cannabinoid effects in striatonigral circuits. *Neuron* **109**, 1513-1526 e1511, doi:10.1016/j.neuron.2021.03.007 (2021).
32 den Boon, F. S. *et al.* Excitability of prefrontal cortical pyramidal neurons is modulated by activation of intracellular type-2 cannabinoid receptors. *Proc Natl Acad Sci U S A* **109**, 3534-3539, doi:10.1073/pnas.1118167109 (2012).
33 Mendizabal-Zubiaga, J. *et al.* Cannabinoid CB1 Receptors Are Localized in Striated Muscle Mitochondria and Regulate Mitochondrial Respiration. *Front Physiol* **7**, 476, doi:10.3389/fphys.2016.00476 (2016).
34 Navarrete, M., Diez, A. & Araque, A. Astrocytes in endocannabinoid signalling. *Philos Trans R Soc Lond B Biol Sci* **369**, 20130599, doi:10.1098/rstb.2013.0599 (2014).
35 Eraso-Pichot, A. *et al.* Endocannabinoid signaling in astrocytes. *Glia*, doi:10.1002/glia.24246 (2022).
36 Navarrete, M. & Araque, A. Endocannabinoids mediate neuron-astrocyte communication. *Neuron* **57**, 883-893, doi:10.1016/j.neuron.2008.01.029 (2008).
37 Navarrete, M. & Araque, A. Endocannabinoids potentiate synaptic transmission through stimulation of astrocytes. *Neuron* **68**, 113-126, doi:10.1016/j.neuron.2010.08.043 (2010).

38 Martin-Fernandez, M. *et al.* Synapse-specific astrocyte gating of amygdala-related behavior. *Nat Neurosci* **20**, 1540-1548, doi:10.1038/nn.4649 (2017).
39 Ho, M. K. & Wong, Y. H. Structure and function of the pertussis-toxin-insensitive Gz protein. *Biol Signals Recept* **7**, 80-89, doi:10.1159/000014533 (1998).
40 Jeong, S. W. & Ikeda, S. R. G protein alpha subunit G alpha z couples neurotransmitter receptors to ion channels in sympathetic neurons. *Neuron* **21**, 1201-1212, doi:10.1016/s0896-6273(00)80636-4 (1998).
41 Fong, H. K., Yoshimoto, K. K., Eversole-Cire, P. & Simon, M. I. Identification of a GTP-binding protein alpha subunit that lacks an apparent ADP-ribosylation site for pertussis toxin. *Proc Natl Acad Sci U S A* **85**, 3066-3070, doi:10.1073/pnas.85.9.3066 (1988).
42 Durkee, C. A. *et al.* Gi/o protein-coupled receptors inhibit neurons but activate astrocytes and stimulate gliotransmission. *Glia* **67**, 1076-1093, doi:10.1002/glia.23589 (2019).
43 Serrat, R. *et al.* Astroglial ER-mitochondria calcium transfer mediates endocannabinoid-dependent synaptic integration. *Cell Rep* **37**, 110133, doi:10.1016/j.celrep.2021.110133 (2021).
44 Walker, J. M. & Huang, S. M. Cannabinoid analgesia. *Pharmacol Ther* **95**, 127-135, doi:10.1016/s0163-7258(02)00252-8 (2002).
45 Guindon, J. & Beaulieu, P. Antihyperalgesic effects of local injections of anandamide, ibuprofen, rofecoxib and their combinations in a model of neuropathic pain. *Neuropharmacology* **50**, 814-823, doi:10.1016/j.neuropharm.2005.12.002 (2006).
46 Agarwal, N. *et al.* Cannabinoids mediate analgesia largely via peripheral type 1 cannabinoid receptors in nociceptors. *Nat Neurosci* **10**, 870-879, doi:10.1038/nn1916 (2007).
47 Guindon, J., Desroches, J. & Beaulieu, P. The antinociceptive effects of intraplantar injections of 2-arachidonoyl glycerol are mediated by cannabinoid CB2 receptors. *Br J Pharmacol* **150**, 693-701, doi:10.1038/sj.bjp.0706990 (2007).
48 Nyilas, R. *et al.* Molecular architecture of endocannabinoid signaling at nociceptive synapses mediating analgesia. *Eur J Neurosci* **29**, 1964-1978, doi:10.1111/j.1460-9568.2009.06751.x (2009).
49 Smith, P. B. & Martin, B. R. Spinal mechanisms of delta 9-tetrahydrocannabinol-induced analgesia. *Brain Res* **578**, 8-12, doi:10.1016/0006-8993(92)90222-u (1992).
50 Garcia-Ovejero, D. *et al.* The endocannabinoid system is modulated in response to spinal cord injury in rats. *Neurobiol Dis* **33**, 57-71, doi:10.1016/j.nbd.2008.09.015 (2009).
51 Palazzo, E., Luongo, L., Novellis, V., Rossi, F. & Maione, S. The Role of Cannabinoid Receptors in the Descending Modulation of Pain. *Pharmaceuticals (Basel)* **3**, 2661-2673, doi:10.3390/ph3082661 (2010).
52 Guindon, J. & Hohmann, A. G. The endocannabinoid system and pain. *CNS Neurol Disord Drug Targets* **8**, 403-421, doi:10.2174/187152709789824660 (2009).
53 Finn, D. P. *et al.* Cannabinoids, the endocannabinoid system, and pain: a review of preclinical studies. *Pain* **162**, S5-S25, doi:10.1097/j.pain.0000000000002268 (2021).
54 Feinberg, I., Jones, R., Walker, J., Cavness, C. & Floyd, T. Effects of marijuana extract and tetrahydrocannabinol on electroencephalographic sleep patterns. *Clin Pharmacol Ther* **19**, 782-794, doi:10.1002/cpt1976196782 (1976).
55 Bonn-Miller, M. O., Boden, M. T., Bucossi, M. M. & Babson, K. A. Self-reported cannabis use characteristics, patterns and helpfulness among medical cannabis users. *Am J Drug Alcohol Abuse* **40**, 23-30, doi:10.3109/00952990.2013.821477 (2014).
56 Valenti, M. *et al.* Differential diurnal variations of anandamide and 2-arachidonoyl-glycerol levels in rat brain. *Cell Mol Life Sci* **61**, 945-950, doi:10.1007/s00018-003-3453-5 (2004).
57 Pava, M. J., Makriyannis, A. & Lovinger, D. M. Endocannabinoid Signaling Regulates Sleep Stability. *PLoS One* **11**, e0152473, doi:10.1371/journal.pone.0152473 (2016).

58 Vaughn, L. K. *et al.* Endocannabinoid signalling: has it got rhythm? *Br J Pharmacol* **160**, 530-543, doi:10.1111/j.1476-5381.2010.00790.x (2010).
59 Acuna-Goycolea, C., Obrietan, K. & van den Pol, A. N. Cannabinoids excite circadian clock neurons. *J Neurosci* **30**, 10061-10066, doi:10.1523/JNEUROSCI.5838-09.2010 (2010).
60 Hablitz, L. M., Gunesch, A. N., Cravetchi, O., Moldavan, M. & Allen, C. N. Cannabinoid Signaling Recruits Astrocytes to Modulate Presynaptic Function in the Suprachiasmatic Nucleus. *eNeuro* **7**, doi:10.1523/ENEURO.0081-19.2020 (2020).
61 Kesner, A. J. & Lovinger, D. M. Cannabinoids, Endocannabinoids and Sleep. *Front Mol Neurosci* **13**, 125, doi:10.3389/fnmol.2020.00125 (2020).
62 Watkins, B. A. & Kim, J. The endocannabinoid system: directing eating behavior and macronutrient metabolism. *Front Psychol* **5**, 1506, doi:10.3389/fpsyg.2014.01506 (2014).
63 Kruk-Slomka, M., Dzik, A., Budzynska, B. & Biala, G. Endocannabinoid System: the Direct and Indirect Involvement in the Memory and Learning Processes-a Short Review. *Mol Neurobiol* **54**, 8332-8347, doi:10.1007/s12035-016-0313-5 (2017).
64 Parsons, L. H. & Hurd, Y. L. Endocannabinoid signalling in reward and addiction. *Nat Rev Neurosci* **16**, 579-594, doi:10.1038/nrn4004 (2015).
65 Pecoraro, N. *et al.* From Malthus to motive: how the HPA axis engineers the phenotype, yoking needs to wants. *Prog Neurobiol* **79**, 247-340, doi:10.1016/j.pneurobio.2006.07.004 (2006).
66 Patel, S., Roelke, C. T., Rademacher, D. J., Cullinan, W. E. & Hillard, C. J. Endocannabinoid signaling negatively modulates stress-induced activation of the hypothalamic-pituitary-adrenal axis. *Endocrinology* **145**, 5431-5438, doi:10.1210/en.2004-0638 (2004).
67 Wade, M. R., Degroot, A. & Nomikos, G. G. Cannabinoid CB1 receptor antagonism modulates plasma corticosterone in rodents. *Eur J Pharmacol* **551**, 162-167, doi:10.1016/j.ejphar.2006.08.083 (2006).
68 Patel, S., Roelke, C. T., Rademacher, D. J. & Hillard, C. J. Inhibition of restraint stress-induced neural and behavioural activation by endogenous cannabinoid signalling. *Eur J Neurosci* **21**, 1057-1069, doi:10.1111/j.1460-9568.2005.03916.x (2005).
69 Wang, M. *et al.* Acute restraint stress enhances hippocampal endocannabinoid function via glucocorticoid receptor activation. *J Psychopharmacol* **26**, 56-70, doi:10.1177/0269881111409606 (2012).
70 Bedse, G. *et al.* Role of the basolateral amygdala in mediating the effects of the fatty acid amide hydrolase inhibitor URB597 on HPA axis response to stress. *Eur Neuropsychopharmacol* **24**, 1511-1523, doi:10.1016/j.euroneuro.2014.07.005 (2014).
71 Morena, M., Patel, S., Bains, J. S. & Hill, M. N. Neurobiological Interactions Between Stress and the Endocannabinoid System. *Neuropsychopharmacology* **41**, 80-102, doi:10.1038/npp.2015.166 (2016).
72 Hill, M. N. *et al.* Recruitment of prefrontal cortical endocannabinoid signaling by glucocorticoids contributes to termination of the stress response. *J Neurosci* **31**, 10506-10515, doi:10.1523/JNEUROSCI.0496-11.2011 (2011).
73 Evanson, N. K., Tasker, J. G., Hill, M. N., Hillard, C. J. & Herman, J. P. Fast feedback inhibition of the HPA axis by glucocorticoids is mediated by endocannabinoid signaling. *Endocrinology* **151**, 4811-4819, doi:10.1210/en.2010-0285 (2010).
74 Hill, M. N., Karatsoreos, I. N., Hillard, C. J. & McEwen, B. S. Rapid elevations in limbic endocannabinoid content by glucocorticoid hormones in vivo. *Psychoneuroendocrinology* **35**, 1333-1338, doi:10.1016/j.psyneuen.2010.03.005 (2010).
75 Bedse, G. *et al.* Functional Redundancy Between Canonical Endocannabinoid Signaling Systems in the Modulation of Anxiety. *Biol Psychiatry* **82**, 488-499, doi:10.1016/j.biopsych.2017.03.002 (2017).

76 Roberts, C. J., Stuhr, K. L., Hutz, M. J., Raff, H. & Hillard, C. J. Endocannabinoid signaling in hypothalamic-pituitary-adrenocortical axis recovery following stress: effects of indirect agonists and comparison of male and female mice. *Pharmacol Biochem Behav* **117**, 17-24, doi:10.1016/j.pbb.2013.11.026 (2014).
77 Shonesy, B. C. *et al.* Genetic disruption of 2-arachidonoylglycerol synthesis reveals a key role for endocannabinoid signaling in anxiety modulation. *Cell Rep* **9**, 1644-1653, doi:10.1016/j.celrep.2014.11.001 (2014).
78 Bluett, R. J. *et al.* Endocannabinoid signalling modulates susceptibility to traumatic stress exposure. *Nat Commun* **8**, 14782, doi:10.1038/ncomms14782 (2017).
79 Marcus, D. J. *et al.* Endocannabinoid Signaling Collapse Mediates Stress-Induced Amygdalo-Cortical Strengthening. *Neuron* **105**, 1062-1076 e1066, doi:10.1016/j.neuron.2019.12.024 (2020).
80 Holleran, K. M. *et al.* Ketamine and MAG Lipase Inhibitor-Dependent Reversal of Evolving Depressive-Like Behavior During Forced Abstinence From Alcohol Drinking. *Neuropsychopharmacology* **41**, 2062-2071, doi:10.1038/npp.2016.3 (2016).
81 Patel, S., Hill, M. N., Cheer, J. F., Wotjak, C. T. & Holmes, A. The endocannabinoid system as a target for novel anxiolytic drugs. *Neurosci Biobehav Rev* **76**, 56-66, doi:10.1016/j.neubiorev.2016.12.033 (2017).
82 Bianco, I. H. & Wilson, S. W. The habenular nuclei: a conserved asymmetric relay station in the vertebrate brain. *Philos Trans R Soc Lond B Biol Sci* **364**, 1005-1020, doi:10.1098/rstb.2008.0213 (2009).
83 Herkenham, M. & Nauta, W. J. Afferent connections of the habenular nuclei in the rat. A horseradish peroxidase study, with a note on the fiber-of-passage problem. *J Comp Neurol* **173**, 123-146, doi:10.1002/cne.901730107 (1977).
84 Hu, H., Cui, Y. & Yang, Y. Circuits and functions of the lateral habenula in health and in disease. *Nat Rev Neurosci* **21**, 277-295, doi:10.1038/s41583-020-0292-4 (2020).
85 Aizawa, H., Kobayashi, M., Tanaka, S., Fukai, T. & Okamoto, H. Molecular characterization of the subnuclei in rat habenula. *J Comp Neurol* **520**, 4051-4066, doi:10.1002/cne.23167 (2012).
86 Jhou, T. C., Geisler, S., Marinelli, M., Degarmo, B. A. & Zahm, D. S. The mesopontine rostromedial tegmental nucleus: A structure targeted by the lateral habenula that projects to the ventral tegmental area of Tsai and substantia nigra compacta. *J Comp Neurol* **513**, 566-596, doi:10.1002/cne.21891 (2009).
87 Sego, C. *et al.* Lateral habenula and the rostromedial tegmental nucleus innervate neurochemically distinct subdivisions of the dorsal raphe nucleus in the rat. *J Comp Neurol* **522**, 1454-1484, doi:10.1002/cne.23533 (2014).
88 Lammel, S. *et al.* Input-specific control of reward and aversion in the ventral tegmental area. *Nature* **491**, 212-217, doi:10.1038/nature11527 (2012).
89 Brinschwitz, K. *et al.* Glutamatergic axons from the lateral habenula mainly terminate on GABAergic neurons of the ventral midbrain. *Neuroscience* **168**, 463-476, doi:10.1016/j.neuroscience.2010.03.050 (2010).
90 Omelchenko, N., Bell, R. & Sesack, S. R. Lateral habenula projections to dopamine and GABA neurons in the rat ventral tegmental area. *Eur J Neurosci* **30**, 1239-1250, doi:10.1111/j.1460-9568.2009.06924.x (2009).
91 Zhou, L. *et al.* Organization of Functional Long-Range Circuits Controlling the Activity of Serotonergic Neurons in the Dorsal Raphe Nucleus. *Cell Rep* **18**, 3018-3032, doi:10.1016/j.celrep.2017.02.077 (2017).
92 Hikosaka, O. The habenula: from stress evasion to value-based decision-making. *Nat Rev Neurosci* **11**, 503-513, doi:10.1038/nrn2866 (2010).
93 Lecca, S. *et al.* Aversive stimuli drive hypothalamus-to-habenula excitation to promote escape behavior. *Elife* **6**, doi:10.7554/eLife.30697 (2017).

94 Wang, D. *et al.* Learning shapes the aversion and reward responses of lateral habenula neurons. *Elife* **6**, doi:10.7554/eLife.23045 (2017).
95 Matsumoto, M. & Hikosaka, O. Lateral habenula as a source of negative reward signals in dopamine neurons. *Nature* **447**, 1111-1115, doi:10.1038/nature05860 (2007).
96 Salas, R., Baldwin, P., de Biasi, M. & Montague, P. R. BOLD Responses to Negative Reward Prediction Errors in Human Habenula. *Front Hum Neurosci* **4**, 36, doi:10.3389/fnhum.2010.00036 (2010).
97 Lalive, A. L. *et al.* Synaptic inhibition in the lateral habenula shapes reward anticipation. *Curr Biol* **32**, 1829-1836 e1824, doi:10.1016/j.cub.2022.02.035 (2022).
98 Barker, D. J. *et al.* Lateral Preoptic Control of the Lateral Habenula through Convergent Glutamate and GABA Transmission. *Cell Rep* **21**, 1757-1769, doi:10.1016/j.celrep.2017.10.066 (2017).
99 Shabel, S. J., Proulx, C. D., Trias, A., Murphy, R. T. & Malinow, R. Input to the lateral habenula from the basal ganglia is excitatory, aversive, and suppressed by serotonin. *Neuron* **74**, 475-481, doi:10.1016/j.neuron.2012.02.037 (2012).
100 Lazaridis, I. *et al.* A hypothalamus-habenula circuit controls aversion. *Mol Psychiatry* **24**, 1351-1368, doi:10.1038/s41380-019-0369-5 (2019).
101 Ootsuka, Y. & Mohammed, M. Activation of the habenula complex evokes autonomic physiological responses similar to those associated with emotional stress. *Physiol Rep* **3**, doi:10.14814/phy2.12297 (2015).
102 Yang, Y. *et al.* Ketamine blocks bursting in the lateral habenula to rapidly relieve depression. *Nature* **554**, 317-322, doi:10.1038/nature25509 (2018).
103 Nair, S. G., Strand, N. S. & Neumaier, J. F. DREADDing the lateral habenula: a review of methodological approaches for studying lateral habenula function. *Brain Res* **1511**, 93-101, doi:10.1016/j.brainres.2012.10.011 (2013).
104 Jacinto, L. R., Mata, R., Novais, A., Marques, F. & Sousa, N. The habenula as a critical node in chronic stress-related anxiety. *Exp Neurol* **289**, 46-54, doi:10.1016/j.expneurol.2016.12.003 (2017).
105 Murphy, C. A., DiCamillo, A. M., Haun, F. & Murray, M. Lesion of the habenular efferent pathway produces anxiety and locomotor hyperactivity in rats: a comparison of the effects of neonatal and adult lesions. *Behav Brain Res* **81**, 43-52, doi:10.1016/s0166-4328(96)00041-1 (1996).
106 Mathis, V. *et al.* The lateral habenula interacts with the hypothalamo-pituitary adrenal axis response upon stressful cognitive demand in rats. *Behav Brain Res* **341**, 63-70, doi:10.1016/j.bbr.2017.12.016 (2018).
107 Gold, P. W. & Kadriu, B. A Major Role for the Lateral Habenula in Depressive Illness: Physiologic and Molecular Mechanisms. *Front Psychiatry* **10**, 320, doi:10.3389/fpsyt.2019.00320 (2019).
108 Caldecott-Hazard, S., Mazziotta, J. & Phelps, M. Cerebral correlates of depressed behavior in rats, visualized using 14C-2-deoxyglucose autoradiography. *J Neurosci* **8**, 1951-1961 (1988).
109 Andalman, A. S. *et al.* Neuronal Dynamics Regulating Brain and Behavioral State Transitions. *Cell* **177**, 970-985 e920, doi:10.1016/j.cell.2019.02.037 (2019).
110 Morris, J. S., Smith, K. A., Cowen, P. J., Friston, K. J. & Dolan, R. J. Covariation of activity in habenula and dorsal raphe nuclei following tryptophan depletion. *Neuroimage* **10**, 163-172, doi:10.1006/nimg.1999.0455 (1999).
111 Li, B. *et al.* Synaptic potentiation onto habenula neurons in the learned helplessness model of depression. *Nature* **470**, 535-539, doi:10.1038/nature09742 (2011).
112 Good, C. H. *et al.* Dopamine D4 receptor excitation of lateral habenula neurons via multiple cellular mechanisms. *J Neurosci* **33**, 16853-16864, doi:10.1523/JNEUROSCI.1844-13.2013 (2013).

113 Zhang, L. *et al.* A GABAergic cell type in the lateral habenula links hypothalamic homeostatic and midbrain motivation circuits with sex steroid signaling. *Transl Psychiatry* **8**, 50, doi:10.1038/s41398-018-0099-5 (2018).
114 Kowski, A. B., Veh, R. W. & Weiss, T. Dopaminergic activation excites rat lateral habenular neurons in vivo. *Neuroscience* **161**, 1154-1165, doi:10.1016/j.neuroscience.2009.04.026 (2009).
115 Reisine, T. D. *et al.* Evidence for a dopaminergic innervation of the cat lateral habenula: its role in controlling serotonin transmission in the basal ganglia. *Brain Res* **308**, 281-288, doi:10.1016/0006-8993(84)91067-9 (1984).
116 Chan, J., Ni, Y., Zhang, P., Zhang, J. & Chen, Y. D1-like dopamine receptor dysfunction in the lateral habenula nucleus increased anxiety-like behavior in rat. *Neuroscience* **340**, 542-550, doi:10.1016/j.neuroscience.2016.11.005 (2017).
117 Shelton, K., Bogyo, K., Schick, T. & Ettenberg, A. Pharmacological modulation of lateral habenular dopamine D2 receptors alters the anxiogenic response to cocaine in a runway model of drug self-administration. *Behav Brain Res* **310**, 42-50, doi:10.1016/j.bbr.2016.05.002 (2016).
118 Stamatakis, A. M. *et al.* A unique population of ventral tegmental area neurons inhibits the lateral habenula to promote reward. *Neuron* **80**, 1039-1053, doi:10.1016/j.neuron.2013.08.023 (2013).
119 Stuber, G. D., Stamatakis, A. M. & Kantak, P. A. Considerations when using cre-driver rodent lines for studying ventral tegmental area circuitry. *Neuron* **85**, 439-445, doi:10.1016/j.neuron.2014.12.034 (2015).
120 Root, D. H. *et al.* Single rodent mesohabenular axons release glutamate and GABA. *Nat Neurosci* **17**, 1543-1551, doi:10.1038/nn.3823 (2014).
121 Yoo, J. H. *et al.* Ventral tegmental area glutamate neurons co-release GABA and promote positive reinforcement. *Nat Commun* **7**, 13697, doi:10.1038/ncomms13697 (2016).
122 Root, D. H. *et al.* Norepinephrine activates dopamine D4 receptors in the rat lateral habenula. *J Neurosci* **35**, 3460-3469, doi:10.1523/JNEUROSCI.4525-13.2015 (2015).
123 Zhang, H. *et al.* Dorsal raphe projection inhibits the excitatory inputs on lateral habenula and alleviates depressive behaviors in rats. *Brain Struct Funct* **223**, 2243-2258, doi:10.1007/s00429-018-1623-3 (2018).
124 Klein, A. K. *et al.* Activation of 5-HT1B receptors in the Lateral Habenula attenuates the anxiogenic effects of cocaine. *Behav Brain Res* **357-358**, 1-8, doi:10.1016/j.bbr.2018.04.014 (2019).
125 Xie, G. *et al.* Serotonin modulates glutamatergic transmission to neurons in the lateral habenula. *Sci Rep* **6**, 23798, doi:10.1038/srep23798 (2016).
126 Tchenio, A., Valentinova, K. & Mameli, M. Can the Lateral Habenula Crack the Serotonin Code? *Front Synaptic Neurosci* **8**, 34, doi:10.3389/fnsyn.2016.00034 (2016).
127 Kobayashi, R. M., Palkovits, M., Kopin, I. J. & Jacobowitz, D. M. Biochemical mapping of noradrenergic nerves arising from the rat locus coeruleus. *Brain Res* **77**, 269-279, doi:10.1016/0006-8993(74)90790-2 (1974).
128 Yetnikoff, L., Cheng, A. Y., Lavezzi, H. N., Parsley, K. P. & Zahm, D. S. Sources of input to the rostromedial tegmental nucleus, ventral tegmental area, and lateral habenula compared: A study in rat. *J Comp Neurol* **523**, 2426-2456, doi:10.1002/cne.23797 (2015).
129 Gottesfeld, Z. Origin and distribution of noradrenergic innervation in the habenula: a neurochemical study. *Brain Res* **275**, 299-304, doi:10.1016/0006-8993(83)90990-3 (1983).

130 Purvis, E. M., Klein, A. K. & Ettenberg, A. Lateral habenular norepinephrine contributes to states of arousal and anxiety in male rats. *Behav Brain Res* **347**, 108-115, doi:10.1016/j.bbr.2018.03.012 (2018).
131 Smith, S. M. & Vale, W. W. The role of the hypothalamic-pituitary-adrenal axis in neuroendocrine responses to stress. *Dialogues Clin Neurosci* **8**, 383-395 (2006).
132 Silberman, Y. & Winder, D. G. Emerging role for corticotropin releasing factor signaling in the bed nucleus of the stria terminalis at the intersection of stress and reward. *Front Psychiatry* **4**, 42, doi:10.3389/fpsyt.2013.00042 (2013).
133 Koob, G. F. The role of CRF and CRF-related peptides in the dark side of addiction. *Brain Res* **1314**, 3-14, doi:10.1016/j.brainres.2009.11.008 (2010).
134 Sanders, J. & Nemeroff, C. The CRF System as a Therapeutic Target for Neuropsychiatric Disorders. *Trends Pharmacol Sci* **37**, 1045-1054, doi:10.1016/j.tips.2016.09.004 (2016).
135 Roberto, M., Spierling, S. R., Kirson, D. & Zorrilla, E. P. Corticotropin-Releasing Factor (CRF) and Addictive Behaviors. *Int Rev Neurobiol* **136**, 5-51, doi:10.1016/bs.irn.2017.06.004 (2017).
136 Chappell, P. B. *et al.* Alterations in corticotropin-releasing factor-like immunoreactivity in discrete rat brain regions after acute and chronic stress. *J Neurosci* **6**, 2908-2914 (1986).
137 Chen, Y., Brunson, K. L., Muller, M. B., Cariaga, W. & Baram, T. Z. Immunocytochemical distribution of corticotropin-releasing hormone receptor type-1 (CRF(1))-like immunoreactivity in the mouse brain: light microscopy analysis using an antibody directed against the C-terminus. *J Comp Neurol* **420**, 305-323, doi:10.1002/(sici)1096-9861(20000508)420:3<305::aid-cne3>3.0.co;2-8 (2000).
138 Rosinger, Z. J., Jacobskind, J. S., Park, S. G., Justice, N. J. & Zuloaga, D. G. Distribution of corticotropin-releasing factor receptor 1 in the developing mouse forebrain: A novel sex difference revealed in the rostral periventricular hypothalamus. *Neuroscience* **361**, 167-178, doi:10.1016/j.neuroscience.2017.08.016 (2017).
139 Justice, N. J., Yuan, Z. F., Sawchenko, P. E. & Vale, W. Type 1 corticotropin-releasing factor receptor expression reported in BAC transgenic mice: implications for reconciling ligand-receptor mismatch in the central corticotropin-releasing factor system. *J Comp Neurol* **511**, 479-496, doi:10.1002/cne.21848 (2008).
140 Authement, M. E. *et al.* A role for corticotropin-releasing factor signaling in the lateral habenula and its modulation by early-life stress. *Sci Signal* **11**, doi:10.1126/scisignal.aan6480 (2018).
141 Zorrilla, E. P. & Koob, G. F. The therapeutic potential of CRF1 antagonists for anxiety. *Expert Opin Investig Drugs* **13**, 799-828, doi:10.1517/13543784.13.7.799 (2004).
142 Schwandt, M. L. *et al.* The CRF1 Antagonist Verucerfont in Anxious Alcohol-Dependent Women: Translation of Neuroendocrine, But not of Anti-Craving Effects. *Neuropsychopharmacology* **41**, 2818-2829, doi:10.1038/npp.2016.61 (2016).
143 Shaham, Y. & de Wit, H. Lost in Translation: CRF1 Receptor Antagonists and Addiction Treatment. *Neuropsychopharmacology* **41**, 2795-2797, doi:10.1038/npp.2016.94 (2016).
144 Wagner, F., Bernard, R., Derst, C., French, L. & Veh, R. W. Microarray analysis of transcripts with elevated expressions in the rat medial or lateral habenula suggest fast GABAergic excitation in the medial habenula and habenular involvement in the regulation of feeding and energy balance. *Brain Struct Funct* **221**, 4663-4689, doi:10.1007/s00429-016-1195-z (2016).
145 Gardon, O. *et al.* Expression of mu opioid receptor in dorsal diencephalic conduction system: new insights for the medial habenula. *Neuroscience* **277**, 595-609, doi:10.1016/j.neuroscience.2014.07.053 (2014).

146 Chen, C. *et al.* Characterization of a Knock-In Mouse Line Expressing a Fusion Protein of kappa Opioid Receptor Conjugated with tdTomato: 3-Dimensional Brain Imaging via CLARITY. *eNeuro* **7**, doi:10.1523/ENEURO.0028-20.2020 (2020).
147 Matthes, H. W. *et al.* Loss of morphine-induced analgesia, reward effect and withdrawal symptoms in mice lacking the mu-opioid-receptor gene. *Nature* **383**, 819-823, doi:10.1038/383819a0 (1996).
148 Kivell, B. & Prisinzano, T. E. Kappa opioids and the modulation of pain. *Psychopharmacology (Berl)* **210**, 109-119, doi:10.1007/s00213-010-1819-6 (2010).
149 Corder, G., Castro, D. C., Bruchas, M. R. & Scherrer, G. Endogenous and Exogenous Opioids in Pain. *Annu Rev Neurosci* **41**, 453-473, doi:10.1146/annurev-neuro-080317-061522 (2018).
150 Bruchas, M. R., Land, B. B. & Chavkin, C. The dynorphin/kappa opioid system as a modulator of stress-induced and pro-addictive behaviors. *Brain Res* **1314**, 44-55, doi:10.1016/j.brainres.2009.08.062 (2010).
151 Darcq, E. & Kieffer, B. L. Opioid receptors: drivers to addiction? *Nat Rev Neurosci* **19**, 499-514, doi:10.1038/s41583-018-0028-x (2018).
152 Welsch, L., Bailly, J., Darcq, E. & Kieffer, B. L. The Negative Affect of Protracted Opioid Abstinence: Progress and Perspectives From Rodent Models. *Biol Psychiatry* **87**, 54-63, doi:10.1016/j.biopsych.2019.07.027 (2020).
153 Waung, M. W. *et al.* A diencephalic circuit in rats for opioid analgesia but not positive reinforcement. *Nat Commun* **13**, 764, doi:10.1038/s41467-022-28332-6 (2022).
154 Ma, Q. P., Shi, Y. S. & Han, J. S. Further studies on interactions between periaqueductal gray, nucleus accumbens and habenula in antinociception. *Brain Res* **583**, 292-295, doi:10.1016/s0006-8993(10)80036-8 (1992).
155 Margolis, E. B. & Fields, H. L. Mu Opioid Receptor Actions in the Lateral Habenula. *PLoS One* **11**, e0159097, doi:10.1371/journal.pone.0159097 (2016).
156 Klein, M. E., Chandra, J., Sheriff, S. & Malinow, R. Opioid system is necessary but not sufficient for antidepressive actions of ketamine in rodents. *Proc Natl Acad Sci U S A* **117**, 2656-2662, doi:10.1073/pnas.1916570117 (2020).
157 Simmons, S. C. *et al.* Early life stress dysregulates kappa opioid receptor signaling within the lateral habenula. *Neurobiol Stress* **13**, 100267, doi:10.1016/j.ynstr.2020.100267 (2020).
158 Berger, A. L. *et al.* The Lateral Habenula Directs Coping Styles Under Conditions of Stress via Recruitment of the Endocannabinoid System. *Biol Psychiatry* **84**, 611-623, doi:10.1016/j.biopsych.2018.04.018 (2018).
159 Patel, S. & Hillard, C. J. Pharmacological evaluation of cannabinoid receptor ligands in a mouse model of anxiety: further evidence for an anxiolytic role for endogenous cannabinoid signaling. *J Pharmacol Exp Ther* **318**, 304-311, doi:10.1124/jpet.106.101287 (2006).
160 Valentinova, K. & Mameli, M. mGluR-LTD at Excitatory and Inhibitory Synapses in the Lateral Habenula Tunes Neuronal Output. *Cell Rep* **16**, 2298-2307, doi:10.1016/j.celrep.2016.07.064 (2016).
161 Park, H., Rhee, J., Lee, S. & Chung, C. Selectively Impaired Endocannabinoid-Dependent Long-Term Depression in the Lateral Habenula in an Animal Model of Depression. *Cell Rep* **20**, 289-296, doi:10.1016/j.celrep.2017.06.049 (2017).
162 Shonesy, B. C. *et al.* CaMKII regulates diacylglycerol lipase-alpha and striatal endocannabinoid signaling. *Nat Neurosci* **16**, 456-463, doi:10.1038/nn.3353 (2013).
163 Fu, R. *et al.* Endocannabinoid signaling in the lateral habenula regulates pain and alcohol consumption. *Transl Psychiatry* **11**, 220, doi:10.1038/s41398-021-01337-3 (2021).

164 Winters, N. D. *et al.* Targeting diacylglycerol lipase reduces alcohol consumption in preclinical models. *J Clin Invest*, doi:10.1172/JCI146861 (2021).
165 Zapata, A. & Lupica, C. R. Lateral habenula cannabinoid CB1 receptor involvement in drug-associated impulsive behavior. *Neuropharmacology* **192**, 108604, doi:10.1016/j.neuropharm.2021.108604 (2021).
166 Ren, M. *et al.* The origins of cannabis smoking: Chemical residue evidence from the first millennium BCE in the Pamirs. *Sci Adv* **5**, eaaw1391, doi:10.1126/sciadv.aaw1391 (2019).
167 Anand, U., Pacchetti, B., Anand, P. & Sodergren, M. H. Cannabis-based medicines and pain: a review of potential synergistic and entourage effects. *Pain Manag* **11**, 395-403, doi:10.2217/pmt-2020-0110 (2021).
168 Patel, S., Hill, M. N. & Hillard, C. J. in *Handbook of Cannabis* (ed R. Pertwee) 189-207 (Oxford Press, 2014).
169 Rock, E. M. & Parker, L. A. Cannabinoids As Potential Treatment for Chemotherapy-Induced Nausea and Vomiting. *Front Pharmacol* **7**, 221, doi:10.3389/fphar.2016.00221 (2016).
170 Goyal, H., Singla, U., Gupta, U. & May, E. Role of cannabis in digestive disorders. *Eur J Gastroenterol Hepatol* **29**, 135-143, doi:10.1097/MEG.0000000000000779 (2017).
171 Berg, C. J., Henriksen, L., Cavazos-Rehg, P. A., Haardoerfer, R. & Freisthler, B. The emerging marijuana retail environment: Key lessons learned from tobacco and alcohol retail research. *Addict Behav* **81**, 26-31, doi:10.1016/j.addbeh.2018.01.040 (2018).
172 Turner, S. E., Williams, C. M., Iversen, L. & Whalley, B. J. Molecular Pharmacology of Phytocannabinoids. *Prog Chem Org Nat Prod* **103**, 61-101, doi:10.1007/978-3-319-45541-9_3 (2017).
173 Banister, S. D., Arnold, J. C., Connor, M., Glass, M. & McGregor, I. S. Dark Classics in Chemical Neuroscience: Delta(9)-Tetrahydrocannabinol. *ACS Chem Neurosci* **10**, 2160-2175, doi:10.1021/acschemneuro.8b00651 (2019).
174 Zimmer, A., Zimmer, A. M., Hohmann, A. G., Herkenham, M. & Bonner, T. I. Increased mortality, hypoactivity, and hypoalgesia in cannabinoid CB1 receptor knockout mice. *Proc Natl Acad Sci U S A* **96**, 5780-5785, doi:10.1073/pnas.96.10.5780 (1999).
175 De Giacomo, V., Ruehle, S., Lutz, B., Haring, M. & Remmers, F. Differential glutamatergic and GABAergic contributions to the tetrad effects of Delta(9)-tetrahydrocannabinol revealed by cell-type-specific reconstitution of the CB1 receptor. *Neuropharmacology* **179**, 108287, doi:10.1016/j.neuropharm.2020.108287 (2020).
176 Ledent, C. *et al.* Unresponsiveness to cannabinoids and reduced addictive effects of opiates in CB1 receptor knockout mice. *Science* **283**, 401-404, doi:10.1126/science.283.5400.401 (1999).
177 Vitale, R. M., Iannotti, F. A. & Amodeo, P. The (Poly)Pharmacology of Cannabidiol in Neurological and Neuropsychiatric Disorders: Molecular Mechanisms and Targets. *Int J Mol Sci* **22**, doi:10.3390/ijms22094876 (2021).
178 Ibeas Bih, C. *et al.* Molecular Targets of Cannabidiol in Neurological Disorders. *Neurotherapeutics* **12**, 699-730, doi:10.1007/s13311-015-0377-3 (2015).
179 VanDolah, H. J., Bauer, B. A. & Mauck, K. F. Clinicians' Guide to Cannabidiol and Hemp Oils. *Mayo Clin Proc* **94**, 1840-1851, doi:10.1016/j.mayocp.2019.01.003 (2019).
180 Wang, Y. H. *et al.* Quantitative Determination of Delta9-THC, CBG, CBD, Their Acid Precursors and Five Other Neutral Cannabinoids by UHPLC-UV-MS. *Planta Med* **84**, 260-266, doi:10.1055/s-0043-124873 (2018).
181 Yamauchi, T., Shoyama, Y., Aramaki, H., Azuma, T. & Nishioka, I. Tetrahydrocannabinolic acid, a genuine substance of tetrahydrocannabinol. *Chem Pharm Bull (Tokyo)* **15**, 1075-1076, doi:10.1248/cpb.15.1075 (1967).

182 Wang, M. *et al.* Decarboxylation Study of Acidic Cannabinoids: A Novel Approach Using Ultra-High-Performance Supercritical Fluid Chromatography/Photodiode Array-Mass Spectrometry. *Cannabis Cannabinoid Res* **1**, 262-271, doi:10.1089/can.2016.0020 (2016).
183 Russell, C., Rueda, S., Room, R., Tyndall, M. & Fischer, B. Routes of administration for cannabis use - basic prevalence and related health outcomes: A scoping review and synthesis. *Int J Drug Policy* **52**, 87-96, doi:10.1016/j.drugpo.2017.11.008 (2018).
184 O'Brien, K. & Blair, P. in *Medicinal Cannabis and CBD in Mental Healthcare* Ch. Routes of Administration, Pharmacokinetics and Safety of Medicinal Cannabis, pp 513–557 (Springer, 2021).
185 Lemberger, L., Martz, R., Rodda, B., Forney, R. & Rowe, H. Comparative pharmacology of Delta9-tetrahydrocannabinol and its metabolite, 11-OH-Delta9-tetrahydrocannabinol. *J Clin Invest* **52**, 2411-2417, doi:10.1172/JCI107431 (1973).
186 Melvin, L. S., Johnson, M. R. & G.M., M. in *186th Natl. Meet. American Chemical. Soc.*
187 Johnson, M. R., Melvin, L. S. & Milne, G. M. Prototype cannabinoid analgetics, prostaglandins and opiates--a search for points of mechanistic interaction. *Life Sci* **31**, 1703-1706, doi:10.1016/0024-3205(82)90190-4 (1982).
188 Melvin, L. S., Johnson, M. R., Harbert, C. A., Milne, G. M. & Weissman, A. A cannabinoid derived prototypical analgesic. *J Med Chem* **27**, 67-71, doi:10.1021/jm00367a013 (1984).
189 Razdan, R. K. Structure-activity relationships in cannabinoids. *Pharmacol Rev* **38**, 75-149 (1986).
190 Weissman, A., Milne, G. M. & Melvin, L. S., Jr. Cannabimimetic activity from CP-47,497, a derivative of 3-phenylcyclohexanol. *J Pharmacol Exp Ther* **223**, 516-523 (1982).
191 Skinner, W. A., Rackur, G. & Uyeno, E. Structure--activity studies on tetrahydro- and hexahydrocannabinol derivatives. *J Pharm Sci* **68**, 330-332, doi:10.1002/jps.2600680319 (1979).
192 Metna-Laurent, M., Mondesir, M., Grel, A., Vallee, M. & Piazza, P. V. Cannabinoid-Induced Tetrad in Mice. *Curr Protoc Neurosci* **80**, 9 59 51-59 59 10, doi:10.1002/cpns.31 (2017).
193 National Academies of Sciences and Medicine, D., Practice, & Agenda. in *The Health Effects of Cannabis and Cannabinoids: The Current State of Evidence and Recommendations for Research The National Academies Collection: Reports funded by National Institutes of Health* (National Academies Press, 2017).
194 Rey, A. A., Purrio, M., Viveros, M. P. & Lutz, B. Biphasic effects of cannabinoids in anxiety responses: CB1 and GABA(B) receptors in the balance of GABAergic and glutamatergic neurotransmission. *Neuropsychopharmacology* **37**, 2624-2634, doi:10.1038/npp.2012.123 (2012).
195 Viveros, M. P., Marco, E. M. & File, S. E. Endocannabinoid system and stress and anxiety responses. *Pharmacol Biochem Behav* **81**, 331-342, doi:10.1016/j.pbb.2005.01.029 (2005).
196 Hill, M. N., Campolongo, P., Yehuda, R. & Patel, S. Integrating Endocannabinoid Signaling and Cannabinoids into the Biology and Treatment of Posttraumatic Stress Disorder. *Neuropsychopharmacology* **43**, 80-102, doi:10.1038/npp.2017.162 (2018).
197 O'Donnell, B., Meissner, H. & Gupta, V. in *StatPearls* (2022).
198 Ware, M. A., Daeninck, P. & Maida, V. A review of nabilone in the treatment of chemotherapy-induced nausea and vomiting. *Ther Clin Risk Manag* **4**, 99-107, doi:10.2147/tcrm.s1132 (2008).
199 Cameron, C., Watson, D. & Robinson, J. Use of a synthetic cannabinoid in a correctional population for posttraumatic stress disorder-related insomnia and nightmares, chronic

pain, harm reduction, and other indications: a retrospective evaluation. *J Clin Psychopharmacol* **34**, 559-564, doi:10.1097/JCP.0000000000000180 (2014).
200 Jetly, R., Heber, A., Fraser, G. & Boisvert, D. The efficacy of nabilone, a synthetic cannabinoid, in the treatment of PTSD-associated nightmares: A preliminary randomized, double-blind, placebo-controlled cross-over design study. *Psychoneuroendocrinology* **51**, 585-588, doi:10.1016/j.psyneuen.2014.11.002 (2015).
201 Fraser, G. A. The use of a synthetic cannabinoid in the management of treatment-resistant nightmares in posttraumatic stress disorder (PTSD). *CNS Neurosci Ther* **15**, 84-88, doi:10.1111/j.1755-5949.2008.00071.x (2009).
202 Whiting, P. F. *et al.* Cannabinoids for Medical Use: A Systematic Review and Meta-analysis. *JAMA* **313**, 2456-2473, doi:10.1001/jama.2015.6358 (2015).
203 Temple, E. C., Driver, M. & Brown, R. F. Cannabis use and anxiety: is stress the missing piece of the puzzle? *Front Psychiatry* **5**, 168, doi:10.3389/fpsyt.2014.00168 (2014).
204 Sharpe, L., Sinclair, J., Kramer, A., de Manincor, M. & Sarris, J. Cannabis, a cause for anxiety? A critical appraisal of the anxiogenic and anxiolytic properties. *J Transl Med* **18**, 374, doi:10.1186/s12967-020-02518-2 (2020).
205 Bitencourt, R. M. & Takahashi, R. N. Cannabidiol as a Therapeutic Alternative for Post-traumatic Stress Disorder: From Bench Research to Confirmation in Human Trials. *Front Neurosci* **12**, 502, doi:10.3389/fnins.2018.00502 (2018).
206 Skelley, J. W., Deas, C. M., Curren, Z. & Ennis, J. Use of cannabidiol in anxiety and anxiety-related disorders. *J Am Pharm Assoc (2003)* **60**, 253-261, doi:10.1016/j.japh.2019.11.008 (2020).
207 Jurkus, R. *et al.* Cannabidiol Regulation of Learned Fear: Implications for Treating Anxiety-Related Disorders. *Front Pharmacol* **7**, 454, doi:10.3389/fphar.2016.00454 (2016).
208 Lee, J. L. C., Bertoglio, L. J., Guimaraes, F. S. & Stevenson, C. W. Cannabidiol regulation of emotion and emotional memory processing: relevance for treating anxiety-related and substance abuse disorders. *Br J Pharmacol* **174**, 3242-3256, doi:10.1111/bph.13724 (2017).
209 Bhamra, S. K., Desai, A., Imani-Berendjestanki, P. & Horgan, M. The emerging role of cannabidiol (CBD) products; a survey exploring the public's use and perceptions of CBD. *Phytother Res* **35**, 5734-5740, doi:10.1002/ptr.7232 (2021).
210 Madras, B. K. Tinkering with THC-to-CBD ratios in Marijuana. *Neuropsychopharmacology* **44**, 215-216, doi:10.1038/s41386-018-0217-3 (2019).
211 McPartland, J. M., Duncan, M., Di Marzo, V. & Pertwee, R. G. Are cannabidiol and Delta(9) -tetrahydrocannabivarin negative modulators of the endocannabinoid system? A systematic review. *Br J Pharmacol* **172**, 737-753, doi:10.1111/bph.12944 (2015).
212 Zanelati, T. V., Biojone, C., Moreira, F. A., Guimaraes, F. S. & Joca, S. R. Antidepressant-like effects of cannabidiol in mice: possible involvement of 5-HT1A receptors. *Br J Pharmacol* **159**, 122-128, doi:10.1111/j.1476-5381.2009.00521.x (2010).
213 Campos, A. C. & Guimaraes, F. S. Involvement of 5HT1A receptors in the anxiolytic-like effects of cannabidiol injected into the dorsolateral periaqueductal gray of rats. *Psychopharmacology (Berl)* **199**, 223-230, doi:10.1007/s00213-008-1168-x (2008).
214 Russo, E. B., Burnett, A., Hall, B. & Parker, K. K. Agonistic properties of cannabidiol at 5-HT1a receptors. *Neurochem Res* **30**, 1037-1043, doi:10.1007/s11064-005-6978-1 (2005).
215 Rock, E. M. *et al.* Cannabidiol, a non-psychotropic component of cannabis, attenuates vomiting and nausea-like behaviour via indirect agonism of 5-HT(1A) somatodendritic autoreceptors in the dorsal raphe nucleus. *Br J Pharmacol* **165**, 2620-2634, doi:10.1111/j.1476-5381.2011.01621.x (2012).

216 Martinez-Aguirre, C. *et al.* Cannabidiol Acts at 5-HT1A Receptors in the Human Brain: Relevance for Treating Temporal Lobe Epilepsy. *Front Behav Neurosci* **14**, 611278, doi:10.3389/fnbeh.2020.611278 (2020).
217 Bakas, T. *et al.* The direct actions of cannabidiol and 2-arachidonoyl glycerol at GABAA receptors. *Pharmacol Res* **119**, 358-370, doi:10.1016/j.phrs.2017.02.022 (2017).
218 Olsen, R. W. Allosteric ligands and their binding sites define gamma-aminobutyric acid (GABA) type A receptor subtypes. *Adv Pharmacol* **73**, 167-202, doi:10.1016/bs.apha.2014.11.005 (2015).
219 Melas, P. A., Scherma, M., Fratta, W., Cifani, C. & Fadda, P. Cannabidiol as a Potential Treatment for Anxiety and Mood Disorders: Molecular Targets and Epigenetic Insights from Preclinical Research. *Int J Mol Sci* **22**, doi:10.3390/ijms22041863 (2021).
220 Wanner, N. M., Colwell, M., Drown, C. & Faulk, C. Subacute cannabidiol alters genome-wide DNA methylation in adult mouse hippocampus. *Environ Mol Mutagen* **61**, 890-900, doi:10.1002/em.22396 (2020).
221 Abu-Sawwa, R., Scutt, B. & Park, Y. Emerging Use of Epidiolex (Cannabidiol) in Epilepsy. *J Pediatr Pharmacol Ther* **25**, 485-499, doi:10.5863/1551-6776-25.6.485 (2020).
222 Iannotti, F. A. *et al.* Nonpsychotropic plant cannabinoids, cannabidivarin (CBDV) and cannabidiol (CBD), activate and desensitize transient receptor potential vanilloid 1 (TRPV1) channels in vitro: potential for the treatment of neuronal hyperexcitability. *ACS Chem Neurosci* **5**, 1131-1141, doi:10.1021/cn5000524 (2014).
223 Kaplan, J. S., Stella, N., Catterall, W. A. & Westenbroek, R. E. Cannabidiol attenuates seizures and social deficits in a mouse model of Dravet syndrome. *Proc Natl Acad Sci U S A* **114**, 11229-11234, doi:10.1073/pnas.1711351114 (2017).
224 Bisogno, T. *et al.* Molecular targets for cannabidiol and its synthetic analogues: effect on vanilloid VR1 receptors and on the cellular uptake and enzymatic hydrolysis of anandamide. *Br J Pharmacol* **134**, 845-852, doi:10.1038/sj.bjp.0704327 (2001).
225 Ryberg, E. *et al.* The orphan receptor GPR55 is a novel cannabinoid receptor. *Br J Pharmacol* **152**, 1092-1101, doi:10.1038/sj.bjp.0707460 (2007).
226 Sharir, H. & Abood, M. E. Pharmacological characterization of GPR55, a putative cannabinoid receptor. *Pharmacol Ther* **126**, 301-313, doi:10.1016/j.pharmthera.2010.02.004 (2010).
227 Sylantyev, S., Jensen, T. P., Ross, R. A. & Rusakov, D. A. Cannabinoid- and lysophosphatidylinositol-sensitive receptor GPR55 boosts neurotransmitter release at central synapses. *Proc Natl Acad Sci U S A* **110**, 5193-5198, doi:10.1073/pnas.1211204110 (2013).
228 FDA. *EPIDIOLEX® (cannabidiol) oral solution*, <https://www.accessdata.fda.gov/drugsatfda_docs/label/2018/210365lbl.pdf> (2018).
229 Ohlsson, A. *et al.* Single-dose kinetics of deuterium-labelled cannabidiol in man after smoking and intravenous administration. *Biomed Environ Mass Spectrom* **13**, 77-83, doi:10.1002/bms.1200130206 (1986).
230 Perucca, E. & Bialer, M. Critical Aspects Affecting Cannabidiol Oral Bioavailability and Metabolic Elimination, and Related Clinical Implications. *CNS Drugs* **34**, 795-800, doi:10.1007/s40263-020-00741-5 (2020).
231 Taylor, L., Gidal, B., Blakey, G., Tayo, B. & Morrison, G. A Phase I, Randomized, Double-Blind, Placebo-Controlled, Single Ascending Dose, Multiple Dose, and Food Effect Trial of the Safety, Tolerability and Pharmacokinetics of Highly Purified Cannabidiol in Healthy Subjects. *CNS Drugs* **32**, 1053-1067, doi:10.1007/s40263-018-0578-5 (2018).
232 Crockett, J., Critchley, D., Tayo, B., Berwaerts, J. & Morrison, G. A phase 1, randomized, pharmacokinetic trial of the effect of different meal compositions, whole

milk, and alcohol on cannabidiol exposure and safety in healthy subjects. *Epilepsia* **61**, 267-277, doi:10.1111/epi.16419 (2020).
233 Deiana, S. *et al.* Plasma and brain pharmacokinetic profile of cannabidiol (CBD), cannabidivarine (CBDV), Delta(9)-tetrahydrocannabivarin (THCV) and cannabigerol (CBG) in rats and mice following oral and intraperitoneal administration and CBD action on obsessive-compulsive behaviour. *Psychopharmacology (Berl)* **219**, 859-873, doi:10.1007/s00213-011-2415-0 (2012).
234 Wheless, J. W. *et al.* Pharmacokinetics and Tolerability of Multiple Doses of Pharmaceutical-Grade Synthetic Cannabidiol in Pediatric Patients with Treatment-Resistant Epilepsy. *CNS Drugs* **33**, 593-604, doi:10.1007/s40263-019-00624-4 (2019).
235 Millar, S. A., Stone, N. L., Yates, A. S. & O'Sullivan, S. E. A Systematic Review on the Pharmacokinetics of Cannabidiol in Humans. *Front Pharmacol* **9**, 1365, doi:10.3389/fphar.2018.01365 (2018).
236 Millar, S. A. *et al.* A systematic review of cannabidiol dosing in clinical populations. *Br J Clin Pharmacol* **85**, 1888-1900, doi:10.1111/bcp.14038 (2019).
237 Assareh, N. *et al.* Cannabidiol disrupts conditioned fear expression and cannabidiolic acid reduces trauma-induced anxiety-related behaviour in mice. *Behav Pharmacol* **31**, 591-596, doi:10.1097/FBP.0000000000000565 (2020).
238 Bedse, G., Hill, M. N. & Patel, S. 2-Arachidonoylglycerol Modulation of Anxiety and Stress Adaptation: From Grass Roots to Novel Therapeutics. *Biol Psychiatry* **88**, 520-530, doi:10.1016/j.biopsych.2020.01.015 (2020).
239 Blum, K. *et al.* Cannabis-Induced Hypodopaminergic Anhedonia and Cognitive Decline in Humans: Embracing Putative Induction of Dopamine Homeostasis. *Front Psychiatry* **12**, 623403, doi:10.3389/fpsyt.2021.623403 (2021).
240 Li, W. *et al.* Activation of glycine receptors in the lateral habenula rescues anxiety- and depression-like behaviors associated with alcohol withdrawal and reduces alcohol intake in rats. *Neuropharmacology* **157**, 107688, doi:10.1016/j.neuropharm.2019.107688 (2019).
241 Xie, Z., Li, G. & Ye, J. H. Acute effects of ethanol on GABAA and glycine currents in the lateral habenula neurons of young rats. *Open J Neurosci* **3**, doi:10.13055/ojns_3_1_5.130821 (2013).
242 Wilson, R. I. & Nicoll, R. A. Endogenous cannabinoids mediate retrograde signalling at hippocampal synapses. *Nature* **410**, 588-592, doi:10.1038/35069076 (2001).
243 Shabel, S. J., Proulx, C. D., Piriz, J. & Malinow, R. GABA/glutamate co-release controls habenula output and is modified by antidepressant treatment. *Science* **345**, 1494-1498, doi:10.1126/science.1250469 (2014).
244 Wallace, M. L. *et al.* Genetically Distinct Parallel Pathways in the Entopeduncular Nucleus for Limbic and Sensorimotor Output of the Basal Ganglia. *Neuron* **94**, 138-152 e135, doi:10.1016/j.neuron.2017.03.017 (2017).
245 Kovacs, A. *et al.* Direct presynaptic and indirect astrocyte-mediated mechanisms both contribute to endocannabinoid signaling in the pedunculopontine nucleus of mice. *Brain Struct Funct* **222**, 247-266, doi:10.1007/s00429-016-1214-0 (2017).
246 Kondev, V. *et al.* The Endocannabinoid 2-Arachidonoylglycerol Bidirectionally Modulates Acute and Protracted Effects of Predator Odor Exposure. *Biol Psychiatry* **In Press**, doi:10.1016/j.biopsych.2022.05.012 (2022).
247 Cong, J. *et al.* Astroglial CB1 Cannabinoid Receptors Mediate CP 55,940-Induced Conditioned Place Aversion Through Cyclooxygenase-2 Signaling in Mice. *Front Cell Neurosci* **15**, 772549, doi:10.3389/fncel.2021.772549 (2021).
248 Lines, J., Covelo, A., Gomez, R., Liu, L. & Araque, A. Synapse-Specific Regulation Revealed at Single Synapses Is Concealed When Recording Multiple Synapses. *Front Cell Neurosci* **11**, 367, doi:10.3389/fncel.2017.00367 (2017).

249 Guzikowski, N. J. & Kavalali, E. T. Nano-Organization at the Synapse: Segregation of Distinct Forms of Neurotransmission. *Front Synaptic Neurosci* **13**, 796498, doi:10.3389/fnsyn.2021.796498 (2021).
250 Kang, S., Li, J., Bekker, A. & Ye, J. H. Rescue of glutamate transport in the lateral habenula alleviates depression- and anxiety-like behaviors in ethanol-withdrawn rats. *Neuropharmacology* **129**, 47-56, doi:10.1016/j.neuropharm.2017.11.013 (2018).
251 Hegyi, Z. *et al.* CB1 receptor activation induces intracellular Ca(2+) mobilization and 2-arachidonoylglycerol release in rodent spinal cord astrocytes. *Sci Rep* **8**, 10562, doi:10.1038/s41598-018-28763-6 (2018).
252 Viollet, C. *et al.* Somatostatin-IRES-Cre Mice: Between Knockout and Wild-Type? *Front Endocrinol (Lausanne)* **8**, 131, doi:10.3389/fendo.2017.00131 (2017).
253 Kim, U. & Chang, S. Y. Dendritic morphology, local circuitry, and intrinsic electrophysiology of neurons in the rat medial and lateral habenular nuclei of the epithalamus. *J Comp Neurol* **483**, 236-250, doi:10.1002/cne.20410 (2005).
254 Lee, J. H. *et al.* Global and local fMRI signals driven by neurons defined optogenetically by type and wiring. *Nature* **465**, 788-792, doi:10.1038/nature09108 (2010).
255 Fasinu, P. S., Phillips, S., ElSohly, M. A. & Walker, L. A. Current Status and Prospects for Cannabidiol Preparations as New Therapeutic Agents. *Pharmacotherapy* **36**, 781-796, doi:10.1002/phar.1780 (2016).
256 Sholler, D. J., Schoene, L. & Spindle, T. R. Therapeutic Efficacy of Cannabidiol (CBD): A Review of the Evidence from Clinical Trials and Human Laboratory Studies. *Curr Addict Rep* **7**, 405-412, doi:10.1007/s40429-020-00326-8 (2020).
257 Janak, P. H. & Tye, K. M. From circuits to behaviour in the amygdala. *Nature* **517**, 284-292, doi:10.1038/nature14188 (2015).
258 Mahan, A. L. & Ressler, K. J. Fear conditioning, synaptic plasticity and the amygdala: implications for posttraumatic stress disorder. *Trends Neurosci* **35**, 24-35, doi:10.1016/j.tins.2011.06.007 (2012).
259 Hartley, N. D. *et al.* Dynamic remodeling of a basolateral-to-central amygdala glutamatergic circuit across fear states. *Nat Neurosci* **22**, 2000-2012, doi:10.1038/s41593-019-0528-7 (2019).
260 Swartz, J. R., Knodt, A. R., Radtke, S. R. & Hariri, A. R. A neural biomarker of psychological vulnerability to future life stress. *Neuron* **85**, 505-511, doi:10.1016/j.neuron.2014.12.055 (2015).
261 Todd, S. M. & Arnold, J. C. Neural correlates of interactions between cannabidiol and Delta(9) -tetrahydrocannabinol in mice: implications for medical cannabis. *Br J Pharmacol* **173**, 53-65, doi:10.1111/bph.13333 (2016).
262 Resstel, L. B., Joca, S. R., Moreira, F. A., Correa, F. M. & Guimaraes, F. S. Effects of cannabidiol and diazepam on behavioral and cardiovascular responses induced by contextual conditioned fear in rats. *Behav Brain Res* **172**, 294-298, doi:10.1016/j.bbr.2006.05.016 (2006).
263 Song, C., Stevenson, C. W., Guimaraes, F. S. & Lee, J. L. Bidirectional Effects of Cannabidiol on Contextual Fear Memory Extinction. *Front Pharmacol* **7**, 493, doi:10.3389/fphar.2016.00493 (2016).
264 Das, R. K. *et al.* Cannabidiol enhances consolidation of explicit fear extinction in humans. *Psychopharmacology (Berl)* **226**, 781-792, doi:10.1007/s00213-012-2955-y (2013).
265 Hsiao, Y. T., Yi, P. L., Li, C. L. & Chang, F. C. Effect of cannabidiol on sleep disruption induced by the repeated combination tests consisting of open field and elevated plus-maze in rats. *Neuropharmacology* **62**, 373-384, doi:10.1016/j.neuropharm.2011.08.013 (2012).

266 Fusar-Poli, P. *et al.* Modulation of effective connectivity during emotional processing by Delta 9-tetrahydrocannabinol and cannabidiol. *Int J Neuropsychopharmacol* **13**, 421-432, doi:10.1017/S1461145709990617 (2010).
267 Fusar-Poli, P. *et al.* Distinct effects of {delta}9-tetrahydrocannabinol and cannabidiol on neural activation during emotional processing. *Arch Gen Psychiatry* **66**, 95-105, doi:10.1001/archgenpsychiatry.2008.519 (2009).
268 Gilpin, N. W., Herman, M. A. & Roberto, M. The central amygdala as an integrative hub for anxiety and alcohol use disorders. *Biol Psychiatry* **77**, 859-869, doi:10.1016/j.biopsych.2014.09.008 (2015).
269 Sharp, B. M. Basolateral amygdala and stress-induced hyperexcitability affect motivated behaviors and addiction. *Transl Psychiatry* **7**, e1194, doi:10.1038/tp.2017.161 (2017).
270 Fadok, J. P. *et al.* A competitive inhibitory circuit for selection of active and passive fear responses. *Nature* **542**, 96-100, doi:10.1038/nature21047 (2017).
271 Kong, M. S. & Zweifel, L. S. Central amygdala circuits in valence and salience processing. *Behav Brain Res* **410**, 113355, doi:10.1016/j.bbr.2021.113355 (2021).
272 Sanford, C. A. *et al.* A Central Amygdala CRF Circuit Facilitates Learning about Weak Threats. *Neuron* **93**, 164-178, doi:10.1016/j.neuron.2016.11.034 (2017).
273 Moscarello, J. M. & Penzo, M. A. The central nucleus of the amygdala and the construction of defensive modes across the threat-imminence continuum. *Nat Neurosci* **25**, 999-1008, doi:10.1038/s41593-022-01130-5 (2022).
274 Shearman, L. P. *et al.* Antidepressant-like and anorectic effects of the cannabinoid CB1 receptor inverse agonist AM251 in mice. *Behav Pharmacol* **14**, 573-582, doi:10.1097/00008877-200312000-00001 (2003).
275 Griebel, G., Stemmelin, J. & Scatton, B. Effects of the cannabinoid CB1 receptor antagonist rimonabant in models of emotional reactivity in rodents. *Biol Psychiatry* **57**, 261-267, doi:10.1016/j.biopsych.2004.10.032 (2005).
276 Tzavara, E. T. *et al.* The CB1 receptor antagonist SR141716A selectively increases monoaminergic neurotransmission in the medial prefrontal cortex: implications for therapeutic actions. *Br J Pharmacol* **138**, 544-553, doi:10.1038/sj.bjp.0705100 (2003).
277 Park, H., Cheon, M., Kim, S. & Chung, C. Temporal variations in presynaptic release probability in the lateral habenula. *Sci Rep* **7**, 40866, doi:10.1038/srep40866 (2017).
278 Bano-Otalora, B. & Piggins, H. D. Contributions of the lateral habenula to circadian timekeeping. *Pharmacol Biochem Behav* **162**, 46-54, doi:10.1016/j.pbb.2017.06.007 (2017).
279 Mendoza, J. Circadian neurons in the lateral habenula: Clocking motivated behaviors. *Pharmacol Biochem Behav* **162**, 55-61, doi:10.1016/j.pbb.2017.06.013 (2017).
280 Millar, S. A., Maguire, R. F., Yates, A. S. & O'Sullivan, S. E. Towards Better Delivery of Cannabidiol (CBD). *Pharmaceuticals (Basel)* **13**, doi:10.3390/ph13090219 (2020).
281 Stevens, J. S. *et al.* Amygdala Reactivity and Anterior Cingulate Habituation Predict Posttraumatic Stress Disorder Symptom Maintenance After Acute Civilian Trauma. *Biol Psychiatry* **81**, 1023-1029, doi:10.1016/j.biopsych.2016.11.015 (2017).
282 Ressler, K. J. Amygdala activity, fear, and anxiety: modulation by stress. *Biol Psychiatry* **67**, 1117-1119, doi:10.1016/j.biopsych.2010.04.027 (2010).
283 Hill, M. N. *et al.* Suppression of amygdalar endocannabinoid signaling by stress contributes to activation of the hypothalamic-pituitary-adrenal axis. *Neuropsychopharmacology* **34**, 2733-2745, doi:10.1038/npp.2009.114 (2009).
284 Duvarci, S. & Pare, D. Amygdala microcircuits controlling learned fear. *Neuron* **82**, 966-980, doi:10.1016/j.neuron.2014.04.042 (2014).
285 Sergerie, K., Chochol, C. & Armony, J. L. The role of the amygdala in emotional processing: a quantitative meta-analysis of functional neuroimaging studies. *Neurosci Biobehav Rev* **32**, 811-830, doi:10.1016/j.neubiorev.2007.12.002 (2008).

286 Shin, L. M., Rauch, S. L. & Pitman, R. K. Amygdala, medial prefrontal cortex, and hippocampal function in PTSD. *Ann N Y Acad Sci* **1071**, 67-79, doi:10.1196/annals.1364.007 (2006).
287 Fallah, M. S., Dlugosz, L., Scott, B. W., Thompson, M. D. & Burnham, W. M. Antiseizure effects of the cannabinoids in the amygdala-kindling model. *Epilepsia* **62**, 2274-2282, doi:10.1111/epi.16973 (2021).
288 Li, H. *et al.* Experience-dependent modification of a central amygdala fear circuit. *Nat Neurosci* **16**, 332-339, doi:10.1038/nn.3322 (2013).
289 Grant, B. F. *et al.* Epidemiology of DSM-5 Alcohol Use Disorder: Results From the National Epidemiologic Survey on Alcohol and Related Conditions III. *JAMA Psychiatry* **72**, 757-766, doi:10.1001/jamapsychiatry.2015.0584 (2015).
290 Kranzler, H. R. & Soyka, M. Diagnosis and Pharmacotherapy of Alcohol Use Disorder: A Review. *JAMA* **320**, 815-824, doi:10.1001/jama.2018.11406 (2018).
291 Centers for Disease Control and Prevention, C. D. C. *Excessive Alcohol Use: A Drain on the American Economy*, <https://www.cdc.gov/alcohol/onlinemedia/infographics/excessive-alcohol-economy.html> (2019).
292 Evoy, K. E. *et al.* National outpatient medication utilization for opioid and alcohol use disorders from 2014 to 2016. *J Subst Abuse Treat* **119**, 108141, doi:10.1016/j.jsat.2020.108141 (2020).
293 Kunos, G. Interactions Between Alcohol and the Endocannabinoid System. *Alcohol Clin Exp Res* **44**, 790-805, doi:10.1111/acer.14306 (2020).
294 Henderson-Redmond, A. N., Guindon, J. & Morgan, D. J. Roles for the endocannabinoid system in ethanol-motivated behavior. *Prog Neuropsychopharmacol Biol Psychiatry* **65**, 330-339, doi:10.1016/j.pnpbp.2015.06.011 (2016).
295 Bedse, G., Centanni, S. W., Winder, D. G. & Patel, S. Endocannabinoid Signaling in the Central Amygdala and Bed Nucleus of the Stria Terminalis: Implications for the Pathophysiology and Treatment of Alcohol Use Disorder. *Alcohol Clin Exp Res* **43**, 2014-2027, doi:10.1111/acer.14159 (2019).
296 Caille, S., Alvarez-Jaimes, L., Polis, I., Stouffer, D. G. & Parsons, L. H. Specific alterations of extracellular endocannabinoid levels in the nucleus accumbens by ethanol, heroin, and cocaine self-administration. *J Neurosci* **27**, 3695-3702, doi:10.1523/JNEUROSCI.4403-06.2007 (2007).
297 Alvarez-Jaimes, L., Stouffer, D. G. & Parsons, L. H. Chronic ethanol treatment potentiates ethanol-induced increases in interstitial nucleus accumbens endocannabinoid levels in rats. *J Neurochem* **111**, 37-48, doi:10.1111/j.1471-4159.2009.06301.x (2009).
298 Basavarajappa, B. S., Saito, M., Cooper, T. B. & Hungund, B. L. Stimulation of cannabinoid receptor agonist 2-arachidonylglycerol by chronic ethanol and its modulation by specific neuromodulators in cerebellar granule neurons. *Biochim Biophys Acta* **1535**, 78-86, doi:10.1016/s0925-4439(00)00085-5 (2000).
299 Basavarajappa, B. S., Ninan, I. & Arancio, O. Acute ethanol suppresses glutamatergic neurotransmission through endocannabinoids in hippocampal neurons. *J Neurochem* **107**, 1001-1013, doi:10.1111/j.1471-4159.2008.05685.x (2008).
300 Vinod, K. Y. *et al.* Genetic and pharmacological manipulations of the CB(1) receptor alter ethanol preference and dependence in ethanol preferring and nonpreferring mice. *Synapse* **62**, 574-581, doi:10.1002/syn.20533 (2008).
301 Marinho, E. A. *et al.* Effects of rimonabant on the development of single dose-induced behavioral sensitization to ethanol, morphine and cocaine in mice. *Prog Neuropsychopharmacol Biol Psychiatry* **58**, 22-31, doi:10.1016/j.pnpbp.2014.11.010 (2015).

302 Perra, S. *et al.* Involvement of the endogenous cannabinoid system in the effects of alcohol in the mesolimbic reward circuit: electrophysiological evidence in vivo. *Psychopharmacology (Berl)* **183**, 368-377, doi:10.1007/s00213-005-0195-0 (2005).
303 Soyka, M. *et al.* Cannabinoid receptor 1 blocker rimonabant (SR 141716) for treatment of alcohol dependence: results from a placebo-controlled, double-blind trial. *J Clin Psychopharmacol* **28**, 317-324, doi:10.1097/JCP.0b013e318172b8bc (2008).
304 Robinson, J. D. *et al.* Pooled analysis of three randomized, double-blind, placebo controlled trials with rimonabant for smoking cessation. *Addict Biol* **23**, 291-303, doi:10.1111/adb.12508 (2018).
305 Pataky, Z. *et al.* Efficacy of rimonabant in obese patients with binge eating disorder. *Exp Clin Endocrinol Diabetes* **121**, 20-26, doi:10.1055/s-0032-1329957 (2013).
306 Sam, A. H., Salem, V. & Ghatei, M. A. Rimonabant: From RIO to Ban. *J Obes* **2011**, 432607, doi:10.1155/2011/432607 (2011).
307 Bisogno, T. *et al.* Cloning of the first sn1-DAG lipases points to the spatial and temporal regulation of endocannabinoid signaling in the brain. *J Cell Biol* **163**, 463-468, doi:10.1083/jcb.200305129 (2003).
308 Ogasawara, D. *et al.* Rapid and profound rewiring of brain lipid signaling networks by acute diacylglycerol lipase inhibition. *Proc Natl Acad Sci U S A* **113**, 26-33, doi:10.1073/pnas.1522364112 (2016).
309 Hermanson, D. J., Gamble-George, J. C., Marnett, L. J. & Patel, S. Substrate-selective COX-2 inhibition as a novel strategy for therapeutic endocannabinoid augmentation. *Trends Pharmacol Sci* **35**, 358-367, doi:10.1016/j.tips.2014.04.006 (2014).
310 Lallemand, F. & de Witte, P. Ethanol induces higher BEC in CB1 cannabinoid receptor knockout mice while decreasing ethanol preference. *Alcohol Alcohol* **40**, 54-62, doi:10.1093/alcalc/agh115 (2005).
311 Pruett, S., Tan, W., Howell, G. E., 3rd & Nanduri, B. Dosage scaling of alcohol in binge exposure models in mice: An empirical assessment of the relationship between dose, alcohol exposure, and peak blood concentrations in humans and mice. *Alcohol* **89**, 9-17, doi:10.1016/j.alcohol.2020.03.011 (2020).
312 Hopf, F. W. & Lesscher, H. M. Rodent models for compulsive alcohol intake. *Alcohol* **48**, 253-264, doi:10.1016/j.alcohol.2014.03.001 (2014).
313 Cho, S. B. *et al.* Positive and negative reinforcement are differentially associated with alcohol consumption as a function of alcohol dependence. *Psychol Addict Behav* **33**, 58-68, doi:10.1037/adb0000436 (2019).
314 George, O. *et al.* Recruitment of medial prefrontal cortex neurons during alcohol withdrawal predicts cognitive impairment and excessive alcohol drinking. *Proc Natl Acad Sci U S A* **109**, 18156-18161, doi:10.1073/pnas.1116523109 (2012).
315 Becker, H. C. Animal models of excessive alcohol consumption in rodents. *Curr Top Behav Neurosci* **13**, 355-377, doi:10.1007/7854_2012_203 (2013).
316 Centanni, S. W. *et al.* Endocannabinoid control of the insular-bed nucleus of the stria terminalis circuit regulates negative affective behavior associated with alcohol abstinence. *Neuropsychopharmacology* **44**, 526-537, doi:10.1038/s41386-018-0257-8 (2019).
317 Driessen, M. *et al.* The course of anxiety, depression and drinking behaviours after completed detoxification in alcoholics with and without comorbid anxiety and depressive disorders. *Alcohol Alcohol* **36**, 249-255, doi:10.1093/alcalc/36.3.249 (2001).
318 Centanni, S. W., Bedse, G., Patel, S. & Winder, D. G. Driving the Downward Spiral: Alcohol-Induced Dysregulation of Extended Amygdala Circuits and Negative Affect. *Alcohol Clin Exp Res* **43**, 2000-2013, doi:10.1111/acer.14178 (2019).

319 Alvarez-Jaimes, L., Polis, I. & Parsons, L. H. Regional Influence of Cannabinoid CB1 Receptors in the Regulation of Ethanol Self-Administration by Wistar Rats. *Open Neuropsychopharmacol J* **2**, 77-85, doi:10.2174/1876523800902020077 (2009).
320 Guan, Y. *et al.* GABAergic actions mediate opposite ethanol effects on dopaminergic neurons in the anterior and posterior ventral tegmental area. *J Pharmacol Exp Ther* **341**, 33-42, doi:10.1124/jpet.111.187963 (2012).
321 Buczynski, M. W. *et al.* Diacylglycerol lipase disinhibits VTA dopamine neurons during chronic nicotine exposure. *Proc Natl Acad Sci U S A* **113**, 1086-1091, doi:10.1073/pnas.1522672113 (2016).
322 Melis, M. *et al.* Enhanced endocannabinoid-mediated modulation of rostromedial tegmental nucleus drive onto dopamine neurons in Sardinian alcohol-preferring rats. *J Neurosci* **34**, 12716-12724, doi:10.1523/JNEUROSCI.1844-14.2014 (2014).
323 Riegel, A. C. & Lupica, C. R. Independent presynaptic and postsynaptic mechanisms regulate endocannabinoid signaling at multiple synapses in the ventral tegmental area. *J Neurosci* **24**, 11070-11078, doi:10.1523/JNEUROSCI.3695-04.2004 (2004).
324 Melis, M. *et al.* Electrophysiological properties of dopamine neurons in the ventral tegmental area of Sardinian alcohol-preferring rats. *Psychopharmacology (Berl)* **201**, 471-481, doi:10.1007/s00213-008-1309-2 (2009).
325 Gianessi, C. A. *et al.* Endocannabinoid contributions to alcohol habits and motivation: Relevance to treatment. *Addict Biol* **25**, e12768, doi:10.1111/adb.12768 (2020).
326 Morales, I., Rodriguez-Borillo, O., Font, L. & Pastor, R. Effects of naltrexone on alcohol, sucrose, and saccharin binge-like drinking in C57BL/6J mice: a study with a multiple bottle choice procedure. *Behav Pharmacol* **31**, 256-271, doi:10.1097/FBP.0000000000000553 (2020).
327 Navarro, M., Luhn, K. L., Kampov-Polevoy, A. B., Garbutt, J. C. & Thiele, T. E. Bupropion, Alone and in Combination with Naltrexone, Blunts Binge-Like Ethanol Drinking and Intake Following Chronic Intermittent Access to Ethanol in Male C57BL/6J Mice. *Alcohol Clin Exp Res* **43**, 783-790, doi:10.1111/acer.13992 (2019).
328 Crabbe, J. C. *et al.* High Drinking in the Dark (HDID) mice are sensitive to the effects of some clinically relevant drugs to reduce binge-like drinking. *Pharmacol Biochem Behav* **160**, 55-62, doi:10.1016/j.pbb.2017.08.002 (2017).
329 Ho, A. M. *et al.* Combined Effects of Acamprosate and Escitalopram on Ethanol Consumption in Mice. *Alcohol Clin Exp Res* **40**, 1531-1539, doi:10.1111/acer.13099 (2016).
330 Cavener, V. S. *et al.* Inhibition of Diacylglycerol Lipase Impairs Fear Extinction in Mice. *Front Neurosci* **12**, 479, doi:10.3389/fnins.2018.00479 (2018).
331 Jenniches, I. *et al.* Anxiety, Stress, and Fear Response in Mice With Reduced Endocannabinoid Levels. *Biol Psychiatry* **79**, 858-868, doi:10.1016/j.biopsych.2015.03.033 (2016).
332 Hartley, N. D. *et al.* 2-arachidonoylglycerol signaling impairs short-term fear extinction. *Transl Psychiatry* **6**, e749, doi:10.1038/tp.2016.26 (2016).
333 Lominac, K. D. *et al.* Behavioral and neurochemical interactions between Group 1 mGluR antagonists and ethanol: potential insight into their anti-addictive properties. *Drug Alcohol Depend* **85**, 142-156, doi:10.1016/j.drugalcdep.2006.04.003 (2006).
334 Cozzoli, D. K. *et al.* The Effect of mGluR5 Antagonism During Binge Drinkingon Subsequent Ethanol Intake in C57BL/6J Mice: Sex- and Age-Induced Differences. *Alcohol Clin Exp Res* **38**, 730-738, doi:10.1111/acer.12292 (2014).
335 Kumar, J., Hapidin, H., Bee, Y. T. & Ismail, Z. Effects of the mGluR5 antagonist MPEP on ethanol withdrawal induced anxiety-like syndrome in rats. *Behav Brain Funct* **9**, 43, doi:10.1186/1744-9081-9-43 (2013).

336 Lee, K. M., Coelho, M. A., Class, M. A. & Szumlinski, K. K. mGlu5-dependent modulation of anxiety during early withdrawal from binge-drinking in adult and adolescent male mice. *Drug Alcohol Depend* **184**, 1-11, doi:10.1016/j.drugalcdep.2017.10.031 (2018).
337 Kasten, C. R., Holmgren, E. B. & Wills, T. A. Metabotropic Glutamate Receptor Subtype 5 in Alcohol-Induced Negative Affect. *Brain Sci* **9**, doi:10.3390/brainsci9080183 (2019).
338 Ceccarini, J. *et al.* Recovery of Decreased Metabotropic Glutamate Receptor 5 Availability in Abstinent Alcohol-Dependent Patients. *J Nucl Med* **61**, 256-262, doi:10.2967/jnumed.119.228825 (2020).
339 Kasten, C. R. *et al.* Adolescent alcohol exposure produces sex differences in negative affect-like behavior and group I mGluR BNST plasticity. *Neuropsychopharmacology* **45**, 1306-1315, doi:10.1038/s41386-020-0670-7 (2020).
340 Grueter, B. A. *et al.* Extracellular-signal regulated kinase 1-dependent metabotropic glutamate receptor 5-induced long-term depression in the bed nucleus of the stria terminalis is disrupted by cocaine administration. *J Neurosci* **26**, 3210-3219, doi:10.1523/JNEUROSCI.0170-06.2006 (2006).
341 Healey, J. C., Winder, D. G. & Kash, T. L. Chronic ethanol exposure leads to divergent control of dopaminergic synapses in distinct target regions. *Alcohol* **42**, 179-190, doi:10.1016/j.alcohol.2008.01.003 (2008).
342 Morgan, A. J. *et al.* Detection of Cyclooxygenase-2-Derived Oxygenation Products of the Endogenous Cannabinoid 2-Arachidonoylglycerol in Mouse Brain. *ACS Chem Neurosci* **9**, 1552-1559, doi:10.1021/acschemneuro.7b00499 (2018).